

DISTRIBUTIONAL ASSOCIATIONS VS IN-CONTEXT REASONING: A STUDY OF FEED-FORWARD AND ATTENTION LAYERS

Anonymous authors

Paper under double-blind review

ABSTRACT

Large language models have been successful at tasks involving basic forms of in-context reasoning, such as generating coherent language, as well as storing vast amounts of knowledge. At the core of the Transformer architecture behind such models are feed-forward and attention layers, which are often associated to knowledge and reasoning, respectively. In this paper, we study this distinction empirically and theoretically in a controlled synthetic setting where certain next-token predictions involve both distributional and in-context information. We find that feed-forward layers tend to learn simple distributional associations such as bigrams, while attention layers focus on in-context reasoning. Our theoretical analysis identifies the noise in the gradients as a key factor behind this discrepancy. Finally, we illustrate how similar disparities emerge in pre-trained models through ablations on the Pythia model family on simple reasoning tasks.

1 INTRODUCTION

Large language models (LLMs) have shown impressive capabilities on a variety of tasks, from generating coherent and grammatically correct text, to language understanding and basic mathematical reasoning (Brown et al., 2020; Touvron et al., 2023). At the heart of this success is the Transformer architecture (Vaswani et al., 2017), which relies on a sequence of self-attention and feed-forward layers to efficiently combine information from the input context and patterns learned from training data. Despite recent progress on interpreting the mechanisms learned by different layers (Meng et al., 2022; Wang et al., 2022), these models remain largely black boxes. A better understanding of the role of Transformer layers and how they are affected by the training process could enable new monitoring and editing techniques, better training data, and ultimately more reliable LLMs.

The task of next-token prediction in language modeling inherently involves different subtasks that may be at odds with each other, as shown in Figure 1. For instance, given the context “John gave a book to”, the word “the” is a natural and grammatically correct next word to predict, and relying on global bigram statistics might be enough to predict it given the last word “to”. Nonetheless, if another character is present in the context, say Mary, then the name “Mary” may be a better prediction, and this would require a more involved form of reasoning over the context to retrieve this name. In the context of Transformer language models, previous work on interpretability has found that circuits of attention heads seem responsible for such in-context predictions (Wang et al., 2022), while feed-forward layers may be storing more general statistics such as the bigram “to the” or factual knowledge (Geva et al., 2021; Meng et al., 2022; Bietti et al., 2023). To further strengthen this observation, the recent work (Sharma et al., 2023) found that selectively replacing certain layer weights to their low-rank approximation, particularly late feed-forward layers, may improve performance on various reasoning benchmarks, and observed that the truncated components were often responsible for predicting “generic” tokens such as the word “the”.

In this paper, we provide a finer understanding of these phenomena by studying how such mechanisms arise during training, in particular how simple *distributional associations*, such as the bigram “to the”, tend to be localized in feed-forward layers, while attention focuses on in-context reasoning. We first provide a fine-grained study of training dynamics on a synthetic task with two-layer transformers

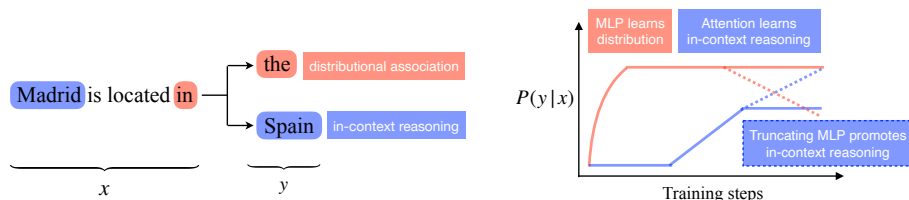


Figure 1: **Distributional association v.s. in-context reasoning.** In this work, we decompose tasks of next-token prediction into the distributional and the in-context ones, finding that MLPs learn distributional associations before attention develops in-context reasoning capabilities. Furthermore, truncating MLPs promotes in-context reasoning by weakening distributional associations. See Figure 5 for an example of this on the Pythia model (Biderman et al., 2023).

exhibiting similar properties, where the task is in-context recall (Bietti et al., 2023) with additional noise on in-context tokens consisting of a fixed “generic” token:

- In a two-layer model with feed-forward layers (FF), we show that the generic noise token is mainly learned in FF and the attention attends towards correct in-context targets. Removing the feed-forward layers then leads to clean in-context predictions. We provide some theoretical justification through early training steps.
- In a model without FF, we show that the generic noise can be identified in a rank-one subspace of the value matrix in attention block. When the noise level is small, low-rank truncation can filter it out and predict clean outputs.

We then investigate such a separation between distributional association and in-context reasoning on pre-trained language models, namely the Pythia family, which has checkpoints available at different training steps (Biderman et al., 2023). Overall, we provide a useful description of how distributional associations and in-context reasoning mechanisms are learned during training, and tend to be disentangled in different parts of the model, such that selectively removing certain components may lead to better predictions in reasoning tasks.

Related work. Sharma et al. (2023) recently empirically observed that a low-rank approximation of some weights in some pre-trained LLMs can improve reasoning capabilities. Several interpretability works have looked at the role of attention versus feed-forward layers for different tasks. The prominence of feed-forward/MLP layers for storing “global” or “persistent” associations or facts has been observed in (Sukhbaatar et al., 2019; Geva et al., 2021; Meng et al., 2022; Geva et al., 2023). In contrast, several works have investigated the role of attention heads for “reasoning” or computation over the context, *e.g.*, for simple copying mechanisms with so-called induction heads (Elhage et al., 2021; Olsson et al., 2022; Bietti et al., 2023), or for more complex tasks (Merrill et al., 2022; Wang et al., 2022; Zhang et al., 2022; Liu et al., 2023; Sanford et al., 2024b).

Training dynamics of transformers and attention have been studied in various works (Snell et al., 2021; Jelassi et al., 2022; Li et al., 2023; Oymak et al., 2023; Tian et al., 2023; Bietti et al., 2023; Reddy, 2024; Tian et al., 2024; Zhang et al., 2024; Nichani et al., 2024; Edelman et al., 2024). In particular, the two-layer model and copy task we consider are similar to Bietti et al. (2023), yet their data model does not involve noise on in-context predictions, and they do not study learning of global associations. Chan et al. (2022); Reddy (2024) study in-context vs. in-weights learning empirically, on different tasks than ours. Cabannes et al. (2024) study training dynamics of linear associative memories, but focuses on deterministic data while our setup has generic noise. Training dynamics were also studied empirically for interpretability (Olsson et al., 2022; Nanda et al., 2023; Quirke et al., 2023; Chen et al., 2024). Edelman et al. (2022); Bai et al. (2023); Abernethy et al. (2024) studied sample complexity of self-attention and in-context learning, but did not consider training dynamics.

2 PRELIMINARIES

In this section, we provide some background and motivation on reasoning tasks, and describe the weight truncation technique which we use for ablating weights.

2.1 REASONING FROM CONTEXT

Recent LLMs have shown promising results in more complex “reasoning” tasks which may involve multiple steps of logical or computational processing from context or prompt (Srivastava et al., 2022; Wei et al., 2022; Bubeck et al., 2023; Dziri et al., 2024), as opposed to simple pattern matching or memorization of training data, for instance using learned n-gram predictions.

While it is difficult to clearly separate reasoning from memorization, in this work we will make the simplifying distinction that **in-context reasoning** involves dependencies between *multiple tokens* potentially far away in the context, while we consider **distributional associations** as simpler predictions that only depend on the *last token*, e.g., through a bigram model. Thus, due to the residual structure of Transformers, reasoning will typically require using attention operations in Transformers over context, while feed-forward layers should suffice for learning distributional associations. We note that our assumption of distributional associations depending only on the last token is mainly for convenience of our analysis, and could be extended to depend on the last token’s *residual stream* (Elhage et al., 2021), which may contain additional information from the context. For instance, this could include previous tokens thanks to position-based attention heads (Voita et al., 2019; Elhage et al., 2021; Akyürek et al., 2024), which allows capturing n-grams instead of just bigrams.

Under this definition, we list a few simple examples of reasoning that we will consider below:

- *In-context recall*: when the last token is *a*, we’d like to copy the token that follows previous occurrences of *a* in the context. This $[\dots a b \dots a] \rightarrow b$ pattern typically requires a two-layer *induction head* mechanism (Elhage et al., 2021; Bietti et al., 2023; Sanford et al., 2024a);
- *Indirect object identification (IOI)*: we consider contexts of the form “When Mary and John went to the store, John gave the ice cream to” where the prediction should be “Mary” (IO, the indirect object), instead of “John” (S, the subject). Wang et al. (2022) found a circuit of several attention heads that perform this task by copying the name which only occurs once in the context;
- *Factual recall*: sentences of the form “Paul Citroen is a native speaker of” with target “Dutch” as in (Sharma et al., 2023). While this may be seen as retrieving a distributional association, we will treat it here as reasoning since it involves combining the subject and relation from the context, while a bigram model that only depends on the last token “of” might instead predict the generic word “the”.

2.2 TRUNCATING WEIGHTS WITH LASER (SHARMA ET AL., 2023)

In order to assess the importance of different weight components for certain predictions, we use the weight truncation technique introduced by Sharma et al. (2023). They observed that reducing the rank of MLP matrices in certain layers of LLMs effectively brings better performance on several reasoning benchmarks. Their proposed method, Layer-Selective Rank Reduction (LASER), replaces any matrix in the full model by its low-rank approximation with fraction ρ , *i.e.*, a matrix $\mathbf{W} \in \mathbb{R}^{d_{in}, d_{out}}$ would be replaced by its rank- $\lfloor \rho \cdot \min\{d_{in}, d_{out}\} \rfloor$ approximation via Singular Value Decomposition (SVD). After searching for the best parameters of different models on different datasets, Sharma et al. (2023) found that applying their method to weight matrices of MLPs on relatively deep layers can enhance in-context reasoning performance on various benchmarks, consistent with our findings. The optimal ρ is smaller than 0.2 for many datasets.

Another observation from Sharma et al. (2023) is that, when LASER improves the model’s prediction on some samples, the full model often predicts “generic” words while the improved model is able to predict the ground-truth answer. For instance, given an input “Madrid is located in”, the full

Table 1: Probabilities of the top-5 next-tokens in Pythia-1B before and after LASER. The input prompt is “Madrid is located in”. Probabilities of two generic words, *i.e.*, “the” and “a”, drop sharply after LASER, while probabilities of meaningful words increase, especially the target “Spain”.

	“the”	“Spain”	“a”	“southern”	“northern”
Full	0.499	0.079	0.069	0.023	0.021
LASER	0.027	0.300	0.002	0.044	0.046

model predicts “the” while the truncated model predicts the target “Spain” in Table 1. Here, the generic word is consistent with our definition of distributional associations in Section 2.1, as it may naturally follow from a bigram distribution conditioned on “in”, while the factual answer is more akin to reasoning from context. Thus, we would like to better understand how such a modification of feed-forward layers improves the model from predicting generic words to inferring the answer from context, and how such a gap appears during training.

3 TWO-LAYER TRANSFORMER ON NOISY IN-CONTEXT RECALL

In this section, we consider simple one- or two-layer transformers on an in-context recall task with added generic token noise, which allows us to study the trade-offs between MLPs and attention layers for storing in-context versus distributional associations, in a controlled setting. We empirically show how transformers solve this task by storing the generic noise token in feed-forward layers, while attention implements the in-context mechanism. We then provide theory showing that feed-forward layers are more likely to store the distributional association (generic token) while attention learns to attend to in-context targets. Finally, we show that when the model has no feed-forward layers, the value matrix in attention stores both in-context and distributional information, in different subspaces.

Data and task. The data model we consider is similar to Bietti et al. (2023), with additional noise. Consider a vocabulary $\mathcal{V} = \{1, 2, \dots, N, N + 1\}$. The token $\tau \triangleq N + 1$ is the generic noise token. We fix a *trigger* token $q \in [N]$, which governs in-context recall, and a context length T . Each sequence of tokens $z_{1:T} = [z_1, z_2, \dots, z_T]$ is generated as follows:

- i. Sample a correct *output* token \bar{y} uniformly in $[N]$.
- ii. Sample $z_{1:T-1}$ according to the following Markov process (π_u, π_b are distributions on $[N]$ defined later): $z_1 \sim \pi_u(\cdot)$, and

$$z_{t+1}|z_t \sim \begin{cases} \pi_b(\cdot|z_t), & \text{if } z_t \neq q, \\ p_{\alpha, \bar{y}}(\cdot), & \text{otherwise,} \end{cases} \quad p_{\alpha, \bar{y}}(x) = \begin{cases} 1 - \alpha, & \text{if } x = \bar{y}, \\ \alpha, & \text{if } x = \tau, \\ 0, & \text{otherwise.} \end{cases}$$

- iii. Set $z_T = q$, and sample the final output $y = z_{T+1} \sim p_{\alpha, \bar{y}}(\cdot)$.

Note that the true \bar{y} varies across sequences, so that the model needs to infer it from context, e.g., using an induction head as in (Bietti et al., 2023). Predicting \bar{y} may thus be seen as a basic “reasoning” task, yet when training with $\alpha > 0$, the noisy output also requires the model to learn a distributional trigger-noise association, similar to the “of/in the” bigram discussed in Section 2. We also consider using multiple trigger tokens in Appendix B.4 and Figure 9.

Two-layer transformer. We consider a simplified two-layer transformer formulated below. The input is a sequence of tokens $z_{1:T} = [z_1, \dots, z_T] \in [N + 1]^T$, and the output is ξ . The embedding matrix $\mathbf{W}_E \in \mathbb{R}^{(N+1) \times d}$ and un-embedding matrix $\mathbf{W}_U \in \mathbb{R}^{(N+1) \times d}$ are fixed at random initialization. The two attention layers have learnable weights $\mathbf{W}_{QK}^1, \mathbf{W}_V^1, \mathbf{W}_{QK}^2, \mathbf{W}_V^2 \in \mathbb{R}^{d \times d}$ with $\sigma(\cdot)$ the softmax on a vector. The two feed-forward layers F_1, F_2 are also learnable, and typically we set them as two-layer MLPs with ReLU activation. We will discuss different architectural choices of F_1, F_2 in Appendix B.5. We use the cross-entropy loss to predict $y = z_{T+1}$ from the logits $\xi_T \in \mathbb{R}^{N+1}$.

$$\begin{aligned} x_t &\triangleq \mathbf{W}_E(z_t) + p_t, \\ h_t^1 &\triangleq \sum_{s \leq t} [\sigma(x_t^\top \mathbf{W}_{QK}^1 x_{1:t})]_s \cdot \mathbf{W}_V^1 x_s, \\ x_t^1 &\triangleq x_t + h_t^1 + F_1(x_t + h_t^1), \\ h_t^2 &\triangleq \sum_{s \leq t} [\sigma(x_t^{1 \top} \mathbf{W}_{QK}^2 x_{1:t}^1)]_s \cdot \mathbf{W}_V^2 x_s^1, \\ x_t^2 &\triangleq x_t^1 + h_t^2 + F_2(x_t^1 + h_t^2), \\ \xi_t &\triangleq \mathbf{W}_U x_t^2. \end{aligned} \tag{1}$$

Experimental observations. Following Bietti et al. (2023), we take π_u and π_b to be the unigram and bigram character-level distributions estimated from the tiny Shakespeare dataset with $N = 65$. The model setup includes $d = 256$ and two-layer MLPs with ReLU for both F_1, F_2 . The training setup includes batch size as 512 and the context length $T = 256$. When evaluating trained models, we consider LASER on the input weight U_{in} of F_2 . We consider a noise level $\alpha = 0.5$ for training data

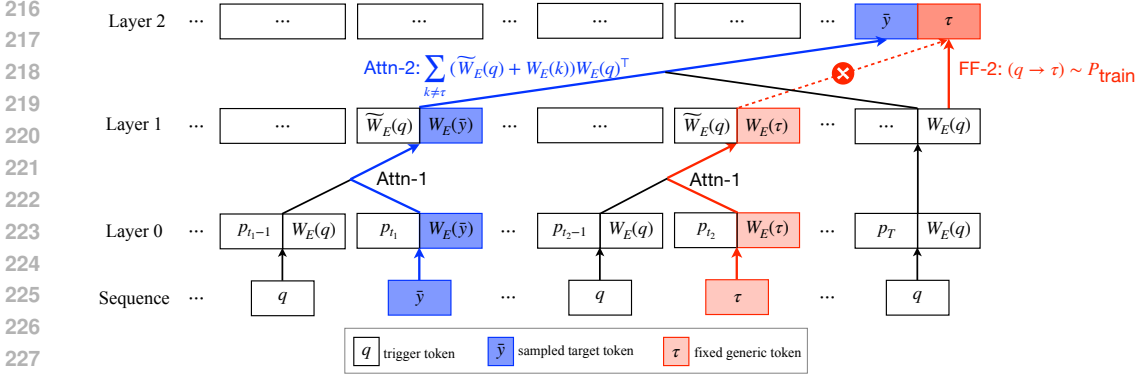


Figure 2: **Noisy in-context recall.** *Purpose of design:* understand mechanisms of attention and feed-forward layers for tasks with **in-context reasoning** (predict \bar{y}) and **distributional association** (predict τ). *Task:* predict tokens \bar{y} v.s. τ from a sentence $[\dots, q, \bar{y}, \dots, q, \tau, \dots, q]$ where q is trigger, \bar{y} is sampled target token for a sentence, and τ is a fixed generic token across sentences. *Our findings:* in a two-layer transformer, the second-layer attention (Attn-2) only attends towards target tuples $[q, \bar{y}]$ while the feed-forward layer (FF-2) learns to predict τ .

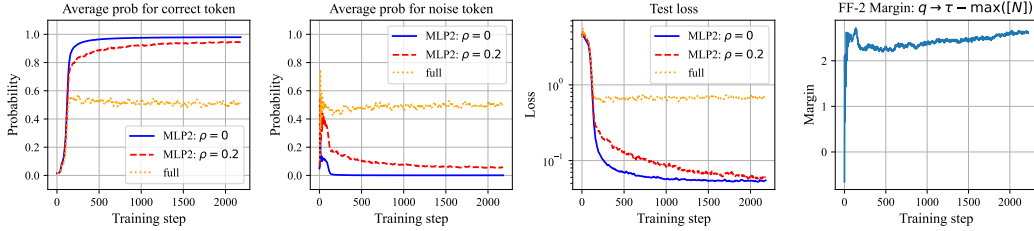


Figure 3: **Left three:** Average probability of predicting correct and noise tokens, and test loss on clean data ($\alpha = 0$), with different fractions ρ of preserved rank in U_{in} of the second-layer MLP F_2 . The full model learns to predict noise with probability around $\alpha = 0.5$, as expected from training data. When F_2 is dropped ($\rho = 0$), the model predicts the correct token \bar{y} with probability ≈ 0.98 . **Rightmost:** the FF-2 margin of τ v.s. all the other tokens with input as q , i.e., $[\mathbf{W}_U F_2(\mathbf{W}_E(q))]_{\tau} - \max_{k \leq N} [\mathbf{W}_U F_2(\mathbf{W}_E(q))]_k$. It reveals that FF-2 learns trigger-noise association in early steps.

(though any other constant value would lead to similar observations). During test time, we set $\alpha = 0$ to compute the test loss, aiming to measure how likely the (full or after-truncation) model predicts the ground-truth \bar{y} .

Experimental results are reported in Figure 3 and 8. The full model predicts noise with probability close to α , which is expected since it is trained to predict the noise token w.p. α . However, when dropping the second-layer MLP F_2 , the truncated model predicts the ground-truth \bar{y} with an almost perfect probability ≈ 0.98 . This suggests that F_2 is responsible for storing the distributional association “[trigger] + [noise]”. Another observation is that the full model first learns to predict the noise with high probability in very early steps, after which it starts learning to predict the correct \bar{y} , which resembles the dynamics observed for learning the “to/in the” bigram in Pythia models in Figure 5. This suggests that learning the (distributional) trigger-noise association is easier than predicting \bar{y} , and we will study this theoretically in Section 3.1.

After the distributional noise association is learned, we observe a slower learning of an induction head mechanism, with similar dynamics to Bietti et al. (2023). Compared to Bietti et al. (2023), we notice that the induction head (i.e., the second layer attention head) filters out the noise tokens and only attends to non-noisy output tokens following the trigger, corresponding to the correct \bar{y} , as

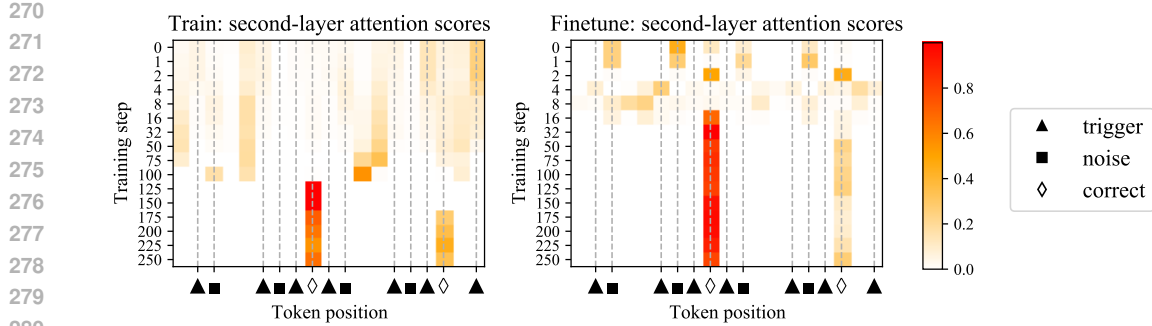


Figure 4: The second-layer attention scores of models trained with noise (left), fine-tuned with noise (right, initialized as a model pre-trained without noise), given the same input. It turns out both models learn to attend to the informative structure “[trigger]+ \bar{y} ” instead of “[trigger]+noise”. This implies that the attention in these models is only responsible to predict \bar{y} , although the training input and output have noise with probability $\alpha = \Theta(1)$. The fine-tuning setting is in Appendix B.1.

shown in Figure 4. We present theoretical understanding for this mechanism in Section 3.2. Figure 2 and Appendix B.2 summarize the roles of all components of the two-layer transformer in this task.

Simplified architecture and data for theoretical analysis. Understanding the full dynamics of the model used in our experiments is out of the scope of the present paper, due to the many moving parts and the complexity of non-linear MLPs. Instead, we focus on a simpler model involving one linear feed-forward layer and one attention layer, and look at the gradient dynamics near initialization. We consider the following simplified 1-layer model. The input $x_t \in \mathbb{R}^d$ at position t is defined as $x_t \triangleq \mathbf{W}_E(z_t) + \widetilde{\mathbf{W}}_E(z_{t-1})$, where $z_t \in [N+1]$ is the token at position t , $\mathbf{W}_E(z_t)$ is its embedding and $\widetilde{\mathbf{W}}_E(z_{t-1})$ is a different embedding of the previous token to a different direction, as in the *previous token head* construction of Bietti et al. (2023), where the value matrix remaps the previous token to a different subspace. We assume all embeddings to be orthogonal (Assumption D.1), which requires large enough d , and holds in the infinite-width limit with random embeddings. This model allows us to simplify our analysis by considering a single attention layer with no positional embeddings, while capturing the difficulty of long-range interactions. We note that such a simplification is standard in the in-context learning literature (e.g., Akyürek et al., 2023; Mahankali et al., 2024; Zhang et al., 2024). For data generation, π_u and π_b are uniform distributions on $[N]$. Given a sequence of inputs, $x_{1:T} \in \mathbb{R}^{T \times d}$, the output of model is $\xi \triangleq \xi_{\text{attn}} + \xi_{\text{ff}}$ as

$$\begin{aligned}
 x_t &\triangleq \mathbf{W}_E(z_t) + \widetilde{\mathbf{W}}_E(z_{t-1}) \in \mathbb{R}^d, \\
 \phi(x_T, x_{1:T}) &\triangleq \sum_{t \leq T} [\sigma(x_T^\top \mathbf{W}_{QK} x_{1:T})]_t \cdot \mathbf{W}_V x_t \in \mathbb{R}^d, \\
 \xi_{\text{attn}}(x_{1:T}) &\triangleq \mathbf{W}_U \phi(x_T, x_{1:T}) \in \mathbb{R}^{N+1}, \\
 \xi_{\text{ff}}(x_{1:T}) &\triangleq \mathbf{W}_U F(x_T) = \mathbf{W}_U \mathbf{W}_F x_T \in \mathbb{R}^{N+1},
 \end{aligned} \tag{2}$$

where $\mathbf{W}_U \in \mathbb{R}^{(N+1) \times d}$ is the unembedding matrix, $\phi(s, t)$ is the attention module with query s and context t , and $F(\cdot)$ is a linear feed-forward layer. This architecture is similar to a one-layer transformer, but already highlights the difference between feed-forward and attention layers in a way that we expect to still hold for more layers. In the above parametrization, the learnable matrices are $\mathbf{W}_{QK}, \mathbf{W}_F, \mathbf{W}_V \in \mathbb{R}^{d \times d}$. At initialization, we set $\mathbf{W}_{QK}, \mathbf{W}_F, \mathbf{W}_V = 0$, noting that random initialization in high dimension would lead to similar behaviors thanks to near-orthogonality.

3.1 FEED-FORWARD LAYERS STORE THE GENERIC NOISE

As we saw in Figure 3 and 8, the model very quickly learns to predict the noise token after a few steps. Then the gap between $\rho = 0$ and 1 in Figure 3 suggests that the feed-forward layer F_2 is responsible for storing the distributional association about noise, which is verified in Figure 7 (middle). We now provide theoretical justification for this behavior. In particular, we will show that, at initialization, the

gradients over the feed-forward parameters are much more informative than the attention gradient, which is dominated by noise unless the sample size is very large. This shows that the feed-forward layer is much more likely to capture the distributional association.

We now look at the first gradient step from initialization, which has commonly been used to understand feature learning and sample complexity in neural networks (Damian et al., 2022; Ba et al., 2022; Dandi et al., 2023; Oymak et al., 2023; Bietti et al., 2023). Note that \mathbf{W}_{QK} has no gradient at initialization, so that the gradient of \mathbf{W}_V is most relevant initially (see also Snell et al., 2021; Li et al., 2023; Oymak et al., 2023; Bietti et al., 2023).

Theorem 1 (Logits after one gradient step). *Assume $N, T \gg 1, \alpha = \Theta(1)$. For the model in Eq(2), consider one gradient step update from zero-initialization on m i.i.d. samples of $z_{1:T}$ with separate learning rates η_f for \mathbf{W}_F and η_v for \mathbf{W}_V (note that the gradient on \mathbf{W}_{QK} is zero). With probability $1 - \delta$, the resulting logits for the feed-forward and attention blocks satisfy, for any test sequence $z_{1:T}$,*

$$\begin{aligned} |\Delta(\xi_{ff}(x_{1:T})) - \eta_f \cdot \alpha| &\leq \eta_f \cdot O\left(\sqrt{\frac{\ln \frac{2(N+1)}{\delta}}{m}}\right), \\ \left|\Delta(\xi_{att}(x_{1:T})) - \frac{\eta_v}{N} \cdot \hat{\alpha}\right| &\leq \eta_v \cdot O\left(\sqrt{\frac{(\frac{1}{TN} + \frac{1}{N^2}) \ln \frac{2(N+1)}{\delta}}{m}} + \frac{\ln \frac{2(N+1)}{\delta}}{m}\right), \end{aligned}$$

where $\Delta(\xi) = \xi_{N+1} - \max_{j \in [N]} \xi_j$ is the margin of predicting the generic noise token and $\hat{\alpha} = (\alpha^2 \hat{q} + \alpha(1 - \hat{q}))$, where $\hat{q} = \frac{1}{T} \sum_{t \leq T} \mathbb{1}\{z_t = N + 1\}$ is the fraction of noise tokens in $z_{1:T}$.

The margin $\Delta(\xi)$ reflects how much signal there is in the logits for predicting the noise token, and the theorem provides concentration bounds on the contributions of the updates on \mathbf{W}_F and \mathbf{W}_V to the margin. Note that $\hat{q} \ll 1$ w.h.p. for large N, T , so $\hat{\alpha} \approx \alpha$. We make the following observations:

- i. When $m = \tilde{\Omega}(1)$, there is enough signal in \mathbf{W}_F to predict the noise, say with $\eta_f = 1$, and a choice of $\eta_v = O(1)$ will lead to a small but controlled contribution to the prediction from \mathbf{W}_V .
- ii. When $m = \tilde{\Omega}(N)$, \mathbf{W}_V can also reliably predict the noise by setting $\eta_v = \Theta(N)$ (i.e., with small deviation on the r.h.s.), at the cost of many more samples.

Our result shows that in the initial phase of training, feed-forward layers are more likely to pick up the noise token, leading to a structure of the form $\mathbf{W}_F \approx \mathbf{W}_U(N + 1)\mathbf{W}_E(q)^\top$, while attention will be slower due to additional noise and possibly smaller step-sizes. We may then expect the attention layers to focus instead on in-context reasoning, as we observe empirically and discuss next.

3.2 ATTENTION ATTENDS TO IN-CONTEXT TARGETS AND AVOIDS NOISE

When the feed-forward weight learns to predict the noise as shown in Theorem 1, Figure 4 reveals that the second-layer attention in the two-layer model attends only towards the correct tokens. In contrast, a model pre-trained without noise has second-layer attention attend towards all tokens just after the triggers (Bietti et al., 2023), as observed in the attention pattern at the first step in Figure 4(right). Then, after being fine-tuned on noise data, the attention becomes only focused on the correct tokens. Understanding this mechanism requires the analysis of the dynamics of \mathbf{W}_{QK} .

Following the simplified model and data distribution in Eq(2), we take a step towards understanding how attention ‘‘avoids’’ the noise tokens. Concretely, this mechanism appears because, after the initial training phase when FF learns noise association much faster than the attention, \mathbf{W}_V has a structure of $\sum_{k \leq N+1} \mathbf{W}_U(k)(\mathbf{W}_E(k) + \tilde{\mathbf{W}}_E(k))^\top$, similar to the non-noise setting in Bietti et al. (2023). After such a \mathbf{W}_V is learned, the trigger-label association provides a stronger gradient signal on \mathbf{W}_{QK} than the trigger-noise association. We show this in the following theorem.

Theorem 2 (Attention attends to in-context targets). *Assume $N, T \gg 1$ and Assumption F.1 hold. Consider the simplified model in Eq(2) with infinite samples as $m \rightarrow \infty$. After \mathbf{W}_F learns the noise association as in Theorem 1, in one step the attention weight \mathbf{W}_{QK} learns to attend to positions $t \in [T]$ where the correct label follows a trigger word, i.e., $z_{t-1} = q, z_t = \bar{y}$.*

378 *More concretely, \mathbf{W}_{QK} has the following structure*

$$379 \xi_{q \rightarrow j} - \xi_{q \rightarrow N+1} = \Omega(N^{-4}) > 0, \quad \forall j \leq N, \\ 380 \xi_{q \rightarrow j} - \xi_{k \rightarrow l} = \Omega(N^{-3}) > 0, \quad \text{if } k \neq q, \forall j, l, \\ 381 \\ 382$$

383 where $\xi_{i \rightarrow j} \triangleq \mathbf{W}_E(q)^\top \mathbf{W}_{QK}(\widetilde{\mathbf{W}}_E(i) + \mathbf{W}_E(j))$ denotes the attention logit for different combina-
384 tions of $z_{t-1} = i, z_t = j$, with $i, j \leq N + 1$.
385

386 Note that a set of logits induces a probability distribution via differences between them as
387 $\exp(\xi_i) / \sum_j \exp(\xi_j) = 1 / \sum_j \exp(\xi_j - \xi_i)$. Therefore, the above theorem reveals that the at-
388 tention has two patterns: i) \mathbf{W}_{QK} attends to indices with the trigger q as the previous token, which
389 is $z_{t-1} = q$, the same as Bietti et al. (2023), and ii) among all indices following q , \mathbf{W}_{QK} pays less
390 attention to the noise, *i.e.*, $z_t = N + 1$ than correct tokens $z_t = \bar{y} \leq N$. Such a key difference for
391 attention between noisy and non-noise tasks verifies our experimental observations in Figure 4.
392

393 3.3 NO FEED-FORWARD LAYERS: VALUE MATRIX STORES GENERIC NOISE ASSOCIATION

394 In the above discussion, we’ve seen separate roles of attention and feed-forward layers play to
395 conduct noisy in-context learning. A natural question is, when there is *no feed-forward layer*, how
396 the attention layer stores both in-context and distributional information. Figure 13 indicates that the
397 value matrix stores the noise association in subspace with smaller singular values. In this section, we
398 propose a setting of *linear associative memory with noise* to understand this mechanism.
399

400 Unlike Theorem 1 and 2 showing the separate roles of attention and FF, the attention in a non-FF
401 model has to handle both noise and in-context information once the model is sufficiently trained to
402 reach a global minimum. Due to symmetry from uniformly random sampling \bar{y} from N tokens, we
403 consider passing the output $x \in \mathbb{R}^d$ of the attention to the value matrix \mathbf{W}_V and output matrix \mathbf{W}_U
404 to predict next-token probability $y \in \mathbb{R}^{N+1}$ given $z_{1:T} \in [N + 1]^T$ with noise probability of α as
405 follows

$$405 x|\bar{y}, z_{1:T} \triangleq \mathbf{W}_E(\bar{y}) + \overline{\mathbf{W}}(z_{1:T}) \in \mathbb{R}^d, \quad \xi \triangleq \mathbf{W}_U \mathbf{W}_V x \in \mathbb{R}^{N+1}, \\ 406 p_\alpha(y|\bar{y}) = (1 - \alpha) \cdot \mathbb{1}\{y = \bar{y}\} + \alpha \cdot \mathbb{1}\{y = N + 1\}, \quad (3) \\ 407$$

408 where $\overline{\mathbf{W}}(z_{1:T})$ is an aggregate embedding independent of \bar{y} . When $T \rightarrow \infty$, $\overline{\mathbf{W}}(z_{1:T})$ converges
409 to a fixed embedding $\overline{\mathbf{W}}$ independent of \bar{y} , so that we may consider a simplified model $x|\bar{y} \triangleq$
410 $\mathbf{W}_E(\bar{y}), \xi \triangleq \mathbf{W}x \in \mathbb{R}^{N+1}$ with $\mathbf{W} \in \mathbb{R}^{(N+1) \times d}$, since $\overline{\mathbf{W}}$ only contributes a fixed offset in all
411 logits that can be easily canceled in the softmax predictions. Therefore, we investigate the following
412 *linear associative memory with noise*.

413 **Model and data.** Consider a learnable weight matrix $\mathbf{W} \in \mathbb{R}^{d \times d}$ with $d > N$. Consider embeddings
414 for N input tokens as $\{e_i\}_{i=1}^N \subset \mathbb{R}^d$ and embeddings for $(N + 1)$ output tokens as $\{u_i\}_{i=1}^{N+1} \subset$
415 \mathbb{R}^d . Given any pair of input and output tokens, the associative memory model takes the form
416 $f(i, j; \mathbf{W}) \triangleq \langle u_j, \mathbf{W}e_i \rangle, \forall i, j \in [N] \times [N + 1]$, as logits to approximate $p_\alpha(\cdot|i)$ in (3). When
417 $k \leq d$, we denote the rank- k approximation of f as $f^{(k)}$ by replacing \mathbf{W} with $\mathbf{W}^{(k)}$, where $\mathbf{W}^{(k)}$ is
418 its rank- k approximation.

419 **Experiments.** During training, the dataset \mathcal{D}_α is generated with non-zero noise probability $\alpha > 0$.
420 At test time, the dataset \mathcal{D}_0 is without noise as $\alpha = 0$, so the computed loss is called **pure-label** loss.
421 The *full* model is trained with Gradient Descent (GD) subjected to cross-entropy loss. The results are
422 reported in Figure 18, with more discussions in Appendix G.1.
423

424 **Low-rank subspace stores noise.** In Figure 18, the rank-1 subspace corresponding to the smallest
425 non-zero singular value is responsible to store the noise. We prove this mechanism as follows. Note
426 that, here $N = 2$ is for simplicity, which is easy to extend to any $N > 2$.

427 **Theorem 3.** Assume Assumptions G.1 and G.2 hold, considering $N = 2$ and $\alpha \in (0.2, 0.4)$, we train
428 the full model $f(\cdot, \cdot; \mathbf{W})$ with gradient flow. Denote $P(i, j; \mathbf{W})$ as the model’s predicted probability
429 for output j conditioned on input i . Then, for $t \rightarrow \infty$ and $i \in \{1, 2\}$, we have

$$430 P(i, j; \mathbf{W}) = (1 - \alpha) \cdot \mathbb{1}\{j = i\} + \alpha \cdot \mathbb{1}\{j = N + 1\}, \\ 431 P(i, j; \mathbf{W}^{(1)}) = (1 - \Theta(t^{-1/2})) \cdot \mathbb{1}\{j = i\} + \Theta(t^{-1/2}) \cdot \mathbb{1}\{j = N + 1\}.$$

The above theorem implies, the full model always predicts noise w.p. α , while the rank-1 model eventually predicts correctly without noise, although training is only on the full model with noise. Actually when $N > 2$, the noise is stored in rank-1 subspace and the correct correspondence is stored in rank- $(N - 1)$ space. Therefore, this explains how the value matrix stores both in-context and noise information when the model is without FF.

4 EXPERIMENTS

In this section, we empirically investigate how LLMs process distributional vs in-context associations, and how this evolves during training. Meanwhile, we provide numerical results of how much low-rank truncation improves complex reasoning on a real-world reasoning benchmark, GSM8K.

4.1 AN INVESTIGATION ON GPT-2 SMALL AND PYTHIA MODELS

We consider GPT-2 small and Pythia models on the indirect object identification (IOI) and factual recall tasks described in Section 2.1.

Quick demonstration: IOI on GPT2 Small. Different from Wang et al. (2022), we would like to consider whether a model proposes an output beyond the input x . A quick demonstration is to consider the IOI task with input $x =$ “When Mary and John went to a store, John gave a drink to”¹. The top 4 predicted tokens for GPT-2 Small (Radford et al., 2019) on x are [“Mary”, “them”, “the”, “John”]. Although GPT-2 Small successfully predicts Mary (the IO target) instead of John (S), the other two top candidate tokens, *i.e.*, “them” and “the”, do not even appear in the context. This prominence of such “generic” words is similar to the factual recall example from Section 2.2, and plausibly follows from a distributional associative mechanism conditioned on the preposition “to”.

Comprehensive experiment: IOI on Pythia-1B. Now we would like to verify this observation on more models and, more comprehensively, track the behavior of these models along training. We choose to conduct the IOI experiments on Pythia (Biderman et al., 2023), a family of models ranging in sizes from 14M to 12B trained on web data, with hundreds of training checkpoints for each size. We generate an IOI dataset of 100 sentences with random names for [IO] and [S] in each sample. Figure 5 reports the test results of Pythia-1B along training. Here LASER is conducted on MLP weights, with parameters given in Appendix C.2. LASER boosts the probability ratio of [IO] over “the” from $2.3\times$ to $12.3\times$ at 14K steps.

Factual recall on Pythia-1B. As in Table 1, we verify factual recall with input as “Madrid is located in”. The full model of Pythia-1B generates “Madrid is located in the north of Spain”, while the model after LASER generates “Madrid is located in Spain”. We track the probability of predicting “Spain” and “the” along training in Figure 5. LASER turns out to boost the probability ratio of “Spain” over “the” from $0.16\times$ to $11.3\times$ at 14K steps. We note that better prompting could avoid the need for LASER in this case (e.g., “Madrid is located in the country of” predicts “Spain”), but increases the context length and thus the inference cost, though this is outside the scope of this paper.

Training dynamics on Pythia. The behavior of the Pythia models on the IOI and factual recall tasks during their pre-training process displays several phases, as shown in Figure 5. For IOI, we observe:

- i. Initialization: all tokens have similar logits since the weights are random initialized.
- ii. Between 10 and 1000 steps: the models consistently output “the”. They cannot solve IOI task at all, as long as they have almost the same prediction for [IO] and [S]. After 500 steps, [IO] starts the growth towards one of the top predictions.
- iii. After 2000 steps: Pythia starts to be able to solve IOI task by preferring [IO] than [S] and “the”. Meanwhile, the benefit of LASER appears as enhancing the leading position of [IO].

Therefore, the training process reveals the capacity of predicting “the” is learnt much earlier than predicting [IO]. The reason might be that predicting “the” requires a simpler grammar structure, while predicting [IO] requires a complicated architecture of attention heads of different roles across layer (Wang et al., 2022). Then we note that the IOI task always has “to” before the masked [IO], which means “to” may be an indicator for the model to predict “the” with non-negligible probability.

¹Note that here we use “a” store instead of “the” store in the original example of Wang et al. (2022). The reason is to rule out the word “the” from the input context.

486
487
488
489
490
491
492
493
494
495
496
497
498
499
500
501
502
503
504
505
506
507
508
509
510
511
512
513
514
515
516
517
518
519
520
521
522
523
524
525
526
527
528
529
530
531
532
533
534
535
536
537
538
539

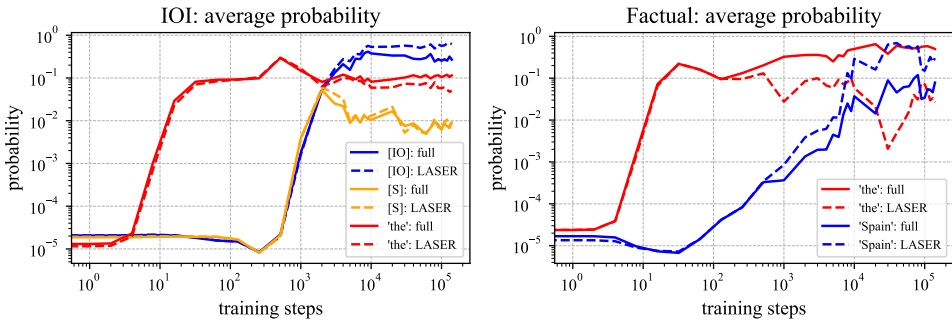


Figure 5: **Left:** average probability of tokens [IO], [S] and “the” in 100-sentence IOI task in the prediction by Pythia-1B along training. **Right:** average probability of tokens “Spain” and “the” in a factual task predicted by Pythia-1B along training, with input as “Madrid is located in”. In both tasks, the full model learns to predict “the” with high probability starting from ~ 10 steps, and then learns to solve the tasks. LASER boosts the probability of correct answers against “the” in both tasks: the average probability ratio of correct answers against “the” improves from $2.3\times$ to $12.3\times$ (in IOI) and from $0.16\times$ to $11.3\times$ (in factual) at 14K steps.

Similarly, for factual recall we see early learning of the “generic” answer, while the factual answer is learned later. Conceptually, if LLMs are able to write natural text or have been trained sufficiently with natural texts, it is not surprising for the model to predict “the” with high probability after seeing “to”. This is verified in Appendix C.1.

4.2 THE EFFECT OF TRUNCATING FEED-FORWARD LAYERS ON GSM8K

As our previous examples of in-context reasoning tasks are too simple for real-world reasoning, we verify whether truncating MLPs improves reasoning on the GSM8K benchmark (Cobbe et al., 2021). As shown in Table 2, LASER improves the few-shot Chain-of-Thought (Wei et al., 2022) reasoning performance on GSM8K when only using 1 or 2 shots, although the performance is worse in the standard 8-shot setting. This suggests that truncating MLPs may help promote in-context reasoning even in more complex settings, perhaps by removing spurious distributional associations.

Table 2: Few-shot accuracy (%) of pretrained and finetuned language models on GSM8K. Truncating MLPs (LASER) improves reasoning performances in few-shot CoT settings while it has worse performance in the standard 8-shot setting. The LASER hyper-parameters are in Appendix C.2.

	1-shot	2-shot	4-shot	8-shot (standard)
Phi-3 (Abdin et al., 2024)	56.0	72.2	78.2	82.7
Phi-3 + LASER	66.1	74.4	77.0	82.3
Llama-3.1-8B (AI@Meta, 2024)	44.7	50.0	57.6	56.0
Llama-3.1-8B + LASER	46.1	50.7	55.9	53.8
Llama-3.1-8B-Instruct (AI@Meta, 2024)	72.6	74.7	78.5	79.7
Llama-3.1-8B-Instruct + LASER	73.6	75.6	77.7	77.0

5 DISCUSSION AND LIMITATIONS

In this paper, we studied the questions of how transformer language models learn to process distributional associations differently than in-context inputs, and how truncating specific weights or layers, particularly feed-forward layers, can help in-context reasoning. While our work provides some initial theoretical understanding of how this may arise on simple controlled settings, it would be interesting to study how these ideas may extend to more complex tasks where in-context reasoning and distributional knowledge interact in more intricate ways.

REFERENCES

- 540
541
542 Marah Abdin, Sam Ade Jacobs, Ammar Ahmad Awan, Jyoti Aneja, Ahmed Awadallah, Hany
543 Awadalla, Nguyen Bach, Amit Bahree, Arash Bakhtiari, Harkirat Behl, et al. Phi-3 technical report:
544 A highly capable language model locally on your phone. *arXiv preprint arXiv:2404.14219*, 2024.
- 545 Jacob Abernethy, Alekh Agarwal, Teodor Vanislavov Marinov, and Manfred K Warmuth. A mecha-
546 nism for sample-efficient in-context learning for sparse retrieval tasks. In *International Conference*
547 *on Algorithmic Learning Theory*, 2024.
- 548 AI@Meta. Llama 3 model card. 2024. URL [https://github.com/meta-llama/llama3/
549 blob/main/MODEL_CARD.md](https://github.com/meta-llama/llama3/blob/main/MODEL_CARD.md).
- 551 Ekin Akyürek, Dale Schuurmans, Jacob Andreas, Tengyu Ma, and Denny Zhou. What learning
552 algorithm is in-context learning? investigations with linear models. In *International Conference*
553 *on Learning Representations (ICLR)*, 2023.
- 554 Ekin Akyürek, Bailin Wang, Yoon Kim, and Jacob Andreas. In-context language learning: Architec-
555 tures and algorithms. *arXiv preprint arXiv:2401.12973*, 2024.
- 556 AI Anthropic. The claude 3 model family: Opus, sonnet, haiku. *Claude-3 Model Card*, 2024.
- 557 Jimmy Ba, Murat A Erdogdu, Taiji Suzuki, Zhichao Wang, Denny Wu, and Greg Yang. High-
558 dimensional asymptotics of feature learning: How one gradient step improves the representation.
559 *Advances in Neural Information Processing Systems*, 2022.
- 560 Yu Bai, Fan Chen, Huan Wang, Caiming Xiong, and Song Mei. Transformers as statisticians:
561 Provable in-context learning with in-context algorithm selection. *Advances in neural information*
562 *processing systems*, 2023.
- 563 Stella Biderman, Hailey Schoelkopf, Quentin Gregory Anthony, Herbie Bradley, Kyle O’Brien, Eric
564 Hallahan, Mohammad Aflah Khan, Shivanshu Purohit, USVSN Sai Prashanth, Edward Raff, et al.
565 Pythia: A suite for analyzing large language models across training and scaling. In *International*
566 *Conference on Machine Learning*, pages 2397–2430. PMLR, 2023.
- 567 Alberto Bietti, Vivien Cabannes, Diane Bouchacourt, Herve Jegou, and Leon Bottou. Birth of a
568 transformer: A memory viewpoint. *Advances in Neural Information Processing Systems*, 2023.
- 569 Tom Brown, Benjamin Mann, Nick Ryder, Melanie Subbiah, Jared D Kaplan, Prafulla Dhariwal,
570 Arvind Neelakantan, Pranav Shyam, Girish Sastry, Amanda Askell, et al. Language models are
571 few-shot learners. In *Advances in Neural Information Processing Systems*, 2020.
- 572 Sébastien Bubeck, Varun Chandrasekaran, Ronen Eldan, Johannes Gehrke, Eric Horvitz, Ece Kamar,
573 Peter Lee, Yin Tat Lee, Yuanzhi Li, Scott Lundberg, et al. Sparks of artificial general intelligence:
574 Early experiments with gpt-4. *arXiv preprint arXiv:2303.12712*, 2023.
- 575 Vivien Cabannes, Berfin Simsek, and Alberto Bietti. Learning associative memories with gradient
576 descent. *arXiv preprint arXiv:2402.18724*, 2024.
- 577 Stephanie Chan, Adam Santoro, Andrew Lampinen, Jane Wang, Aaditya Singh, Pierre Richemond,
578 James McClelland, and Felix Hill. Data distributional properties drive emergent in-context learning
579 in transformers. 2022.
- 580 Angelica Chen, Ravid Schwartz-Ziv, Kyunghyun Cho, Matthew L Leavitt, and Naomi Saphra.
581 Sudden drops in the loss: Syntax acquisition, phase transitions, and simplicity bias in mlms. In
582 *International Conference on Learning Representations*, 2024.
- 583 Karl Cobbe, Vineet Kosaraju, Mohammad Bavarian, Mark Chen, Heewoo Jun, Lukasz Kaiser,
584 Matthias Plappert, Jerry Tworek, Jacob Hilton, Reiichiro Nakano, Christopher Hesse, and John
585 Schulman. Training verifiers to solve math word problems. *arXiv preprint arXiv:2110.14168*,
586 2021.
- 587 Alexandru Damian, Jason Lee, and Mahdi Soltanolkotabi. Neural networks can learn representations
588 with gradient descent. In *Conference on Learning Theory*, 2022.

- 594 Yatin Dandi, Florent Krzakala, Bruno Loureiro, Luca Pesce, and Ludovic Stephan. Learning two-layer
595 neural networks, one (giant) step at a time. *arXiv preprint arXiv:2305.18270*, 2023.
596
- 597 Nouha Dziri, Ximing Lu, Melanie Sclar, Xiang Lorraine Li, Liwei Jiang, Bill Yuchen Lin, Sean
598 Welleck, Peter West, Chandra Bhagavatula, Ronan Le Bras, et al. Faith and fate: Limits of
599 transformers on compositionality. *Advances in Neural Information Processing Systems*, 2024.
- 600 Benjamin L Edelman, Surbhi Goel, Sham Kakade, and Cyril Zhang. Inductive biases and variable
601 creation in self-attention mechanisms. In *International Conference on Machine Learning*, 2022.
602
- 603 Benjamin L Edelman, Ezra Edelman, Surbhi Goel, Eran Malach, and Nikolaos Tsilivis. The evolution
604 of statistical induction heads: In-context learning markov chains. *arXiv preprint arXiv:2402.11004*,
605 2024.
- 606 Nelson Elhage, Neel Nanda, Catherine Olsson, Tom Henighan, Nicholas Joseph, Ben Mann, Amanda
607 Askell, Yuntao Bai, Anna Chen, Tom Conerly, Nova DasSarma, Dawn Drain, Deep Ganguli, Zac
608 Hatfield-Dodds, Danny Hernandez, Andy Jones, Jackson Kernion, Liane Lovitt, Kamal Ndousse,
609 Dario Amodei, Tom Brown, Jack Clark, Jared Kaplan, Sam McCandlish, and Chris Olah. A
610 mathematical framework for transformer circuits. *Transformer Circuits Thread*, 2021.
611
- 612 Mor Geva, Roei Schuster, Jonathan Berant, and Omer Levy. Transformer feed-forward layers are
613 key-value memories. In *Conference on Empirical Methods in Natural Language Processing*
614 (*EMNLP*), 2021.
- 615 Mor Geva, Jasmijn Bastings, Katja Filippova, and Amir Globerson. Dissecting recall of factual
616 associations in auto-regressive language models. In *Conference on Empirical Methods in Natural*
617 *Language Processing (EMNLP)*, 2023.
- 618 Samy Jelassi, Michael Sander, and Yuanzhi Li. Vision transformers provably learn spatial structure.
619 In *Advances in Neural Information Processing Systems*, 2022.
620
- 621 Diederik P Kingma. Adam: A method for stochastic optimization. *arXiv preprint arXiv:1412.6980*,
622 2014.
- 623 Yuchen Li, Yuanzhi Li, and Andrej Risteski. How do transformers learn topic structure: Towards a
624 mechanistic understanding. In *International Conference on Machine Learning*, 2023.
625
- 626 Bingbin Liu, Jordan T Ash, Surbhi Goel, Akshay Krishnamurthy, and Cyril Zhang. Transformers
627 learn shortcuts to automata. In *International Conference on Learning Representations*, 2023.
628
- 629 Arvind Mahankali, Tatsunori B Hashimoto, and Tengyu Ma. One step of gradient descent is provably
630 the optimal in-context learner with one layer of linear self-attention. In *International Conference*
631 *on Learning Representations (ICLR)*, 2024.
- 632 Kevin Meng, David Bau, Alex Andonian, and Yonatan Belinkov. Locating and editing factual
633 associations in gpt. *Advances in Neural Information Processing Systems*, 2022.
634
- 635 William Merrill, Ashish Sabharwal, and Noah A Smith. Saturated transformers are constant-depth
636 threshold circuits. *Transactions of the Association for Computational Linguistics*, 10:843–856,
637 2022.
- 638 Neel Nanda, Lawrence Chan, Tom Liberum, Jess Smith, and Jacob Steinhardt. Progress measures for
639 grokking via mechanistic interpretability. In *International Conference on Learning Representations*,
640 2023.
- 641 Eshaan Nichani, Alex Damian, and Jason D Lee. How transformers learn causal structure with
642 gradient descent. In *International Conference on Learning Representations*, 2024.
643
- 644 Catherine Olsson, Nelson Elhage, Neel Nanda, Nicholas Joseph, Nova DasSarma, Tom Henighan,
645 Ben Mann, Amanda Askell, Yuntao Bai, Anna Chen, Tom Conerly, Dawn Drain, Deep Ganguli,
646 Zac Hatfield-Dodds, Danny Hernandez, Scott Johnston, Andy Jones, Jackson Kernion, Liane
647 Lovitt, Kamal Ndousse, Dario Amodei, Tom Brown, Jack Clark, Jared Kaplan, Sam McCandlish,
and Chris Olah. In-context learning and induction heads. *Transformer Circuits Thread*, 2022.

- 648 Samet Oymak, Ankit Singh Rawat, Mahdi Soltanolkotabi, and Christos Thrampoulidis. On the role
649 of attention in prompt-tuning. In *International Conference on Machine Learning*, 2023.
- 650
651 Lucia Quirke, Lovis Heindrich, Wes Gurnee, and Neel Nanda. Training dynamics of contextual
652 n-grams in language models. *arXiv preprint arXiv:2311.00863*, 2023.
- 653 Alec Radford, Jeffrey Wu, Rewon Child, David Luan, Dario Amodei, Ilya Sutskever, et al. Language
654 models are unsupervised multitask learners. *Technical report, OpenAI*, 2019.
- 655
656 Gautam Reddy. The mechanistic basis of data dependence and abrupt learning in an in-context
657 classification task. In *International Conference on Learning Representations*, 2024.
- 658 Clayton Sanford, Daniel Hsu, and Matus Telgarsky. One-layer transformers fail to solve the induction
659 heads task. *arXiv preprint arXiv:2408.14332*, 2024a.
- 660
661 Clayton Sanford, Daniel Hsu, and Matus Telgarsky. Transformers, parallel computation, and logarithmic
662 depth. *arXiv preprint arXiv:2402.09268*, 2024b.
- 663 Pratyusha Sharma, Jordan T Ash, and Dipendra Misra. The truth is in there: Improving reasoning in
664 language models with layer-selective rank reduction. *arXiv preprint arXiv:2312.13558*, 2023.
- 665
666 Charlie Snell, Ruiqi Zhong, Dan Klein, and Jacob Steinhardt. Approximating how single head
667 attention learns. *arXiv preprint arXiv:2103.07601*, 2021.
- 668 Aarohi Srivastava, Abhinav Rastogi, Abhishek Rao, Abu Awal Md Shoeb, Abubakar Abid, Adam
669 Fisch, Adam R Brown, Adam Santoro, Aditya Gupta, Adrià Garriga-Alonso, et al. Beyond the
670 imitation game: Quantifying and extrapolating the capabilities of language models. *arXiv preprint
671 arXiv:2206.04615*, 2022.
- 672 Sainbayar Sukhbaatar, Edouard Grave, Guillaume Lample, Herve Jegou, and Armand Joulin. Aug-
673 menting self-attention with persistent memory. *arXiv preprint arXiv:1907.01470*, 2019.
- 674
675 Yuandong Tian, Yiping Wang, Beidi Chen, and Simon S Du. Scan and snap: Understanding training
676 dynamics and token composition in 1-layer transformer. In *Advances in Neural Information
677 Processing Systems*, 2023.
- 678 Yuandong Tian, Yiping Wang, Zhenyu Zhang, Beidi Chen, and Simon Du. Joma: Demystifying
679 multilayer transformers via joint dynamics of mlp and attention. 2024.
- 680
681 Hugo Touvron, Louis Martin, Kevin Stone, Peter Albert, Amjad Almahairi, Yasmine Babaei, Nikolay
682 Bashlykov, Soumya Batra, Prajjwal Bhargava, Shruti Bhosale, et al. Llama 2: Open foundation
683 and fine-tuned chat models. *arXiv preprint arXiv:2307.09288*, 2023.
- 684 Ashish Vaswani, Noam Shazeer, Niki Parmar, Jakob Uszkoreit, Llion Jones, Aidan N Gomez, Łukasz
685 Kaiser, and Illia Polosukhin. Attention is all you need. In *Advances in Neural Information
686 Processing Systems*, 2017.
- 687
688 Elena Voita, David Talbot, Fedor Moiseev, Rico Sennrich, and Ivan Titov. Analyzing multi-head
689 self-attention: Specialized heads do the heavy lifting, the rest can be pruned. In *Proceedings of the
690 57th Annual Meeting of the Association for Computational Linguistics*, 2019.
- 691
692 Kevin Wang, Alexandre Variengien, Arthur Conmy, Buck Shlegeris, and Jacob Steinhardt. Inter-
693 pretability in the wild: a circuit for indirect object identification in gpt-2 small. *arXiv preprint
694 arXiv:2211.00593*, 2022.
- 695
696 Jason Wei, Xuezhi Wang, Dale Schuurmans, Maarten Bosma, Fei Xia, Ed Chi, Quoc V Le, Denny
697 Zhou, et al. Chain-of-thought prompting elicits reasoning in large language models. *Advances in
698 neural information processing systems*, 2022.
- 699
700 Ruiqi Zhang, Spencer Frei, and Peter L Bartlett. Trained transformers learn linear models in-context.
701 *Journal of Machine Learning Research*, 25(49):1–55, 2024.
- 702
703 Yi Zhang, Arturs Backurs, Sébastien Bubeck, Ronen Eldan, Suriya Gunasekar, and Tal Wagner.
Unveiling transformers with lego: a synthetic reasoning task. *arXiv preprint arXiv:2206.04301*,
2022.

702	CONTENTS	
703		
704		
705	1 Introduction	1
706		
707	2 Preliminaries	2
708	2.1 Reasoning from Context	3
709	2.2 Truncating Weights with LASER (Sharma et al., 2023)	3
710		
711		
712	3 Two-layer Transformer on Noisy In-context Recall	4
713	3.1 Feed-forward layers store the generic noise	6
714	3.2 Attention attends to in-context targets and avoids noise	7
715	3.3 No feed-forward Layers: value matrix stores generic noise association	8
716		
717		
718		
719	4 Experiments	9
720	4.1 An Investigation on GPT-2 Small and Pythia Models	9
721	4.2 The effect of truncating feed-forward layers on GSM8K	10
722		
723		
724	5 Discussion and Limitations	10
725		
726	A Contributions and Implications	16
727		
728		
729	B How Does the Two-layer Model Solve Noisy In-context Recall?	16
730	B.1 Training settings	16
731	B.2 Summarizing: roles of key components in the two-layer transformer	17
732	B.3 How does attention attend less towards the noise token?	17
733	B.4 Multiple Triggers	21
734	B.5 Architectural Choices	21
735	B.6 Training Details about Experiments	22
736		
737		
738		
739		
740	C More Experiments on Pythia	22
741	C.1 Learning Association with Prepositions	22
742	C.2 LASER Parameters for Evaluated LLMs	23
743	C.3 Other Pythia models on IOI and More Examples of Factual Recall	24
744		
745		
746	D Proof of Theorem 1	24
747	D.1 Gradient for the Feed-forward Matrix \mathbf{W}_F	24
748	D.2 Gradient for the Value Matrix \mathbf{W}_V	27
749	D.3 Completing the Proof of Theorem 1	36
750		
751		
752		
753	E Proof for First and Second moments in Lemma D.2	37
754	E.1 When $\bar{y} = q$	38
755	E.2 When $\bar{y} \neq q$	44

756	F Proof of Theorem 2: Training Dynamics of the Attention Layer	52
757		
758	G Linear Associative Memory	56
759		
760	G.1 Experiments and Discussions	56
761	G.2 Proof of Theorem 3	58
762		
763	H Useful Lemmas	59
764		
765		
766	I Input Examples for LLMs	61
767		
768	I.1 Examples for Prepositions	61
769	I.2 More Examples of Factual Recall	61
770		
771	J Synthetic IOI Task	62
772		
773		
774		
775		
776		
777		
778		
779		
780		
781		
782		
783		
784		
785		
786		
787		
788		
789		
790		
791		
792		
793		
794		
795		
796		
797		
798		
799		
800		
801		
802		
803		
804		
805		
806		
807		
808		
809		

A CONTRIBUTIONS AND IMPLICATIONS

Our contribution focuses on understanding the different roles of attention and FF weights in disentangling distributional vs in-context associations, both empirically and theoretically. The application of low-rank truncation is simply a way to verify our claims, and is consistent with the findings in the LASER paper that truncating some FF layers may improve performance on some reasoning tasks.

Nevertheless, our perspective based on distributional associations versus in-context reasoning may be helpful in thinking about how to allocate parameters to feed-forward versus attention layers: for instance, in Figure 6 on our synthetic task, we found that for a fixed total parameter budget, models with fewer MLP parameters achieve higher loss on distributional predictions (e.g., non-contextual bigrams) compared to models with more MLP parameters (and fewer attention parameters). These notions may also provide a different way to reason about circuit discovery in mechanistic interpretability from the perspective of training dynamics and properties of the training data. Finally, this disentanglement may inform more effective ways to fine-tune models, e.g., by selectively choosing which layers to fine-tune.

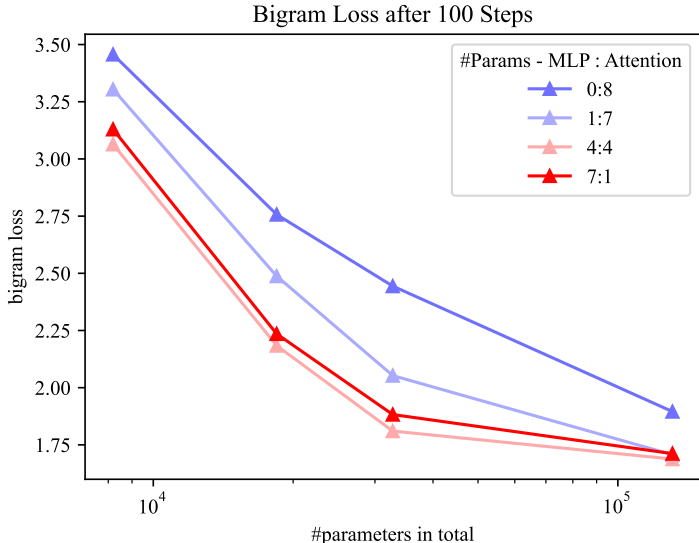


Figure 6: The training loss of approximating the global bigram π_b with various allocations of parameters in MLP and Attention. For each configuration of total parameters and ratios, we use the corresponding best learning rate after search to train 100 steps.

B HOW DOES THE TWO-LAYER MODEL SOLVE NOISY IN-CONTEXT RECALL?

B.1 TRAINING SETTINGS

In most parts of this work, we consistently train the model with a fixed level of $\alpha > 0$. However, we also present numerical results of **fine-tuning** in Figure 8 and 4 to show the mechanism of avoiding generic noise token in the second-layer attention. The details of such a fine-tuning setting is as follows.

Fine-tuning: there are two phases of training as

- phase 1 (pre-training): starting from a model with random initialized weights, we train the model on data generated with $\alpha = 0$. This is exactly the same as Bietti et al. (2023). At the end of this phase, the second-layer attention is expected to attend *all tokens* after the trigger token, i.e., $t \leq T$ such that $z_{t-1} = q$ no matter what z_t is.

- phase 2 (fine-tuning): starting from a model after phase 1, we train all weights in the model on data generated with $\alpha > 0$. At the end of this phase, the second-layer attention learns to avoid the generic noise token, *i.e.*, $t \leq T$ such that $z_t = N_1, z_{t-1} = q$, as shown in Figure 4.

B.2 SUMMARIZING: ROLES OF KEY COMPONENTS IN THE TWO-LAYER TRANSFORMER

Recall the architecture of two-layer transformers in Section 3 as

$$\begin{aligned}
 x_t &\triangleq \mathbf{W}_E(z_t) + p_t, \\
 h_t^1 &\triangleq \sum_{s \leq t} [\sigma(x_t^\top \mathbf{W}_{QK}^1 x_{1:t})]_s \cdot \mathbf{W}_V^1 x_s, \\
 x_t^1 &\triangleq x_t + h_t^1 + F_1(x_t + h_t^1), \\
 h_t^2 &\triangleq \sum_{s \leq t} [\sigma(x_t^{1\top} \mathbf{W}_{QK}^2 x_{1:t}^1)]_s \cdot \mathbf{W}_V^2 x_s^1, \\
 x_t^2 &\triangleq x_t^1 + h_t^2 + F_2(x_t^1 + h_t^2), \\
 \xi_t &\triangleq \mathbf{W}_U x_t^2.
 \end{aligned}$$

When the task is without noise, *i.e.*, $\alpha = 0$, Bietti et al. (2023) point out the first-layer attention attends to the previous token through $\mathbf{W}_{QK}^1 = \sum_{t=2}^T p_{t-1} p_t^\top$. Therefore, when $z_t = \bar{y}$ with $z_{t-1} = q$, the output of the first layer is $x_t^1 \approx \mathbf{W}_E(\bar{y}) + \mathbf{W}_V^1 \mathbf{W}_E(q)$. Then they show that the second-layer attention matches such x_t^1 with $z_T = q$ by $\mathbf{W}_{QK}^2 = (\mathbf{W}_V \mathbf{W}_E(q)) \mathbf{W}_E(q)^\top$, through which the information of \bar{y} in x_t^1 is copied to last token as $h_T^2 \approx \mathbf{W}_V^2 \mathbf{W}_E(\bar{y})$. Finally $\mathbf{W}_V^2 = \sum_{z \in [N]} \mathbf{W}_U(z) \mathbf{W}_E(z)^\top$ helps output the correct label of \bar{y} .

In our work with noise $\alpha > 0$, the key difference is that there is a fixed probability α for a noise token $N + 1$ to appear after each trigger q . This requires \mathbf{W}_{QK}^2 to not only match the trigger but also avoid the noise token after trigger. Let’s first summarize the whole pipeline of this model for our task.

Roles of key components. The first layer will be basically the same as Bietti et al. (2023), where $\mathbf{W}_{QK}^1 = \sum_{t=2}^T p_{t-1} p_t^\top$ attends to the previous token. Consider two positions t_1, t_2 with $z_{t_1-1} = z_{t_2-1} = q, z_{t_1} = \bar{y}, z_{t_2} = N + 1$, then outputs of the first layer at these two positions are $x_{t_1}^1 \approx \mathbf{W}_E(\bar{y}) + \mathbf{W}_V^1 \mathbf{W}_E(q)$, $x_{t_2}^1 \approx \mathbf{W}_E(N + 1) + \mathbf{W}_V^1 \mathbf{W}_E(q)$. Then the second-layer attention $\mathbf{W}_{QK}^2 = (\mathbf{W}_V \mathbf{W}_E(q) - c \cdot \mathbf{W}_E(N + 1)) \mathbf{W}_E(q)^\top$ with some positive c makes the attention attend to t_1 and avoid t_2 simultaneously, matching with the last token $z_T = q$. Therefore, the output of the second-layer attention at T is basically $h_T^2 \approx \mathbf{W}_V^2 \mathbf{W}_E(\bar{y})$. Similar to the noiseless case, $\mathbf{W}_V^2 = \sum_{z \in [N]} \mathbf{W}_U(z) \mathbf{W}_E(z)^\top$ helps output the correct label of \bar{y} . Meanwhile, note that x_T^1 actually contains $\mathbf{W}_E(q)$ through x_T , so F_2 is able to predict the noise $N + 1$ when seeing a fixed $\mathbf{W}_E(q)$. As a result, combining the two streams from h_T^2 and $F_2(x_T^1)$, the full model is able to predict any \bar{y} w.p. $1 - \alpha$ and predict the noise $N + 1$ w.p. α .

Evidence. Figure 4 illustrates that the second-layer attention learns to attend to $z_{t_1} = \bar{y}$ and avoid $z_{t_2} = N + 1$, with Appendix B.3 presenting a primitive exploration on how the avoidance is learnt in a simplified setting. Figure 7 (left) shows the attention pattern from \mathbf{W}_{QK}^1 of attending to the previous token. Figure 7 (middle) shows the memory recall of $\mathbf{W}_U(N + 1)^\top F_2(\mathbf{W}_E(q))$ to predict the noise. Figure 7 (right) illustrates the memory recall of $\mathbf{W}_U(i)^\top \mathbf{W}_V^2 \mathbf{W}_E(i)$ to predict the correct token.

B.3 HOW DOES ATTENTION ATTEND LESS TOWARDS THE NOISE TOKEN?

We use the same simplified model as in Section 3.1 to understand how the second-layer attention learns to avoid the noise. When using the same learning rate $\eta = \eta_v = \eta_f$, Theorem 1 implies that the feed-forward \mathbf{W}_F makes the most contribution for predicting the noise after the first-step update. Denote the logits for the noise of the model at time t as ξ_t . The arguments in this section make the following assumptions, which hold at least after the first-step update:

- \mathbf{W}_F dominates the logits ξ_t of predicting the noise token, compared with \mathbf{W}_V .

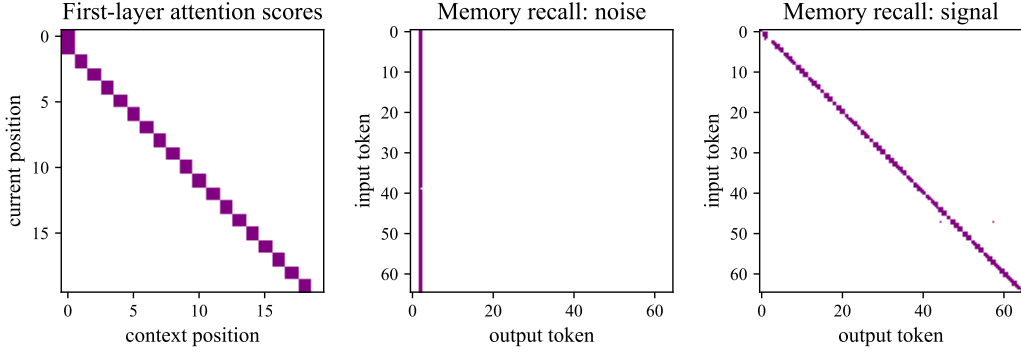


Figure 7: **Left:** first-layer attention attending to the previous token from the current token. **Middle:** logits to predict noise from $\langle F_2(\mathbf{W}_E(i)), \mathbf{W}_U(j) \rangle$ with input $i \in [N + 1]$ and output $j \in [N + 1]$, where the output channel 2 is set as the noise channel. It turns out, for all input i , the logits on output 2 are large, which matches our construction that, at least for trigger q as input, the output 2 has large logits. **Right:** logits to predict signal from $\langle \mathbf{W}_V^2 \mathbf{W}_E(i), \mathbf{W}_U(j) \rangle$ for input $i \in [N + 1]$ and output $j \in [N + 1]$. It matches our construction that $i = j$ has large logits. Meanwhile, $i = j = 2$ does not have large logits since 2 is the noise channel.

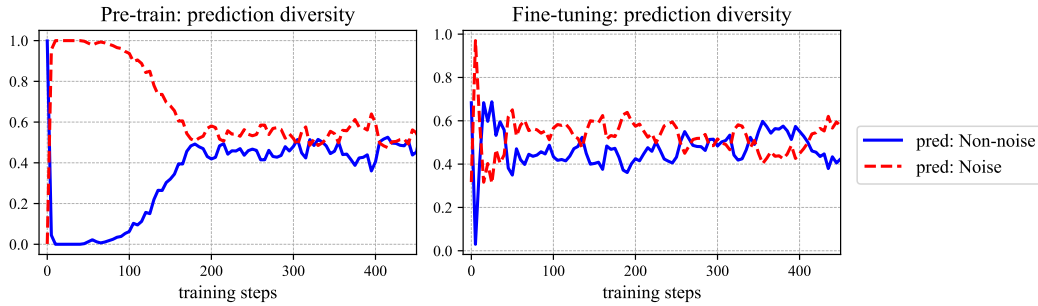


Figure 8: Fractions of predicting the noise token and the other non-noise tokens with $\alpha = 0.5$. (Left) pretraining steps on noisy data; (right) finetuning steps on noisy data, after pretraining on clean data with $\alpha = 0$. In both cases, the models learn to predict noise with probability nearly 0.5. In the first few (~ 5) steps, the models quickly learn to predict noise with probability close to 1. The fine-tuning setting is in Appendix B.1.

- ii. Logits for predicting any $k \leq N$ is close to 0, which means the predicted probability p_t is approximately $p_t \approx \frac{\exp(\xi_t)}{N + \exp(\xi_t)}$.
- iii. The predicted probability $p_t < \alpha$.
- iv. The attention matrix \mathbf{W}_{QK} is approximately 0, inducing a uniform attention.
- v. The dataset has $T, N \gg 1$ and $m \rightarrow \infty$, so the gradient is from population loss.

The first assumption holds after the first step from Theorem 1 with $\eta_f = \eta_v$.

Then, since $|\mathbf{W}_U(k)^\top (\nabla_{\mathbf{w}_F} L) \mathbf{W}_E(q)| = O(\frac{1}{N}) \cdot |\mathbf{W}_U(N+1)^\top (\nabla_{\mathbf{w}_F} L) \mathbf{W}_E(q)|$ for any $k \leq N$ in Lemma D.1, the second assumption holds. Meanwhile, the projection of $\nabla_{\mathbf{w}_V} L$ onto any direction in Lemma D.2 is also smaller than $\mathbf{W}_U(N+1)^\top (\nabla_{\mathbf{w}_F} L) \mathbf{W}_E(q)$ by a factor of $O(1/N)$.

Let's check the condition of the third assumption. In the proof of Lemma D.1, the gradient of \mathbf{W}_F has the form of

$$\mathbf{W}_U(N+1)^\top (-\nabla_{\mathbf{w}_F} L) \mathbf{W}_E(q) = \alpha - p_t.$$

This update induces ξ_t to increase by $\eta(\alpha - p_t)$. This implies

$$\xi_t \approx \xi_{t-1} + \eta \left(\alpha - \frac{\exp(\xi_t)}{N + \exp(\xi_t)} \right), \quad \forall t \geq 1.$$

This sequence $\{\xi_t\}_{t \geq 1}$ has stationary point $\xi^* = \log N + \log(\frac{\alpha}{1-\alpha})$. Denoting $\hat{\xi}_t \triangleq \xi_t - \xi^*$ with $\hat{\xi}_1 = -\xi^* < 0$, the iteration becomes

$$\hat{\xi}_{t+1} \approx \hat{\xi}_t + \eta \left(\alpha - \frac{\exp(\hat{\xi}_t)}{\frac{1-\alpha}{\alpha} + \exp(\hat{\xi}_t)} \right).$$

If we would like to have $\hat{\xi}_t$ not hit the positive region by controlling η , it suffices to bound η with any $\hat{\xi} < 0$,

$$\eta \leq \frac{\hat{\xi}}{\frac{\exp(\hat{\xi})}{\frac{1-\alpha}{\alpha} + \exp(\hat{\xi})} - \alpha},$$

where RHS is continuous and decreasing on $\xi < 0$ when $\alpha < 0.5$. Hence, we have $\eta \leq \frac{1}{\alpha(1-\alpha)}$ evaluated at $\hat{\xi} = 0$ by L'Hospital rule. This bound of η is very strong, since $\eta = O(\log N)$ can still have $\hat{\xi} < 0$ after one step.

The fourth assumption is basically from what we will show at the end of this section, as the second observation.

Then consider the dynamics of \mathbf{W}_V , which is much slower than \mathbf{W}_F . From the proof of Lemma D.2, the gradient of \mathbf{W}_V satisfies

$$\begin{aligned} \nabla_{\mathbf{W}_V} L &= \mathbb{E}_x \left[\sum_{k=1}^{N+1} (p_{\mathbf{W}}(k|x) - \mathbb{1}\{y=k\}) \mathbf{W}_U(k) \left(\frac{1}{T} \sum_{t=1}^t x_t \right)^\top \right], \\ \mathbf{W}_U(N+1)^\top (-\nabla_{\mathbf{W}_V} L) \mathbf{W}_E(k) &\approx \frac{1}{N} \sum_{t \geq 1} (\alpha - p_t) (\mathbb{1}\{k \leq N\} + \alpha \cdot \mathbb{1}\{k = N+1\}) \\ &\triangleq c \cdot \mathbb{1}\{k \leq N\} + c \cdot \alpha \cdot \mathbb{1}\{k = N+1\} = \Theta\left(\frac{1}{N}\right), \end{aligned} \tag{4}$$

where the projection on $\mathbf{W}_E(N+1)$ is always positive and smaller than that on other directions when $p_t < \alpha$. Projections onto other directions $\mathbf{W}_U(j) \mathbf{W}_E(k)^\top, \forall j \leq N$, are smaller as $\Theta(\frac{1}{N^2})$.

Finally, let's consider the dynamics of \mathbf{W}_{QK} . At initialization, $\mathbf{W}_{QK} = 0$ and $\nabla_{\mathbf{W}_{QK}} L = 0$ due to zero initialization of \mathbf{W}_V . After one-step, \mathbf{W}_V has such a structure in Eq.(4). Then, with $\bar{x}_{1:T} \triangleq \frac{1}{T} \sum_{1 \leq t \leq T} x_t$ from uniform attention, the gradient of \mathbf{W}_{QK} satisfies

$$\begin{aligned} -\nabla_{\mathbf{W}_{QK}} L &= \mathbb{E}_x \left[\sum_{k=1}^N (\mathbb{1}\{y=k\} - p_{\mathbf{W}}(k|x)) \frac{1}{T} \sum_{t=1}^T (\mathbf{W}_U(k)^\top \mathbf{W}_V x_t) \cdot (x_t - \bar{x}_{1:T}) \mathbf{W}_E(q)^\top \right] \\ &\approx \sum_{k=1}^N \left(\frac{1-\alpha}{N} - \frac{1-p_t}{N} \right) \underbrace{\mathbb{E} \left[\frac{1}{T} \sum_{t=1}^T \mathbf{W}_U(k)^\top \mathbf{W}_V x_t \cdot (x_t - \bar{x}_{1:T}) \mathbf{W}_E(q)^\top \right]}_{\triangleq A} \\ &\quad + (\alpha - p_t) \underbrace{\mathbb{E} \left[\frac{1}{T} \sum_{t=1}^T (\mathbf{W}_U(N+1)^\top \mathbf{W}_V x_t) \cdot (x_t - \bar{x}_{1:T}) \mathbf{W}_E(q)^\top \right]}_{\triangleq B}. \end{aligned} \tag{5}$$

Then, we have

$$\begin{aligned}
\mathbf{W}_E(N+1)^\top B \mathbf{W}_E(q) &= \mathbb{E} \left[\frac{1}{T} \sum_{t=1}^T (\mathbf{W}_U(N+1)^\top \mathbf{W}_V x_t) \cdot \mathbf{W}_E(N+1)^\top (x_t - \bar{x}_{1:T}) \right] \\
&\stackrel{(a)}{=} \mathbb{E} \left[\frac{1}{T} \sum_{t=1}^T (c + c(\alpha - 1) \cdot \mathbb{1}\{z_t = N+1\}) \cdot \mathbf{W}_E(N+1)^\top (x_t - \bar{x}_{1:T}) \right] \\
&\stackrel{(b)}{=} \mathbb{E} \left[\frac{1}{T} \sum_{t=1}^T (c(\alpha - 1) \cdot \mathbb{1}\{z_t = N+1\}) \cdot \mathbf{W}_E(N+1)^\top (x_t - \bar{x}_{1:T}) \right] \\
&= \frac{\alpha}{N} \cdot c(\alpha - 1) \left(1 - \frac{\alpha}{N}\right) = \Theta\left(\frac{1}{N^2}\right) < 0.
\end{aligned}$$

where (a) is from Eq.(4), (b) is due to $\bar{x}_{1:T} = \frac{1}{T} \sum_t x_t$ and note that $c = \Theta\left(\frac{1}{N}\right)$.

Similarly, we also have

$$\begin{aligned}
\mathbf{W}_E(N+1)^\top A \mathbf{W}_E(q) &= \mathbb{E} \left[\frac{1}{T} \sum_{t=1}^T (\mathbf{W}_U(k)^\top \mathbf{W}_V x_t) \mathbf{W}_E(N+1)^\top \cdot (x_t - \bar{x}_{1:T}) \right] \\
&= \mathbb{E} \left[\frac{1}{T} \sum_{t=1}^T \Theta\left(\frac{1}{N^2}\right) \cdot \mathbb{1}\{z_t = N+1\} \mathbf{W}_E(N+1)^\top \cdot (x_t - \bar{x}_{1:T}) \right] = \Theta\left(\frac{1}{N^3}\right).
\end{aligned}$$

For any $k \leq N$, we have

$$\begin{aligned}
\mathbf{W}_E(k)^\top B \mathbf{W}_E(q) &= \mathbb{E} \left[\frac{1}{T} \sum_{t=1}^T (\mathbf{W}_U(N+1)^\top \mathbf{W}_V x_t) \cdot \mathbf{W}_E(k)^\top (x_t - \bar{x}_{1:T}) \right] \\
&= \mathbb{E} \left[\frac{1}{T} \sum_{t=1}^T (c(\alpha - 1) \cdot \mathbb{1}\{z_t = k\}) \cdot \mathbf{W}_E(N+1)^\top (x_t - \bar{x}_{1:T}) \right] \\
&= \frac{\alpha}{N} \cdot c(\alpha - 1) \left(-\frac{1}{N}\right) = \Theta\left(\frac{1}{N^3}\right) > 0,
\end{aligned}$$

and

$$\begin{aligned}
\mathbf{W}_E(k)^\top A \mathbf{W}_E(q) &= \mathbb{E} \left[\frac{1}{T} \sum_{t=1}^T (\mathbf{W}_U(k)^\top \mathbf{W}_V x_t) \mathbf{W}_E(k)^\top \cdot (x_t - \bar{x}_{1:T}) \right] \\
&= \mathbb{E} \left[\frac{1}{T} \sum_{t=1}^T \Theta\left(\frac{1}{N^2}\right) \cdot \mathbb{1}\{z_t = N+1\} \mathbf{W}_E(k)^\top \cdot (x_t - \bar{x}_{1:T}) \right] = \Theta\left(\frac{1}{N^4}\right).
\end{aligned}$$

Combining the above four estimation of projections of A and B with Eq.(5), we have

$$\begin{aligned}
\mathbf{W}_E(N+1)^\top (-\nabla_{\mathbf{W}_{QK}} L) \mathbf{W}_E(q) &= \Theta\left(\frac{1}{N^2}\right) < 0, \\
\forall k \leq N, \mathbf{W}_E(k)^\top (-\nabla_{\mathbf{W}_{QK}} L) \mathbf{W}_E(q) &= \Theta\left(\frac{1}{N^3}\right) > 0.
\end{aligned}$$

Then we have three observations

- i. \mathbf{W}_{QK} in this phase avoids the noise token $N+1$ and uniformly attends to all tokens $k \leq N$.
- ii. The update of \mathbf{W}_{QK} is in $\Theta\left(\frac{1}{N^2}\right)$, while the update of \mathbf{W}_F is $\Theta(1)$ in Lemma D.1 and that of \mathbf{W}_V is $\Theta\left(\frac{1}{N}\right)$ in Lemma D.2. These three levels of updating speed also coincide with the assumptions that \mathbf{W}_F dominates first and then \mathbf{W}_V has a micro structure that induces the evolving of \mathbf{W}_{QK} .
- iii. The current proof for \mathbf{W}_{QK} strongly depends on the fact that the noise token appears less than other token by a factor α in expectation. The proof will have the opposite result if the noise token is made to appear more by manipulating the data distribution. Therefore, we leave a new proof that is robust to such an assumption in data distribution as future work.

B.4 MULTIPLE TRIGGERS

In Section 3, we assume there is only one fixed trigger $q \in [N]$ for simplicity. Actually the case of multiple triggers has the same mechanism. As discussed by Bietti et al. (2023) and Appendix B.2, for one trigger, the second-layer attention has large logits in $\langle \mathbf{W}_V^1 \mathbf{W}_E(i)^\top, \mathbf{W}_{QK}^2 \mathbf{W}_E(j) \rangle$ only for $i = j = q$. For multiple triggers, basically $\langle \mathbf{W}_V^1 \mathbf{W}_E(i)^\top, \mathbf{W}_{QK}^2 \mathbf{W}_E(j) \rangle$ only have large values when $q \in Q$. This is verified in Figure 9.

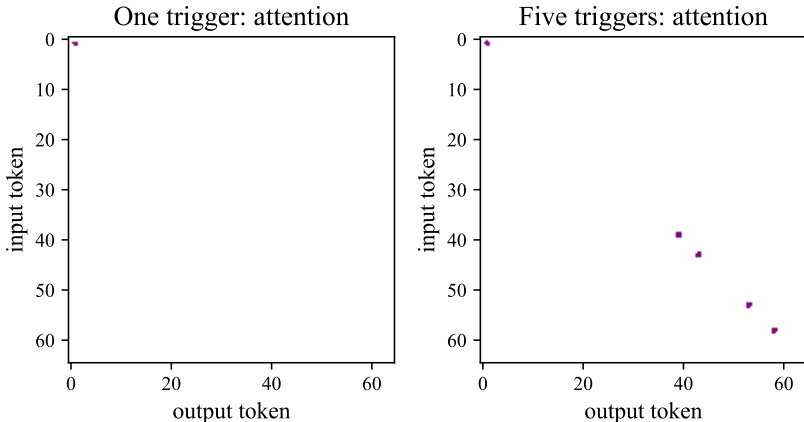


Figure 9: Logits of $\langle \mathbf{W}_V^1 \mathbf{W}_E(i)^\top, \mathbf{W}_{QK}^2 \mathbf{W}_E(j) \rangle$ for input i and output j when there is one trigger (left, $q = 1$) and five triggers (right, $q \in Q = \{1, 39, 43, 53, 58\}$). In both cases, the logits only have large values when $i = j = q$, verifies the matching mechanism in Appendix B.2.

B.5 ARCHITECTURAL CHOICES

In Section 3 and Appendix B.2, we were focused on experiments with both F_1, F_2 being two-layer ReLU MLPs. Meanwhile, we have also tried other choices of F_1, F_2 and then search for the best truncation method for each architecture. In this section, we would like to summarize our experimental results for better understanding of all modules in the two-layer transformer.

Generally, the feed-forward layer can be two-layer ReLU MLPs, one-layer Linear or “None”, where None stands for there is no feed-forward layer so that the value matrices in attention layers are the only weight matrices that transform features.

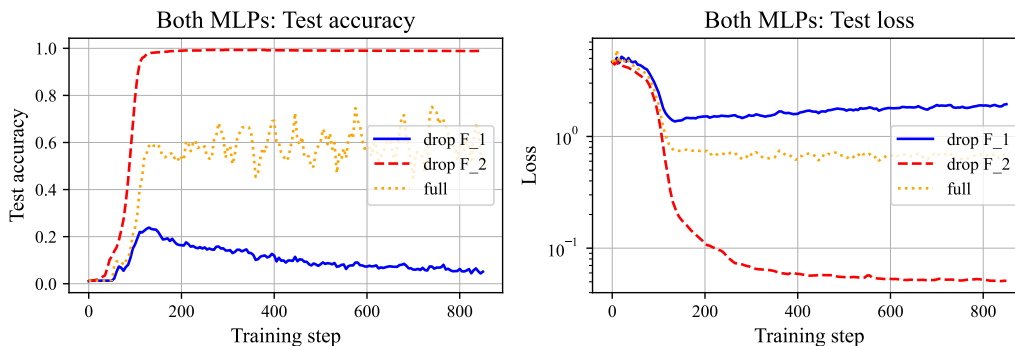
Both F_1, F_2 are two-layer MLPs. This is our main setting. The best truncation method is to *fully* drop F_2 . We also try to fully drop F_1 , as reported in Figure 10. It turns out fully dropping F_1 makes the model predict the noise with high probability.

F_1 is MLPs and F_2 is Linear. Figure 11 reports the results. Dropping F_1 and F_2 both improve the correct prediction, and dropping F_1 is better with lower test loss. Note that, when test accuracies are near 100%, lower test loss is a better measurement of the prediction quality, because accuracies are taken by argmax over the output logits while test loss are about the exactly predicted probability.

F_1 is Linear and F_2 is MLPs. Figure 12 reports the results. Dropping F_2 improves the correct prediction while dropping F_1 makes the model predict noise more.

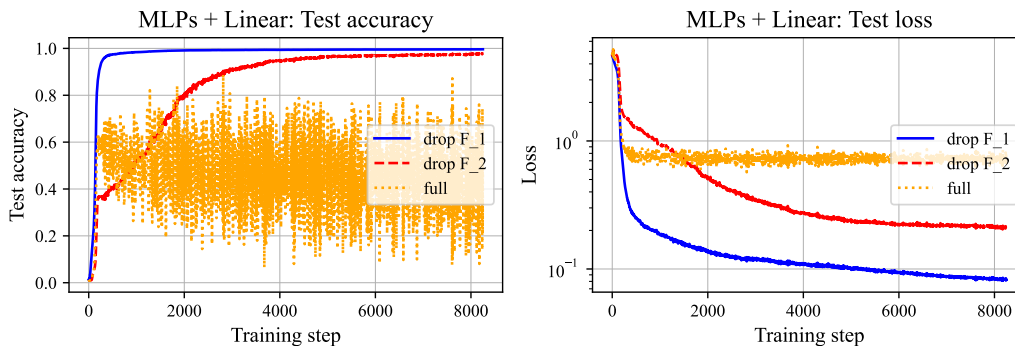
Both F_1 and F_2 are None. Figure 13 reports the results. While there is no feed-forward layer any more, low-rank truncating a part \mathbf{W}_O^1 of the first-layer matrix improves the model’s prediction a little. This implies that, when there is not feed-forward layers, the noise association is possible stored in the first-layer value matrix of attention. Note that the improvement of such low-rank truncation is clearly smaller than *fully* dropping one of feed-forward layers in the previous cases. Meanwhile, a smaller $\rho = 0.01$ destroys the model’s performance. This implies fully dropping is not the optimal choice for low-rank truncation of the value matrix, and there is low-rank subspace in it that is useful for predicting the correct tokens. Our discussion of the role of \mathbf{W}_V^1 in Appendix B.2 is a possible answer to this phenomena.

1134
1135
1136
1137
1138
1139
1140
1141
1142
1143
1144
1145
1146



1147 Figure 10: Test performance of fully dropping F_1, F_2 when both F_1, F_2 are two-layer MLPs. It turns
1148 out, while dropping F_2 makes the model predict correctly w.p. near 1, dropping F_1 has the model
1149 predict noise with high probability.

1150
1151
1152
1153
1154
1155
1156
1157
1158
1159
1160
1161
1162
1163



1164 Figure 11: Test performance of fully dropping F_1, F_2 when both F_1 is MLPs and F_2 Linear. Both
1165 dropping methods turn out to help predict more correctly than the full model. Meanwhile, dropping
1166 the MLP F_1 is better with lower test loss.

1169 B.6 TRAINING DETAILS ABOUT EXPERIMENTS

1170
1171
1172
1173
1174
1175
1176

All of the training is with SGD optimization with learning rate in $\{0.001, 0.03\}$. The batch size is
512. The dimension is 256. The context length is 256. All results in the experiments are stable for
any learning rate between 0.001 and 0.03. Each run of experiments is on a single Nvidia Tesla V100
GPU. It takes 3 hours to finish each run for 2K steps, which probably can be optimized a lot since we
are tracking a lot of measurement along training, not limited to hundreds of possible truncations at
each test time.

1177
1178
1179
1180

C MORE EXPERIMENTS ON PYTHIA

1181
1182

C.1 LEARNING ASSOCIATION WITH PREPOSITIONS

1183
1184
1185
1186
1187

We would like to verify our guess about the structure of “to + the” in Pythia in Section 4.1. To make
the argument generalizable than IOI dataset, we consider a structure of “[preposition] + the”, where
[preposition] has a pool of 30 prepositions in English, including “to”. The input is a raw “[preposition]”
or a random sentence ending with “[preposition]”, with some examples in Appendix I.1. For both
kinds of inputs, Pythia-160M/410M/1B turns out to learn the structure of “[preposition] + the” around
10 steps, as shown in Figure 14.

1188
1189
1190
1191
1192
1193
1194
1195
1196
1197
1198
1199
1200

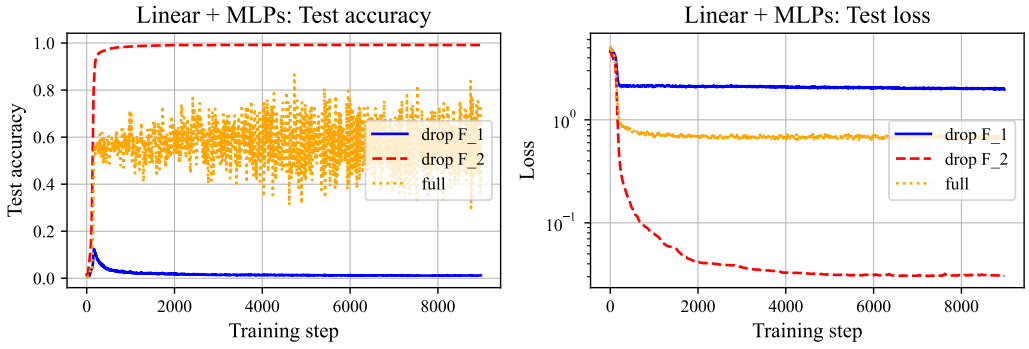


Figure 12: Test performance of fully dropping F_1, F_2 when both F_1 is Linear and F_2 MLPs. Only dropping F_2 helps predict more correctly. Dropping F_1 makes the model predicting noise more.

1201
1202
1203
1204
1205
1206
1207
1208
1209
1210
1211
1212
1213
1214
1215
1216

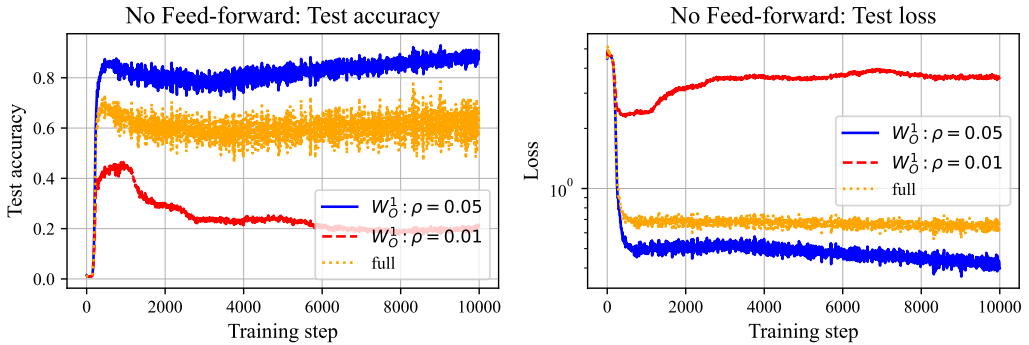


Figure 13: Test performance of low-rank truncating of W_O^1 when there is no F_1, F_2 . Here ρ is the fraction of preserved rank of W_O^1 , where actually we re-parametrize the first-layer value matrix in attention as $W_O^1 W_V^1 \in \mathbb{R}^{d \times d}$. It turns out the best $\rho = 0.05$ improves the model’s prediction a little. Meanwhile, a smaller ρ destroys the model’s performance.

C.2 LASER PARAMETERS FOR EVALUATED LLMs

1223
1224
1225
1226
1227
1228
1229
1230
1231
1232
1233
1234
1235
1236
1237
1238
1239
1240
1241

Following the definition of LASER in Section 2.2, we search for the optimal layer, ρ and target weights in Pythia models and GPT-2 Small for each dataset.

IOI on Pythia-410M. The model has 24 layers. The truncation is on the input matrix of MLPs on the 22-th layer with $\rho = 0.02$.

IOI on Pythia-1B. The model has 16 layers. The truncation is on the input matrix of MLPs on the 11-th layer with $\rho = 0.008$.

Factual recall on Pythia-1B. The truncation is on the input matrix of MLPs on the 16-th layer with $\rho = 0.0125$.

Factual recall on Pythia-1.4B. The model has 24 layers. The truncation is on the input matrix of MLPs on the 24-th layer with $\rho = 0.025$.

Factual recall on Pythia-2.8B. The model has 32 layers. The truncation is on the input matrix of MLPs on the 32-th layer with $\rho = 0.04$.

IOI on GPT2 Small. Related parameters have been contained in Section 4.1.

Phi-3 on GSM8K. The model has 32 layers. The truncation is on the output matrix of MLPs on the 28-th layer with $\rho = 0.02$.

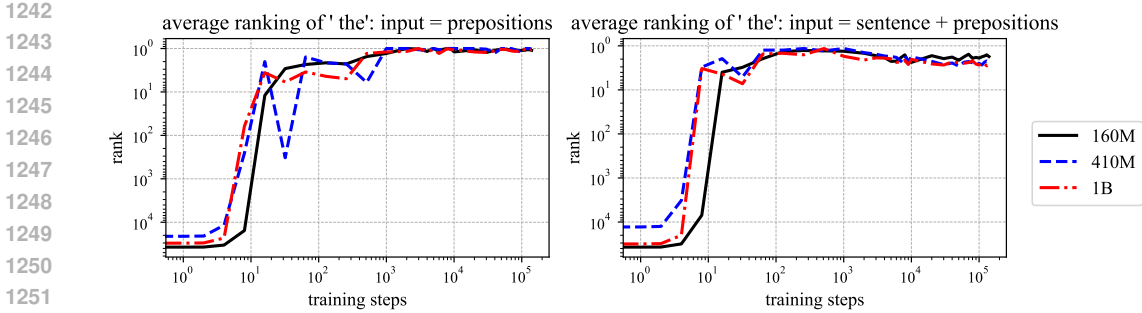


Figure 14: Average ranking of tokens “the” in the prediction by Pythia-160M/410M/1B along training. The inputs are 30 preposition words (left) and 40 sentences ending with prepositions. It turns out “the” becomes one of top predictions around 10 steps.

Llama3.1-8B(-instruct) on GSM8K. The models have 32 layers. The truncation is on the output of MLPs on the 27-th layer with $\rho = 0.02$.

C.3 OTHER PYTHIA MODELS ON IOI AND MORE EXAMPLES OF FACTUAL RECALL

IOI. In the same setting of Figure 5 (left), we plot the prediction distributions of Pythia-410M and 1B on the 100 IOI inputs in Figure 15. The model checkpoints are the final ones after training. LASER turns out to decrease the probability of “the” while keeping that of the correct [IO] high.

More examples of Factual Recall. In addition to the factual query “Madrid is located in” in Figure 5 (right), we consider more such examples in Table 5. We plot the prediction distributions of Pythia-1B, 1.4B and 2.8B on these inputs in Figure 16, where LASER significantly lowers the probability of predicting “the” versus the correct outputs.

D PROOF OF THEOREM 1

In this section, we will present the expectations and variances of $\nabla_{\mathbf{W}_V} \hat{L}$ and $\nabla_{\mathbf{W}_F} \hat{L}$ with $\mathbf{W}_V = \mathbf{W}_F = 0$ at initialization. The targets are to show:

1. a gap between $\lim_{m \rightarrow \infty} \nabla_{\mathbf{W}_V} \hat{L}$ and $\lim_{m \rightarrow \infty} \nabla_{\mathbf{W}_F} \hat{L}$ so that a step of GD with large learning rates is enough to learn the noise in \mathbf{W}_F , and
2. sample complexity of $\nabla_{\mathbf{W}_V} \hat{L}$ and $\nabla_{\mathbf{W}_F} \hat{L}$ based on expectations and variances.

Assumption D.1 (Orthonormal embeddings). *The embeddings $u_k \in \mathbb{R}^d$ are assumed to be orthonormal, i.e., $u_i^\top u_j = \mathbb{1}\{i = j\}$. Meanwhile, if a matrix $\mathbf{W} \in \mathbb{R}^{d \times d}$ is random initialized, it holds $u_i^\top \mathbf{W} u_j = 0$.*

D.1 GRADIENT FOR THE FEED-FORWARD MATRIX \mathbf{W}_F

Lemma D.1. *Consider zero initialization, $\mathbf{W}_V = \mathbf{W}_F = \mathbf{W}_{QK} = 0$ and $N \gg 1$. Then with probability $1 - \delta$, for any $j, k \in [N + 1]$, it holds*

$$\begin{aligned} & \left| \mathbf{W}_U(k)^\top (\nabla_{\mathbf{W}_F} \hat{L}) \mathbf{W}_E(q) - \mu(k) \right| \\ & \leq \sqrt{\frac{4\sigma^2(k) (\ln(N + 1) + \ln(\frac{2}{\delta}))}{m}} + \frac{4R(k) (\ln(N + 1) + \ln(\frac{2}{\delta}))}{m}, \end{aligned} \tag{6}$$

where $\mu(k), \sigma^2(k), R(k)$ are expectation, variance and range for different choices of $k \in [N]$ as follows:

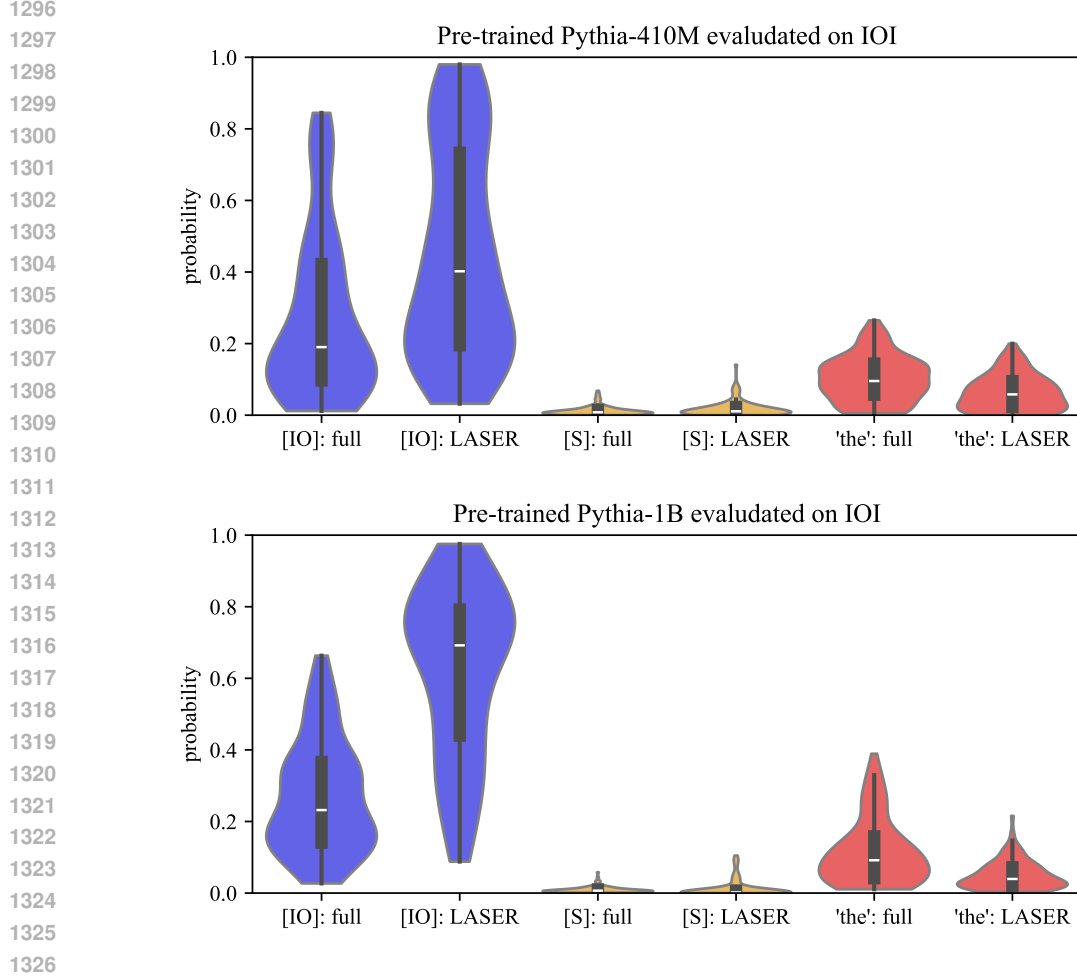


Figure 15: The prediction distributions of Pythia-410M and 1B on the IOI task. The setting is the same as in Figure 5 (left). The evaluated models are the final checkpoints after training. LASER turns out to decrease the probability of “the” while keeping that of the correct [IO] high.

$$\forall k \leq N : \quad \begin{aligned} \mu(N+1) &= -\alpha, & \sigma^2(N+1) &= \alpha(1-\alpha), & R(N+1) &= \max\{\alpha, 1-\alpha\}, \\ \mu(k) &= \frac{1}{N+1} - \frac{1-\alpha}{N}, & \sigma^2(k) &= \frac{1-\alpha}{N}, & R(k) &= 1. \end{aligned}$$

Proof. Due to zero initialization, *i.e.*, $\mathbf{W}_V = \mathbf{W}_F = 0$, the current predicted probability is $\hat{p}_{\mathbf{W}}(k|x_i) \equiv \frac{1}{N+1}$ for all $i \in [m]$ and $k \in [N+1]$. Therefore, from Lemma H.1, we have

$$\nabla_{\mathbf{W}_F} \hat{L} = \frac{1}{m} \sum_{i=1}^m \left[\sum_{k=1}^{N+1} \left(\frac{1}{N+1} - \mathbb{1}\{y_i = k\} \right) \mathbf{W}_U(k) x_{i,T}^\top \right],$$

where $x_{i,T} \in \mathbb{R}^d = \mathbf{W}_E(z_{i,T}) + p_T$ is the input embedding with input token $z_{i,T}$ at position T in sequence i , together with positional encoding p_T for position T . Since $z_{i,T}$ is set to be the trigger q in the data generation process and p_T is assumed to orthogonal to any other vector in \mathbf{W}_E in Assumption D.1, we have the following projections for $\nabla_{\mathbf{W}_F} \hat{L}$: $\forall k \in [N+1]$,

$$\mathbf{W}_U(k)^\top (\nabla_{\mathbf{W}_F} \hat{L}) \mathbf{W}_E(q) = \frac{1}{m} \sum_{i=1}^m \left(\frac{1}{N+1} - \mathbb{1}\{y_i = k\} \right).$$

From the data generation process, it is obvious to get

$$\mathbb{E}_{(x,y)} \left[\frac{1}{N+1} - \mathbb{1}\{y = k\} \right] = \frac{1}{N+1} - \alpha \cdot \mathbb{1}\{k = N+1\} - \frac{1-\alpha}{N} \cdot \mathbb{1}\{k \leq N\}. \quad (7)$$

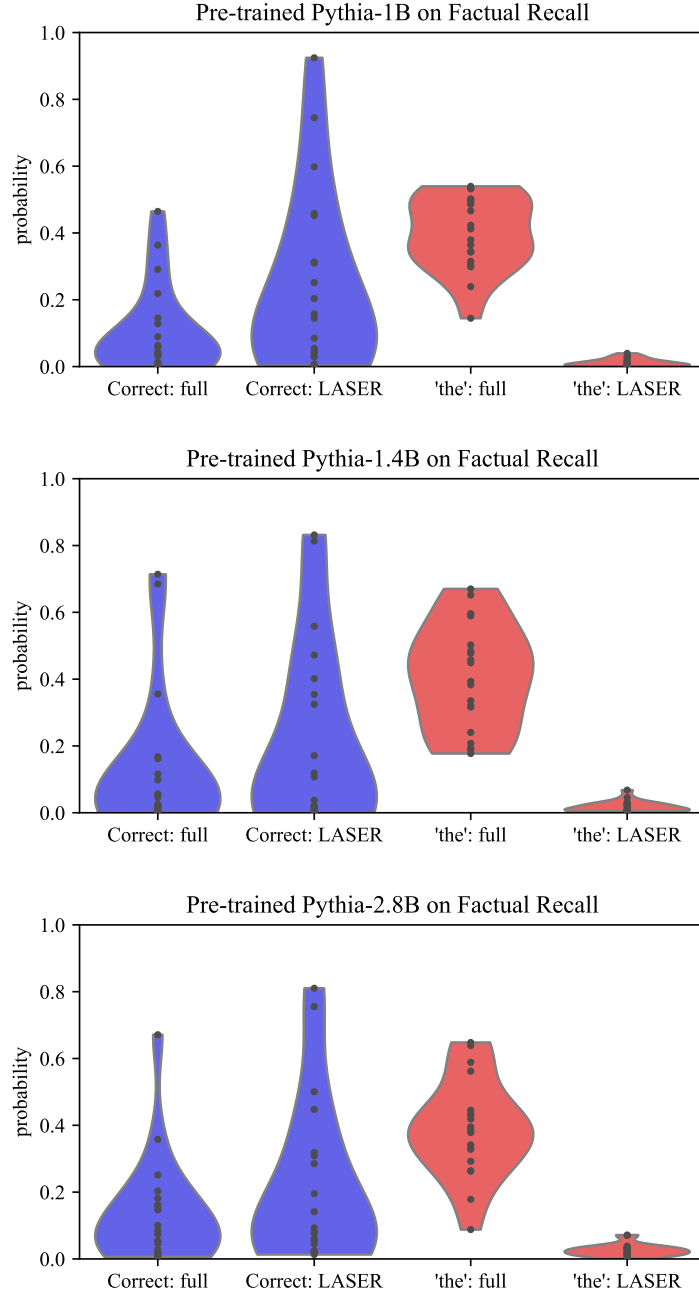


Figure 16: The prediction distributions of Pythia-1B, 1.4B and 2.8B on more examples of factual recall. Compared with the setting in Figure 5 (right), here we use 20 examples in Table 5. LASER turns out to significantly decrease the probability of "the" against the correct tokens.

Since $\alpha = \Theta(1)$ is much larger than $\frac{1}{N+1}$ when $N \gg 1$, due to law of large numbers, we have the population gradient $\nabla_{\mathbf{W}_F} L$ satisfying

$$\mathbf{W}_U(N+1)^\top (-\nabla_{\mathbf{W}_F} L) \mathbf{W}_E(q) \approx \alpha = \Theta(1),$$

$$\forall k \leq N: \quad \mathbf{W}_U(k)^\top (-\nabla_{\mathbf{W}_F} L) \mathbf{W}_E(q) < 0, \text{ with absolute value in } O(1/N).$$

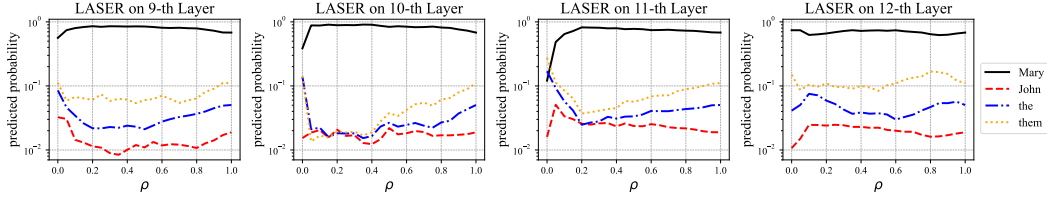


Figure 17: Predicted probability for $c \in \{\text{“Mary”, “them”, “the”, “John”}\}$. LASER is conducted on input matrices of MLP layers on the layer $l = 9, 10, 11, 12$ of GPT-2 Small. The input is “When Mary and John went to a store, John gave a drink to”. The horizontal is the fraction of preserved rank, $\rho \in [0, 1]$, where $\rho = 1$ stands for the full model. It turns out LASER clearly decreases probability of “the” and “them” when $\rho \in [0.1, 0.8]$ for layer $l = 9, 10, 11$, compared with the full model.

The variance of the gradient projection onto $\mathbf{W}_U(N+1)\mathbf{W}_E(q)^\top$ of a single data point follows that of Bernoulli distribution with parameter α , which means

$$\text{Var}\left[\frac{1}{N+1} - \mathbb{1}\{y = N+1\}\right] = \alpha(1-\alpha). \quad (8)$$

Similarly, for any $k \leq N$, the variance of the gradient projection onto $\mathbf{W}_U(N+1)\mathbf{W}_E(q)^\top$ of a single data point follows that of Bernoulli distribution with parameter $\frac{1-\alpha}{N}$, which means

$$\text{Var}\left[\frac{1}{N+1} - \mathbb{1}\{y = k\}\right] = \frac{1-\alpha}{N} \left(1 - \frac{1-\alpha}{N}\right) = \Theta(1/N). \quad (9)$$

The ranges of the gradient projections’ deviation from the expectation are

$$\forall k \leq N : \begin{cases} \left| \frac{1}{N+1} - \mathbb{1}\{y = N+1\} - \left(\frac{1}{N+1} - \alpha\right) \right| \leq \max\{\alpha, 1-\alpha\}, \\ \left| \frac{1}{N+1} - \mathbb{1}\{y = k\} - \left(\frac{1}{N+1} - \frac{1-\alpha}{N}\right) \right| \lesssim 1. \end{cases} \quad (10)$$

For each choice of $k \in [N+1]$ *individually*, after having the expectation $\mu(k)$, variance $\sigma^2(k)$ and range $R(k)$, by applying Bernstein’s inequality, then: for each $k \in [N+1]$, with probability $1 - \delta$, it holds

$$\left| \mathbf{W}_U(k)^\top (\nabla_{\mathbf{W}_F} \hat{L}) \mathbf{W}_E(q) - \mu(k) \right| \leq \sqrt{\frac{4\sigma^2(k) \ln(\frac{2}{\delta})}{m}} + \frac{4R(k) \ln(\frac{2}{\delta})}{m}.$$

Then by the union bound in probability, we need $(N+1)$ events above to hold at the same time, so we can substitute δ with $\frac{\delta}{N+1}$ to have: with probability $1 - \delta$, for any $k \in [N+1]$, it holds

$$\left| \mathbf{W}_U(k)^\top (\nabla_{\mathbf{W}_F} \hat{L}) \mathbf{W}_E(q) - \mu(k) \right| \leq \sqrt{\frac{4\sigma^2(k) (\ln(N+1) + \ln(\frac{2}{\delta}))}{m}} + \frac{4R(k) (\ln(N+1) + \ln(\frac{2}{\delta}))}{m}. \quad (11)$$

□

D.2 GRADIENT FOR THE VALUE MATRIX \mathbf{W}_V

Lemma D.2. Consider zero initialization, $\mathbf{W}_V = \mathbf{W}_F = \mathbf{W}_{QK} = 0$. Then with probability $1 - \delta$, for any $j, k \in [N+1]$, it holds

$$\begin{aligned} & \left| \mathbf{W}_U(j)^\top (\nabla_{\mathbf{W}_V} \hat{L}) \mathbf{W}_E(k) - \mu(j, k) \right| \\ & \leq \sqrt{\frac{4\sigma^2(j, k) (2 \ln(N+1) + \ln(\frac{2}{\delta}))}{m}} + \frac{4R(j, k) (2 \ln(N+1) + \ln(\frac{2}{\delta}))}{m}, \end{aligned} \quad (12)$$

Table 3: $\mu(j, k), \sigma^2(j, k), R(j, k)$ for different choices of (j, k) in Lemma D.2.

j	k	μ	σ^2	R
$N + 1$	$N + 1$	$-\frac{\alpha^2}{N}$	$\frac{\alpha^2}{TN} + \frac{\alpha^3 - \alpha^4}{N^2}$	$\frac{1}{2}$
$N + 1$	q	$-\frac{\alpha}{N}$	$\frac{\alpha}{TN} + \frac{\alpha - \alpha^2}{N^2}$	1
$N + 1$	$[N] \setminus \{q\}$	$-\frac{\alpha}{N}$	$\frac{\alpha}{TN} + \frac{\alpha - \alpha^2}{N^2}$	1
q	$N + 1$	$\frac{2\alpha - 1}{N^2}$	$\frac{1}{TN^2} + \frac{\alpha^2 - \alpha + 1}{N^3}$	$\frac{1}{2}$
q	q	$\frac{2\alpha - 1}{\alpha N^2}$	$\frac{\alpha^3 - \alpha^2 - \alpha + 2}{\alpha^3 TN^2} + \frac{\alpha^2 - \alpha + 1}{\alpha^2 N^3}$	1
q	$[N] \setminus \{q\}$	$\frac{\alpha}{N^2}$	$(2 - \alpha) \cdot \left(\frac{1}{TN^2} + \frac{1}{N^3} \right)$	1
$[N] \setminus \{q\}$	$N + 1$	$\frac{\alpha^2}{N^2}$	$(2 - \alpha) \left(\frac{\alpha}{TN^2} + \frac{\alpha^2}{N^3} \right)$	$\frac{1}{3}$
$[N] \setminus \{q\}$	q	$\frac{\alpha}{N^2}$	$(2 - \alpha) \left(\frac{1}{TN^2} + \frac{1}{N^3} \right)$	$\frac{1}{2}$
$[N] \setminus \{q\}$	j	$-\frac{\alpha^2 + 3\alpha - 1}{N^2}$	$\frac{1 + (1 - \alpha)(2 - \alpha)}{TN^2} + \frac{1 + (1 - \alpha)(2 - \alpha)^2}{N^3}$	1
$[N] \setminus \{q\}$	$[N] \setminus \{q, j\}$	$\frac{\alpha}{N^2}$	$(2 - \alpha) \left(\frac{1}{TN^2} + \frac{1}{N^3} \right)$	1

where $\mu(j, k), \sigma^2(j, k), R(j, k)$ are expectation, variance and range for different choices of (j, k) at listed in Table 3.

Proof. Due to zero initialization, i.e., $\mathbf{W}_V = \mathbf{W}_F = 0$, the current predicted probability is $\hat{p}_{\mathbf{W}}(k|x_i) \equiv \frac{1}{N+1}$ for all $i \in [m]$ and $k \in [N + 1]$. Meanwhile, the attention score is uniform as $\frac{1}{T}$ for all context positions due to $\mathbf{W}_K = 0$. Therefore, from Lemma H.1, we have

$$\nabla_{\mathbf{W}_F} \hat{L} = \frac{1}{m} \sum_{i=1}^m \left[\sum_{k=1}^{N+1} \left(\frac{1}{N+1} - \mathbb{1}\{y_i = k\} \right) \mathbf{W}_U(k) \left(\frac{1}{T} \sum_{t=1}^T x_{i,t} \right)^\top \right],$$

where $x_{i,t} \in \mathbb{R}^d = \mathbf{W}_E(z_{i,t}) + p_t$ is the input embedding with input token $z_{i,t}$ at position t in sequence i , together with positional encoding p_t for position t . With the assumption of orthonormality in Assumption D.1, we have the projection of $\nabla_{\mathbf{W}_F} \hat{L}$: $\forall j, k \in [N + 1]$,

$$\mathbf{W}_U(j)^\top (\nabla_{\mathbf{W}_F} \hat{L}) \mathbf{W}_E(k) = \frac{1}{m} \sum_{i=1}^m \left[\left(\frac{1}{N+1} - \mathbb{1}\{y_i = j\} \right) \left(\frac{1}{T} \sum_{t=1}^T \mathbb{1}\{z_{i,t} = k\} \right) \right].$$

Since each sample is drawn i.i.d., it suffices to discuss the expectation and variance of

$$\Gamma_i(j, k) \triangleq \left(\frac{1}{N+1} - \mathbb{1}\{z_{i,T+1} = j\} \right) \left(\frac{1}{T} \sum_{t=1}^T \mathbb{1}\{z_{i,t} = k\} \right),$$

$$\hat{\Gamma}(j, k) \triangleq \frac{1}{m} \sum_{i=1}^m \Gamma_i(j, k),$$

where we use the fact $y_i = z_{i,T+1}$.

Recall that, for each sample in the data generation process, the trigger q is fixed while the correct next token $\bar{y} \sim \text{Uniform}([N])$. Hence, conditioning on $z_{i,T} = q$, it has probability α for $z_{i,T+1} = N + 1$ and probability $1 - \alpha$ for $z_{i,T+1} = \bar{y}$. This leads to the necessity of discussing whether or not $\bar{y} = k$. Meanwhile, a corner case of $\bar{y} = q$ is also necessary to consider, as this implies an event that increases the counting $\frac{1}{T} \sum_{t=1}^T \mathbb{1}\{z_{i,t} = q\}$ than the case of $\bar{y} \neq q$.

Therefore, generally there are 10 cases due to different choices of (j, k) as follows:

1. $j = N + 1, k = N + 1$,
2. $j = N + 1, k = q$,
3. $j = N + 1, k \in [N] \setminus \{q\}$,

- 1512 4. $j = q, k = N + 1,$
 1513
 1514 5. $j = q, k = q,$
 1515
 1516 6. $j = q, k \in [N] \setminus \{q\},$
 1517
 1518 7. $j \in [N] \setminus \{q\}, k = N + 1,$
 1519
 1520 8. $j \in [N] \setminus \{q\}, k = q,$
 1521
 1522 9. $j \in [N] \setminus \{q\}, k = j,$
 1523
 1524 10. $j \in [N] \setminus \{q\}, k \in [N] \setminus \{q, j\}.$

1524 For each $\Gamma_i(j, k)$ *individually*, if we have its expectation $\mu(j, k)$, variance $\sigma^2(j, k)$ and range $R(j, k)$,
 1525 by applying Bernstein's inequality, then: for each $j, k \in [N + 1]$, with probability $1 - \delta$, it holds
 1526

$$1527 \left| \hat{\Gamma}(j, k) - \mu(j, k) \right| \leq \sqrt{\frac{4\sigma^2(j, k) \ln(\frac{2}{\delta})}{m}} + \frac{4R(j, k) \ln(\frac{2}{\delta})}{m}.$$

1530 Then by the union bound in probability, we need $(N + 1)^2$ events above to hold at the same time, so
 1531 we can substitute δ with $\frac{\delta}{(N+1)^2}$ to have: with probability $1 - \delta$, for any $j, k \in [N + 1]$, it holds
 1532

$$1533 \left| \hat{\Gamma}(j, k) - \mu(j, k) \right| \leq \sqrt{\frac{4\sigma^2(j, k) (2 \ln(N + 1) + \ln(\frac{2}{\delta}))}{m}} + \frac{4R(j, k) (2 \ln(N + 1) + \ln(\frac{2}{\delta}))}{m}. \quad (13)$$

1538 As a final step of the proof, now we elaborate the expectation, variance and range of $\Gamma_i(j, k)$ for these
 1539 10 cases.
 1540

1541 **Case 1:** $j = N + 1, k = N + 1.$

1542 There is probability $\frac{1}{N}$ for $\bar{y} = q$ and probability $\frac{N-1}{N}$ for $\bar{y} \neq q$. Hence, we have

$$1544 \mathbb{E}[\Gamma_i(j, k)] = \frac{1}{N} \mathbb{E}[\Gamma_i(j, k) | \bar{y} = q] + \frac{N-1}{N} \mathbb{E}[\Gamma_i(j, k) | \bar{y} \neq q],$$

$$1546 \mathbb{E}[\Gamma_i(j, k)^2] = \frac{1}{N} \mathbb{E}[\Gamma_i(j, k)^2 | \bar{y} = q] + \frac{N-1}{N} \mathbb{E}[\Gamma_i(j, k)^2 | \bar{y} \neq q].$$

1549 From Lemma E.2 and the independence between $\mathbb{1}\{z_{i,T+1} = N + 1\}$ and $\sum_{t \leq T} \mathbb{1}\{z_{i,t} =$
 1550 $k\}$, we have

$$1551 \mathbb{E}[\Gamma_i(j, k) | \bar{y} = q] \approx -\alpha \cdot \frac{1}{N},$$

$$1553 \mathbb{E}[\Gamma_i(j, k)^2 | \bar{y} = q] \approx \alpha \cdot \left(\frac{1}{TN} + \frac{1}{N^2} \right),$$

1556 where the second is from

$$1557 \mathbb{E} \left[\left(\frac{1}{N+1} - \mathbb{1}\{z_{i,T+1} = N + 1\} \right)^2 \right] = (1 - \alpha) \cdot \left(\frac{1}{N+1} \right)^2 + \alpha \cdot \left(\frac{1}{N+1} - 1 \right)^2 \approx \alpha.$$

1561 Similarly, from Lemma E.5, we have

$$1562 \mathbb{E}[\Gamma_i(j, k) | \bar{y} \neq q] \approx -\alpha \cdot \frac{\alpha}{N},$$

$$1564 \mathbb{E}[\Gamma_i(j, k)^2 | \bar{y} \neq q] \approx \alpha \cdot \left(\frac{\alpha}{TN} + \frac{\alpha^2}{N^2} \right).$$

1566
1567
1568
1569
1570
1571
1572
1573
1574
1575
1576

Therefore, it holds

$$\begin{aligned}\mathbb{E}[\Gamma_i(j, k)] &= \frac{1}{N} \frac{-\alpha}{N} + \frac{N-1}{N} \frac{-\alpha^2}{N} \approx -\frac{\alpha^2}{N}, \\ \mathbb{E}[\Gamma_i(j, k)^2] &= \frac{1}{N} \mathbb{E}[\Gamma_i(j, k)^2 | \bar{y} = q] + \frac{N-1}{N} \mathbb{E}[\Gamma_i(j, k)^2 | \bar{y} \neq q] \\ &\approx \frac{1}{N} \alpha \cdot \left(\frac{1}{TN} + \frac{1}{N^2} \right) + \frac{N-1}{N} \alpha \cdot \left(\frac{\alpha}{TN} + \frac{\alpha^2}{N^2} \right) \approx \frac{\alpha^2}{TN} + \frac{\alpha^3}{N^2}, \\ \text{Var}[\Gamma_i(j, k)] &= \mathbb{E}[\Gamma_i(j, k)^2] - \mathbb{E}[\Gamma_i(j, k)]^2 \approx \frac{\alpha^2}{TN} + \frac{\alpha^3 - \alpha^4}{N^2}.\end{aligned}$$

1577
1578
1579
1580

The range of $\Gamma_i(j, k)$ is

$$|\Gamma_i(j, k) - \mathbb{E}[\Gamma_i(j, k)]| \leq \frac{1}{2},$$

and the extreme case is when half of the sequence is $N + 1$ with the rest all being q .

1581
1582

Case 2: $j = N + 1, k = q$.

1583
1584
1585
1586

Similar to Case 1, we have $\mathbb{1}\{z_{i, T+1} = N + 1\}$ is independent of $\sum_{t \leq T} \mathbb{1}\{z_{i, t} = k\}$.

From Lemma E.1, we have

1587
1588
1589
1590
1591

$$\begin{aligned}\mathbb{E}[\Gamma_i(j, k) | \bar{y} = q] &\approx -\alpha \cdot \frac{1}{\alpha N}, \\ \mathbb{E}[\Gamma_i(j, k)^2 | \bar{y} = q] &\approx \alpha \cdot \left(\frac{1}{\alpha TN} \left(-1 + \frac{2}{\alpha^2} \right) + \frac{1}{\alpha^2 N^2} \right).\end{aligned}$$

1592

From Lemma E.4, we have

1593
1594
1595
1596
1597

$$\begin{aligned}\mathbb{E}[\Gamma_i(j, k) | \bar{y} \neq q] &\approx -\alpha \cdot \frac{1}{N}, \\ \mathbb{E}[\Gamma_i(j, k)^2 | \bar{y} \neq q] &\approx \alpha \cdot \left(\frac{1}{TN} + \frac{1}{N^2} \right).\end{aligned}$$

1598
1599

Therefore, we have

1600
1601
1602
1603
1604
1605
1606

$$\begin{aligned}\mathbb{E}[\Gamma_i(j, k)] &= \frac{1}{N} \mathbb{E}[\Gamma_i(j, k) | \bar{y} = q] + \frac{N-1}{N} \mathbb{E}[\Gamma_i(j, k) | \bar{y} \neq q] \approx -\frac{\alpha}{N}, \\ \mathbb{E}[\Gamma_i(j, k)^2] &= \frac{1}{N} \mathbb{E}[\Gamma_i(j, k)^2 | \bar{y} = q] + \frac{N-1}{N} \mathbb{E}[\Gamma_i(j, k)^2 | \bar{y} \neq q] \approx \frac{\alpha}{TN} + \frac{\alpha}{N^2}, \\ \text{Var}[\Gamma_i(j, k)] &= \mathbb{E}[\Gamma_i(j, k)^2] - \mathbb{E}[\Gamma_i(j, k)]^2 \approx \frac{\alpha}{TN} + \frac{\alpha - \alpha^2}{N^2}.\end{aligned}$$

1607
1608

The range of $\Gamma_i(j, k)$ is

1609

$$|\Gamma_i(j, k) - \mathbb{E}[\Gamma_i(j, k)]| \lesssim 1,$$

1610
1611

and the extreme case is when $\bar{y} = q$ and the sequence is all q 's.

1612
1613

Case 3: $j = N + 1, k \in [N] \setminus \{q\}$.

1614
1615

Similar to Case 1, we have $\mathbb{1}\{z_{i, T+1} = N + 1\}$ is independent of $\sum_{t \leq T} \mathbb{1}\{z_{i, t} = k\}$.

From Lemma E.3, we have

1616
1617
1618
1619

$$\begin{aligned}\mathbb{E}[\Gamma_i(j, k) | \bar{y} = q] &\approx -\alpha \cdot \frac{1}{N}, \\ \mathbb{E}[\Gamma_i(j, k)^2 | \bar{y} = q] &\approx \alpha \cdot \left(\frac{1}{TN} + \frac{1}{N^2} \right).\end{aligned}$$

From Lemma E.7, we have

$$\begin{aligned}\mathbb{E}[\Gamma_i(j, k)|\bar{y} \neq q] &\approx -\alpha \cdot \frac{1}{N}, \\ \mathbb{E}[\Gamma_i(j, k)^2|\bar{y} \neq q] &\approx \alpha \cdot \left(\frac{1}{TN} + \frac{1}{N^2}\right).\end{aligned}$$

Therefore, we have

$$\begin{aligned}\mathbb{E}[\Gamma_i(j, k)] &\approx -\alpha \cdot \frac{1}{N}, \\ \mathbb{E}[\Gamma_i(j, k)^2] &\approx \alpha \cdot \left(\frac{1}{TN} + \frac{1}{N^2}\right), \\ \text{Var}[\Gamma_i(j, k)] &= \mathbb{E}[\Gamma_i(j, k)^2] - \mathbb{E}[\Gamma_i(j, k)]^2 \approx \frac{\alpha}{TN} + \frac{\alpha - \alpha^2}{N^2}.\end{aligned}$$

The range of $\Gamma_i(j, k)$ is

$$|\Gamma_i(j, k) - \mathbb{E}[\Gamma_i(j, k)]| \lesssim 1,$$

and the extreme case is when all of the sequence except the last one is k .

Case 4: $j = q, k = N + 1$.

If $\bar{y} \neq q$, we always have $z_{i, T+1} \neq q$ because $z_{i, T+1} \in \{\bar{y}, N + 1\}$. If conditioning on $\bar{y} = q$, it has probability $1 - \alpha$ for $z_{i, T+1} = q$, independent of $\sum_{t \leq T} \mathbb{1}\{z_{i, t} = N + 1\}$.

From Lemma E.5, we have

$$\begin{aligned}\mathbb{E}[\Gamma_i(j, k)|\bar{y} \neq q] &\approx \frac{1}{N+1} \cdot \frac{\alpha}{N}, \\ \mathbb{E}[\Gamma_i(j, k)^2|\bar{y} \neq q] &\approx \frac{1}{N+1} \cdot \left(\frac{\alpha}{TN} + \frac{\alpha^2}{N^2}\right).\end{aligned}$$

From Lemma E.2, we have

$$\begin{aligned}\mathbb{E}[\Gamma_i(j, k)|\bar{y} = q] &\approx -(1 - \alpha) \cdot \frac{1}{N}, \\ \mathbb{E}[\Gamma_i(j, k)^2|\bar{y} = q] &\approx (1 - \alpha) \cdot \left(\frac{1}{TN} + \frac{1}{N^2}\right).\end{aligned}$$

Therefore, we have

$$\begin{aligned}\mathbb{E}[\Gamma_i(j, k)] &= \frac{1}{N} \mathbb{E}[\Gamma_i(j, k)|\bar{y} = q] + \frac{N-1}{N} \mathbb{E}[\Gamma_i(j, k)|\bar{y} \neq q] \approx \frac{2\alpha - 1}{N^2}, \\ \mathbb{E}[\Gamma_i(j, k)^2] &= \frac{1}{N} \mathbb{E}[\Gamma_i(j, k)^2|\bar{y} = q] + \frac{N-1}{N} \mathbb{E}[\Gamma_i(j, k)^2|\bar{y} \neq q] \approx \frac{1}{TN^2} + \frac{\alpha^2 - \alpha + 1}{N^3}, \\ \text{Var}[\Gamma_i(j, k)] &= \mathbb{E}[\Gamma_i(j, k)^2] - \mathbb{E}[\Gamma_i(j, k)]^2 \approx \frac{1}{TN^2} + \frac{\alpha^2 - \alpha + 1}{N^3}.\end{aligned}$$

The range of $\Gamma_i(j, k)$ is

$$|\Gamma_i(j, k) - \mathbb{E}[\Gamma_i(j, k)]| \lesssim \frac{1}{2},$$

and the extreme case is when $\bar{y} = q$ and half of the sequence is $N + 1$ with the rest all being q .

Case 5: $j = q, k = q$.

Similar to Case 4, if $\bar{y} \neq q$, we always have $z_{i, T+1} \neq q$. If conditioning on $\bar{y} = q$, it has probability $1 - \alpha$ for $z_{i, T+1} = q$, independent of $\sum_{t \leq T} \mathbb{1}\{z_{i, t} = q\}$.

From Lemma E.4, we have

$$\begin{aligned}\mathbb{E}[\Gamma_i(j, k)|\bar{y} \neq q] &\approx \frac{1}{N+1} \cdot \frac{1}{N}, \\ \mathbb{E}[\Gamma_i(j, k)^2|\bar{y} \neq q] &\approx \frac{1}{N+1} \cdot \left(\frac{1}{TN} + \frac{1}{N^2} \right).\end{aligned}$$

From Lemma E.1, we have

$$\begin{aligned}\mathbb{E}[\Gamma_i(j, k)|\bar{y} = q] &\approx -(1-\alpha) \cdot \frac{1}{\alpha N}, \\ \mathbb{E}[\Gamma_i(j, k)^2|\bar{y} = q] &\approx (1-\alpha) \cdot \left(\frac{1}{\alpha TN} \left(-1 + \frac{2}{\alpha^2} \right) + \frac{1}{\alpha^2 N^2} \right).\end{aligned}$$

Therefore, we have

$$\begin{aligned}\mathbb{E}[\Gamma_i(j, k)] &= \frac{1}{N} \mathbb{E}[\Gamma_i(j, k)|\bar{y} = q] + \frac{N-1}{N} \mathbb{E}[\Gamma_i(j, k)|\bar{y} \neq q] \approx \frac{2\alpha-1}{\alpha N^2}, \\ \mathbb{E}[\Gamma_i(j, k)^2] &= \frac{1}{N} \mathbb{E}[\Gamma_i(j, k)^2|\bar{y} = q] + \frac{N-1}{N} \mathbb{E}[\Gamma_i(j, k)^2|\bar{y} \neq q] \\ &\approx \frac{\alpha^3 - \alpha^2 - \alpha + 2}{\alpha^3 TN^2} + \frac{\alpha^2 - \alpha + 1}{\alpha^2 N^3}, \\ \text{Var}[\Gamma_i(j, k)] &= \mathbb{E}[\Gamma_i(j, k)^2] - \mathbb{E}[\Gamma_i(j, k)]^2 \approx \frac{\alpha^3 - \alpha^2 - \alpha + 2}{\alpha^3 TN^2} + \frac{\alpha^2 - \alpha + 1}{\alpha^2 N^3}.\end{aligned}$$

The range of $\Gamma_i(j, k)$ is

$$|\Gamma_i(j, k) - \mathbb{E}[\Gamma_i(j, k)]| \lesssim 1,$$

and the extreme case is when $\bar{y} = q$ and all of the sequence are q .

Case 6: $j = q, k \in [N] \setminus \{q\}$.

Similar to Case 4, if $\bar{y} \neq q$, we always have $z_{i, T+1} \neq q$. If conditioning on $\bar{y} = q$, it has probability $1 - \alpha$ for $z_{i, T+1} = q$, independent of $\sum_{t \leq T} \mathbb{1}\{z_{i, t} = k\}$.

Moreover, we need to consider whether $\bar{y} = k$ or not.

From Lemma E.6, we have

$$\begin{aligned}\mathbb{E}[\Gamma_i(j, k)|\bar{y} \neq q, k = \bar{y}] &\approx \frac{1}{N+1} \cdot \frac{2-\alpha}{N}, \\ \mathbb{E}[\Gamma_i(j, k)^2|\bar{y} \neq q, k = \bar{y}] &\approx \frac{1}{N+1} \cdot \left(\frac{2-\alpha}{TN} + \frac{(2-\alpha)^2}{N^2} \right).\end{aligned}$$

From Lemma E.7, we have

$$\begin{aligned}\mathbb{E}[\Gamma_i(j, k)|\bar{y} \neq q, k \in [N] \setminus \{q, \bar{y}\}] &\approx \frac{1}{N+1} \cdot \frac{1}{N}, \\ \mathbb{E}[\Gamma_i(j, k)^2|\bar{y} \neq q, k \in [N] \setminus \{q, \bar{y}\}] &\approx \frac{1}{N+1} \cdot \left(\frac{1}{TN} + \frac{1}{N^2} \right).\end{aligned}$$

From Lemma E.3, we have

$$\begin{aligned}\mathbb{E}[\Gamma_i(j, k)|\bar{y} = q] &\approx -(1-\alpha) \cdot \frac{1}{N}, \\ \mathbb{E}[\Gamma_i(j, k)^2|\bar{y} = q] &\approx (1-\alpha) \cdot \left(\frac{1}{TN} + \frac{1}{N^2} \right).\end{aligned}$$

1728
1729
1730
1731
1732
1733
1734
1735
1736
1737
1738
1739
1740
1741
1742
1743
1744
1745
1746
1747
1748
1749
1750
1751
1752
1753
1754
1755
1756
1757
1758
1759
1760
1761
1762
1763
1764
1765
1766
1767
1768
1769
1770
1771
1772
1773
1774
1775
1776
1777
1778
1779
1780
1781

Therefore, we have

$$\begin{aligned}\mathbb{E}[\Gamma_i(j, k)] &= \frac{1}{N}\mathbb{E}[\Gamma_i(j, k)|\bar{y} = q] + \frac{1}{N}\mathbb{E}[\Gamma_i(j, k)|\bar{y} \neq q, k = \bar{y}] \\ &\quad + \frac{N-2}{N}\mathbb{E}[\Gamma_i(j, k)|\bar{y} \neq q, k \in [N] \setminus \{q, \bar{y}\}] \\ &\approx \frac{\alpha}{N^2}, \\ \mathbb{E}[\Gamma_i(j, k)^2] &= \frac{1}{N}\mathbb{E}[\Gamma_i(j, k)^2|\bar{y} = q] + \frac{1}{N}\mathbb{E}[\Gamma_i(j, k)^2|\bar{y} \neq q, k = \bar{y}] \\ &\quad + \frac{N-2}{N}\mathbb{E}[\Gamma_i(j, k)^2|\bar{y} \neq q, k \in [N] \setminus \{q, \bar{y}\}] \\ &\approx (2 - \alpha) \cdot \left(\frac{1}{TN^2} + \frac{1}{N^3} \right), \\ \text{Var}[\Gamma_i(j, k)] &= \mathbb{E}[\Gamma_i(j, k)^2] - \mathbb{E}[\Gamma_i(j, k)]^2 \approx (2 - \alpha) \cdot \left(\frac{1}{TN^2} + \frac{1}{N^3} \right).\end{aligned}$$

The range of $\Gamma_i(j, k)$ is

$$|\Gamma_i(j, k) - \mathbb{E}[\Gamma_i(j, k)]| \lesssim 1,$$

and the extreme case is when all of the sequence except the last one are k .

Case 7: $j \in [N] \setminus \{q\}, k = N + 1$.

If $\bar{y} \neq j$, we always have $z_{i, T+1} \neq j$ because $z_{i, T+1} \in \{\bar{y}, N + 1\}$. If conditioning on $\bar{y} = j$, it has probability $1 - \alpha$ for $z_{i, T+1} = j$, independent of $\sum_{t \leq T} \mathbb{1}\{z_{i, t} = N + 1\}$.

Moreover, in the case of $\bar{y} \neq j$, we need to discuss whether or not $\bar{y} = q$.

From Lemma E.2, we have

$$\begin{aligned}\mathbb{E}[\Gamma_i(j, k)|\bar{y} = q] &\approx \frac{1}{N+1} \cdot \frac{1}{N}, \\ \mathbb{E}[\Gamma_i(j, k)^2|\bar{y} = q] &\approx \frac{1}{N+1} \cdot \left(\frac{1}{TN} + \frac{1}{N^2} \right).\end{aligned}$$

From Lemma E.5, we have

$$\begin{aligned}\mathbb{E}[\Gamma_i(j, k)|\bar{y} \neq q, \bar{y} \neq j] &\approx \frac{1}{N+1} \cdot \frac{\alpha}{N}, \\ \mathbb{E}[\Gamma_i(j, k)^2|\bar{y} \neq q, \bar{y} \neq j] &\approx \frac{1}{N+1} \cdot \left(\frac{\alpha}{TN} + \frac{\alpha^2}{N^2} \right).\end{aligned}$$

From Lemma E.5, we have

$$\begin{aligned}\mathbb{E}[\Gamma_i(j, k)|\bar{y} = j] &\approx -(1 - \alpha) \cdot \frac{\alpha}{N}, \\ \mathbb{E}[\Gamma_i(j, k)^2|\bar{y} = j] &\approx (1 - \alpha) \cdot \left(\frac{\alpha}{TN} + \frac{\alpha^2}{N^2} \right).\end{aligned}$$

Therefore, we have

$$\begin{aligned}\mathbb{E}[\Gamma_i(j, k)] &= \frac{1}{N}\mathbb{E}[\Gamma_i(j, k)|\bar{y} = q] + \frac{1}{N}\mathbb{E}[\Gamma_i(j, k)|\bar{y} = j] + \frac{N-2}{N}\mathbb{E}[\Gamma_i(j, k)|\bar{y} \neq q, \bar{y} \neq j] \\ &\approx \frac{\alpha^2}{N^2}, \\ \mathbb{E}[\Gamma_i(j, k)^2] &= \frac{1}{N}\mathbb{E}[\Gamma_i(j, k)^2|\bar{y} = q] + \frac{1}{N}\mathbb{E}[\Gamma_i(j, k)^2|\bar{y} = j] + \frac{N-2}{N}\mathbb{E}[\Gamma_i(j, k)^2|\bar{y} \neq q, \bar{y} \neq j] \\ &\approx (2 - \alpha) \left(\frac{\alpha}{TN^2} + \frac{\alpha^2}{N^3} \right), \\ \text{Var}[\Gamma_i(j, k)] &= \mathbb{E}[\Gamma_i(j, k)^2] - \mathbb{E}[\Gamma_i(j, k)]^2 \approx (2 - \alpha) \left(\frac{\alpha}{TN^2} + \frac{\alpha^2}{N^3} \right).\end{aligned}$$

1782 The range of $\Gamma_i(j, k)$ is

$$1783 \quad |\Gamma_i(j, k) - \mathbb{E}[\Gamma_i(j, k)]| \lesssim \frac{1}{3},$$

1786 and the extreme case is when $\bar{y} = j$ and one-third of the sequence are k , where the sequence
1787 has a repeated pattern like $[q, j, N + 1, q, j, N + 1, \dots]$.

1788 **Case 8:** $j \in [N] \setminus \{q\}, k = q$.

1790 Similar to Case 7, if $\bar{y} \neq j$, we always have $z_{i, T+1} \neq j$. If conditioning on $\bar{y} = j$, it has
1791 probability $1 - \alpha$ for $z_{i, T+1} = j$, independent of $\sum_{t \leq T} \mathbb{1}\{z_{i, t} = N + 1\}$.

1792 Moreover, in the case of $\bar{y} \neq j$, we need to discuss whether or not $\bar{y} = q$.

1793 From Lemma E.1, we have

$$1794 \quad \mathbb{E}[\Gamma_i(j, k) | \bar{y} = q] \approx \frac{1}{N+1} \cdot \frac{1}{\alpha N},$$

$$1795 \quad \mathbb{E}[\Gamma_i(j, k)^2 | \bar{y} = q] \approx \frac{1}{N+1} \cdot \left(\frac{T}{\alpha N} \left(-1 + \frac{2}{\alpha^2} \right) + \frac{T^2}{\alpha^2 N^2} \right).$$

1800 From Lemma E.4, we have

$$1801 \quad \mathbb{E}[\Gamma_i(j, k) | \bar{y} \neq q, \bar{y} \neq j] \approx \frac{1}{N+1} \cdot \frac{1}{N},$$

$$1802 \quad \mathbb{E}[\Gamma_i(j, k)^2 | \bar{y} \neq q, \bar{y} \neq j] \approx \frac{1}{N+1} \cdot \left(\frac{1}{TN} + \frac{1}{N^2} \right).$$

1807 From Lemma E.4, we have

$$1808 \quad \mathbb{E}[\Gamma_i(j, k) | \bar{y} = j] \approx -(1 - \alpha) \cdot \frac{1}{N},$$

$$1809 \quad \mathbb{E}[\Gamma_i(j, k)^2 | \bar{y} = j] \approx (1 - \alpha) \cdot \left(\frac{1}{TN} + \frac{1}{N^2} \right).$$

1813 Therefore, we have

$$1814 \quad \mathbb{E}[\Gamma_i(j, k)] = \frac{1}{N} \mathbb{E}[\Gamma_i(j, k) | \bar{y} = q] + \frac{1}{N} \mathbb{E}[\Gamma_i(j, k) | \bar{y} = j] + \frac{N-2}{N} \mathbb{E}[\Gamma_i(j, k) | \bar{y} \neq q, \bar{y} \neq j]$$

$$1815 \quad \approx \frac{\alpha}{N^2},$$

$$1816 \quad \mathbb{E}[\Gamma_i(j, k)^2] = \frac{1}{N} \mathbb{E}[\Gamma_i(j, k)^2 | \bar{y} = q] + \frac{1}{N} \mathbb{E}[\Gamma_i(j, k)^2 | \bar{y} = j] + \frac{N-2}{N} \mathbb{E}[\Gamma_i(j, k)^2 | \bar{y} \neq q, \bar{y} \neq j]$$

$$1817 \quad \approx (2 - \alpha) \left(\frac{1}{TN^2} + \frac{1}{N^3} \right),$$

$$1818 \quad \text{Var}[\Gamma_i(j, k)] = \mathbb{E}[\Gamma_i(j, k)^2] - \mathbb{E}[\Gamma_i(j, k)]^2 \approx (2 - \alpha) \left(\frac{1}{TN^2} + \frac{1}{N^3} \right).$$

1823 The range of $\Gamma_i(j, k)$ is

$$1824 \quad |\Gamma_i(j, k) - \mathbb{E}[\Gamma_i(j, k)]| \lesssim \frac{1}{2},$$

1825 and the extreme case is when $\bar{y} = j$ and half of the sequence are q .

1826 **Case 9:** $j \in [N] \setminus \{q\}, k = j$.

1827 Similar to Case 7, if $\bar{y} \neq j$, we always have $z_{i, T+1} \neq j$. If conditioning on $\bar{y} = j$, it has
1828 probability $1 - \alpha$ for $z_{i, T+1} = j$, independent of $\sum_{t \leq T} \mathbb{1}\{z_{i, t} = N + 1\}$.

1829 Moreover, in the case of $\bar{y} \neq j$, we need to discuss whether or not $\bar{y} = q$.

1836
1837
1838
1839
1840
1841
1842
1843
1844
1845
1846
1847
1848
1849
1850
1851
1852
1853
1854
1855
1856
1857
1858
1859
1860
1861
1862
1863
1864
1865
1866
1867
1868
1869
1870
1871
1872
1873
1874
1875
1876
1877
1878
1879
1880
1881
1882
1883
1884
1885
1886
1887
1888
1889

From Lemma E.3, we have

$$\begin{aligned}\mathbb{E}[\Gamma_i(j, k)|\bar{y} = q] &\approx \frac{1}{N+1} \cdot \frac{1}{N}, \\ \mathbb{E}[\Gamma_i(j, k)^2|\bar{y} = q] &\approx \frac{1}{N+1} \cdot \left(\frac{1}{TN} + \frac{1}{N^2} \right).\end{aligned}$$

From Lemma E.7, we have

$$\begin{aligned}\mathbb{E}[\Gamma_i(j, k)|\bar{y} \neq q, \bar{y} \neq j] &\approx \frac{1}{N+1} \cdot \frac{1}{N}, \\ \mathbb{E}[\Gamma_i(j, k)^2|\bar{y} \neq q, \bar{y} \neq j] &\approx \frac{1}{N+1} \cdot \left(\frac{1}{TN} + \frac{1}{N^2} \right).\end{aligned}$$

From Lemma E.6, we have

$$\begin{aligned}\mathbb{E}[\Gamma_i(j, k)|\bar{y} = j] &\approx -(1-\alpha) \cdot \frac{2-\alpha}{N}, \\ \mathbb{E}[\Gamma_i(j, k)^2|\bar{y} = j] &\approx (1-\alpha) \cdot \left(\frac{2-\alpha}{TN} + \frac{(2-\alpha)^2}{N^2} \right).\end{aligned}$$

Therefore, we have

$$\begin{aligned}\mathbb{E}[\Gamma_i(j, k)] &= \frac{1}{N}\mathbb{E}[\Gamma_i(j, k)|\bar{y} = q] + \frac{1}{N}\mathbb{E}[\Gamma_i(j, k)|\bar{y} = j] + \frac{N-2}{N}\mathbb{E}[\Gamma_i(j, k)|y \neq q, \bar{y} \neq j] \\ &\approx \frac{-\alpha^2 + 3\alpha - 1}{N^2}, \\ \mathbb{E}[\Gamma_i(j, k)^2] &= \frac{1}{N}\mathbb{E}[\Gamma_i(j, k)^2|\bar{y} = q] + \frac{1}{N}\mathbb{E}[\Gamma_i(j, k)^2|\bar{y} = j] + \frac{N-2}{N}\mathbb{E}[\Gamma_i(j, k)^2|y \neq q, \bar{y} \neq j] \\ &\approx \frac{1 + (1-\alpha)(2-\alpha)}{TN^2} + \frac{1 + (1-\alpha)(2-\alpha)^2}{N^3}, \\ \text{Var}[\Gamma_i(j, k)] &= \mathbb{E}[\Gamma_i(j, k)^2] - \mathbb{E}[\Gamma_i(j, k)]^2 \approx \frac{1 + (1-\alpha)(2-\alpha)}{TN^2} + \frac{1 + (1-\alpha)(2-\alpha)^2}{N^3}.\end{aligned}$$

The range of $\Gamma_i(j, k)$ is

$$|\Gamma_i(j, k) - \mathbb{E}[\Gamma_i(j, k)]| \lesssim 1,$$

and the extreme case is when $\bar{y} = j$ and all of the sequence are $j = k$.

Case 10: $j \in [N] \setminus \{q\}, k \in [N] \setminus \{q, j\}$.

Similar to Case 7, if $\bar{y} \neq j$, we always have $z_{i, T+1} \neq j$. If conditioning on $\bar{y} = j$, it has probability $1 - \alpha$ for $z_{i, T+1} = j$, independent of $\sum_{t \leq T} \mathbb{1}\{z_{i, t} = N + 1\}$.

Moreover, in the case of $\bar{y} \neq j$, we need to discuss whether or not $\bar{y} = q$.

From Lemma E.3, we have

$$\begin{aligned}\mathbb{E}[\Gamma_i(j, k)|\bar{y} = q] &\approx \frac{1}{N+1} \cdot \frac{1}{N}, \\ \mathbb{E}[\Gamma_i(j, k)^2|\bar{y} = q] &\approx \frac{1}{N+1} \cdot \left(\frac{1}{TN} + \frac{1}{N^2} \right).\end{aligned}$$

From Lemma E.7, we have

$$\begin{aligned}\mathbb{E}[\Gamma_i(j, k)|\bar{y} = j] &\approx -(1-\alpha) \cdot \frac{1}{N}, \\ \mathbb{E}[\Gamma_i(j, k)^2|\bar{y} = j] &\approx (1-\alpha) \cdot \left(\frac{1}{TN} + \frac{1}{N^2} \right).\end{aligned}$$

From Lemma E.6, we have

$$\begin{aligned}\mathbb{E}[\Gamma_i(j, k)|\bar{y} = k] &\approx \frac{1}{N+1} \cdot \frac{2-\alpha}{N}, \\ \mathbb{E}[\Gamma_i(j, k)^2|\bar{y} = k] &\approx \frac{1}{N+1} \cdot \left(\frac{2-\alpha}{TN} + \frac{(2-\alpha)^2}{N^2} \right).\end{aligned}$$

From Lemma E.7, we have

$$\begin{aligned}\mathbb{E}[\Gamma_i(j, k)|\bar{y} \neq q, \bar{y} \neq j, \bar{y} \neq k] &\approx \frac{1}{N+1} \cdot \frac{1}{N}, \\ \mathbb{E}[\Gamma_i(j, k)^2|\bar{y} \neq q, \bar{y} \neq j, \bar{y} \neq k] &\approx \frac{1}{N+1} \cdot \left(\frac{1}{TN} + \frac{1}{N^2} \right).\end{aligned}$$

Therefore, we have

$$\begin{aligned}\mathbb{E}[\Gamma_i(j, k)] &= \frac{1}{N}\mathbb{E}[\Gamma_i(j, k)|\bar{y} = q] + \frac{1}{N}\mathbb{E}[\Gamma_i(j, k)|\bar{y} = j] + \frac{1}{N}\mathbb{E}[\Gamma_i(j, k)|\bar{y} = k] \\ &\quad + \frac{N-3}{N}\mathbb{E}[\Gamma_i(j, k)|\bar{y} \neq q, \bar{y} \neq j] \\ &\approx \frac{\alpha}{N^2}, \\ \mathbb{E}[\Gamma_i(j, k)^2] &= \frac{1}{N}\mathbb{E}[\Gamma_i(j, k)^2|\bar{y} = q] + \frac{1}{N}\mathbb{E}[\Gamma_i(j, k)^2|\bar{y} = j] + \frac{1}{N}\mathbb{E}[\Gamma_i(j, k)^2|\bar{y} = k] \\ &\quad + \frac{N-3}{N}\mathbb{E}[\Gamma_i(j, k)^2|\bar{y} \neq q, \bar{y} \neq j] \\ &\approx (2-\alpha) \left(\frac{1}{TN} + \frac{1}{N^2} \right), \\ \text{Var}[\Gamma_i(j, k)] &= \mathbb{E}[\Gamma_i(j, k)^2] - \mathbb{E}[\Gamma_i(j, k)]^2 \approx (2-\alpha) \left(\frac{1}{TN^2} + \frac{1}{N^3} \right).\end{aligned}$$

The range of $\Gamma_i(j, k)$ is

$$|\Gamma_i(j, k) - \mathbb{E}[\Gamma_i(j, k)]| \lesssim 1,$$

and the extreme case is when $\bar{y} = j$ and all of the sequence except the last are k .

□

D.3 COMPLETING THE PROOF OF THEOREM 1

Theorem 4 (Restatement of Theorem 1). *Assume $N, T \gg 1, \alpha = \Theta(1)$. Consider a one gradient step update from zero-initialization on m i.i.d. samples of $z_{1:T}$ with separate learning rates η_f for \mathbf{W}_F and η_v for \mathbf{W}_V (note that the gradient on \mathbf{W}_{QK} is zero). For a test sequence $z_{1:T}$, the resulting logits for the feed-forward and attention blocks satisfy, with probability $1 - \delta$*

$$\begin{aligned}|\Delta(\xi_{ff}(x_{1:T})) - \eta_f \cdot \alpha| &\leq \eta_f \cdot O\left(\sqrt{\frac{\ln \frac{2(N+1)}{\delta}}{m}}\right), \\ \left|\Delta(\xi_{attn}(x_{1:T})) - \frac{\eta_v}{N} \cdot (\alpha^2 \hat{q} + \alpha(1 - \hat{q}))\right| &\leq \eta_v \cdot O\left(\sqrt{\frac{(\frac{1}{TN} + \frac{1}{N^2}) \ln \frac{2(N+1)}{\delta}}{m}} + \frac{\ln \frac{2(N+1)}{\delta}}{m}\right),\end{aligned}$$

where $\Delta(\xi) = \xi_{N+1} - \max_{j \in [N]} \xi_j$ is the margin of predicting the noise token and $\hat{q} = \frac{1}{T} \sum_{t \leq T} \mathbb{1}\{z_t = N+1\}$.

Proof. For \mathbf{W}_F , since the input is always $z_T = q$, the logits will be $[\xi_{\text{ff}}]_k = \mathbf{W}_U(k)^\top \mathbf{W}_F \mathbf{W}_E(q)$, $\forall k \in [N + 1]$. As \mathbf{W}_F is initialized from 0 and updated by GD with learning rate η_f , after one-step update, we have

$$\xi_{\text{ff}} = \mathbf{W}_U(k)^\top \left(-\eta_f \nabla_{\mathbf{W}_F} \hat{L} \Big|_{\mathbf{W}_F=0} \right) \mathbf{W}_E(q) \in \mathbb{R}^{N+1}.$$

By Lemma D.1, with probability $1 - \frac{1}{2}\delta$, we have

$$|[\xi_{\text{ff}}]_{N+1} - \eta_f \cdot \alpha| \leq \eta_f \cdot O \left(\sqrt{\frac{\ln \frac{2(N+1)}{\delta}}{m}} \right),$$

$$\forall k \leq N, \left| [\xi_{\text{ff}}]_k - \eta_f \cdot \left(\frac{1-\alpha}{N} - \frac{1}{N+1} \right) \right| \leq \eta_f \cdot O \left(\sqrt{\frac{\ln \frac{2(N+1)}{\delta}}{Nm}} + \frac{\ln \frac{2(N+1)}{\delta}}{m} \right),$$

and then triangle inequality finishes the proof for ξ_{ff} .

For \mathbf{W}_V , since the gradient on \mathbf{W}_{QK} at initialization is zero, \mathbf{W}_{QK} being zero after the first step induces a uniform attention over the input sequence. Consider the input sequence $\{z_i\}_{i=1}^T$, then the logits will be $[\xi_{\text{attn}}]_j = \mathbf{W}_U(j)^\top \mathbf{W}_V \frac{1}{T} \sum_{t=1}^T \mathbf{W}_E(z_t)$, $\forall j \in [N + 1]$.

Then considering the concentration bound of \mathbf{W}_V after one-step update in Lemma D.2, denoting $\Gamma(j, k) = \mathbf{W}_U(j)^\top \mathbf{W}_V \mathbf{W}_E(k)$, we have

$$[\xi_{\text{attn}}]_j = \frac{1}{T} \sum_{t \leq T} \Gamma(j, z_t) = \frac{1}{T} \sum_{k \leq N+1} n_k \cdot \Gamma(j, k),$$

with concentration bound for each $\Gamma(\cdot, \cdot)$ in Lemma D.2. From Table 3, note that for all $j = N + 1, k \leq N$, the expectation and variances are the same, while $k = N + 1$ has slightly different expectation and variance (but still in the same order of the others). Hence, denoting $\hat{q} = \frac{1}{T} \sum_{t \leq T} \mathbb{1}\{z_t = N + 1\}$ dependent of the test sample $z_{1:T}$, we have

$$\left| [\xi_{\text{attn}}(x_{1:T})]_{N+1} - \frac{\eta_v}{N} \cdot (\alpha^2 \hat{q} + \alpha(1 - \hat{q})) \right| \leq \eta_v \cdot O \left(\sqrt{\frac{(\frac{1}{TN} + \frac{1}{N^2}) \ln \frac{2(N+1)}{\delta}}{m}} + \frac{\ln \frac{2(N+1)}{\delta}}{m} \right).$$

Meanwhile, as the terms in Table 3 for $j \neq N + 1$ always have much smaller mean and variance by a factor $1/N$, using the Bernstein's inequalities for these terms in Lemma D.2 finishes the proof for \mathbf{W}_V .

□

E PROOF FOR FIRST AND SECOND MOMENTS IN LEMMA D.2

In this section, we will show the proof of the first and second moments of $\left[\sum_{1 \leq t \leq T} \mathbb{1}\{z_t = k\} \cdot \right]$ for all cases. Note that we do not consider $z_T = q$, but including it will not change the results, as $T \gg 1$ and z_T is explicitly fixed as q during data generation in Section 3. Generally, there are three factors to classify the cases as follows:

1. The i.i.d. uniformly sampled correct token $\bar{y} \in [N]$:
 - (a) $\bar{y} = q$,
 - (b) $\bar{y} \neq q$.
2. The target token $k \in [N + 1]$:
 - (a) $k = q$,
 - (b) $k = N + 1$.
 - (c) $k \leq N, k \neq q, k \neq \bar{y}$,
 - (d) (if $\bar{y} \neq q$) $k \leq N, k \neq q, k = \bar{y}$,

3. A condition about the token z_0 before the sequence $\{z_t\}_{t \geq 1}$:

- (a) $z_0 = q$,
- (b) $z_0 \in [N + 1] \setminus \{q\}$.

Note that when z_0 will be implicitly or explicitly considered. When there is no condition on the first token, which means $z_1 \sim \text{Uniform}([N])$, this belongs to Case (3b), *i.e.*, $z_0 \in [N + 1] \setminus \{q\}$, following the data generation process.

Table 4 summarizes all lemmas about the seven cases classified by the first two factors. The third factor about z_0 is explicitly presented in the proof of each corresponding lemma.

Table 4: All lemmas about the seven cases classified by \bar{y} and k .

	(2a)	(2b)	(2c)	(2d)
(1a)	E.1	E.2	E.3	N/A
(1b)	E.4	E.5	E.7	E.6

E.1 WHEN $\bar{y} = q$

Lemma E.1 ($\bar{y} = q, k = q$). *Following the data generation process, assuming $N, T \gg 1$ and $\alpha = \Theta(1)$, if $\bar{y} = q$ and $k = q$, it holds*

$$\begin{aligned} \mathbb{E} \left[\sum_{t \leq T} \mathbb{1}\{z_t = k\} \middle| \bar{y} = q, k = q \right] &\approx \frac{T}{\alpha N}, \\ \mathbb{E} \left[\left(\sum_{t \leq T} \mathbb{1}\{z_t = k\} \right)^2 \middle| \bar{y} = q, k = q \right] &\approx \frac{T}{\alpha N} \left(-1 + \frac{2}{\alpha^2} \right) + \frac{T^2}{\alpha^2 N^2}. \end{aligned} \quad (14)$$

Proof. For simplicity, we omit the condition of $\bar{y} = q, k = q$ in this proof. Denote

$$\begin{aligned} Y(T) &\triangleq \mathbb{E} \left[\sum_{t \leq T} \mathbb{1}\{z_t = k\} \middle| z_0 = q \right], \\ \hat{Y}(T) &\triangleq \mathbb{E} \left[\sum_{t \leq T} \mathbb{1}\{z_t = k\} \middle| z_0 \in [N + 1], z_0 \neq q \right]. \end{aligned}$$

Then the data generation process implies, $\forall T \geq 1$,

$$\begin{aligned} Y(T) &= p(z_1 = q | z_0 = q) \cdot (1 + Y(T - 1)) + p(z_1 = N + 1 | z_0 = q) \cdot \hat{Y}(T - 1), \\ \hat{Y}(T) &= p(z_1 = q | z_0 \neq q) \cdot (1 + Y(T - 1)) + p(z_1 \in [N] \setminus \{q\} | z_0 \neq q) \cdot \hat{Y}(T - 1). \end{aligned}$$

The iteration becomes

$$\begin{aligned} Y(T) &= (1 - \alpha) \cdot Y(T - 1) + \alpha \cdot \hat{Y}(T - 1) + 1 - \alpha, \\ \hat{Y}(T) &= \frac{1}{N} \cdot Y(T - 1) + \frac{N - 1}{N} \cdot \hat{Y}(T - 1) + \frac{1}{N}. \end{aligned}$$

This gives

$$\begin{aligned} Y(T) - \hat{Y}(T) &= (1 - \alpha - \frac{1}{N})(Y(T - 1) - \hat{Y}(T - 1)) + 1 - \alpha - \frac{1}{N}, \\ \frac{1}{N}Y(T) + \alpha\hat{Y}(T) &= \frac{1}{N}Y(T - 1) + \alpha\hat{Y}(T - 1) + \frac{1}{N}. \end{aligned}$$

2052 Consider the initialization $Y(0) = \hat{Y}(0) = 0$. This implies

$$2053$$

$$2054 \quad Y(T) - \hat{Y}(T) = \frac{1 - \alpha - \frac{1}{N}}{\alpha + \frac{1}{N}} \left(1 - \left(1 - \alpha - \frac{1}{N} \right)^T \right),$$

$$2055$$

$$2056 \quad \frac{1}{N}Y(T) + \alpha\hat{Y}(T) = \frac{1}{N}T.$$

2057 Then we obtain

$$2058$$

$$2059 \quad Y(T) \approx \frac{1}{\alpha N + 1}(T - \alpha N) + \frac{\alpha}{(\alpha + \frac{1}{N})^2} = \frac{1}{\alpha N + 1} \left(T - \alpha N + \frac{N^2}{\alpha N + 1} \right)$$

$$2060$$

$$2061 \quad \approx \frac{T}{\alpha N} - 1 + \frac{1}{\alpha^2},$$

$$2062$$

$$2063 \quad \hat{Y}(T) \approx \frac{1}{\alpha N + 1}T - \frac{N}{(\alpha N + 1)^2} + \frac{1}{\alpha N + 1}$$

$$2064$$

$$2065 \quad \approx \frac{T}{\alpha N}.$$

2066 Since the data generation process implicitly assumes $z_0 \neq q$, we have the desired expectation as

$$2067$$

$$2068 \quad \mathbb{E} \left[\sum_{t \leq T} \mathbb{1}\{z_t = k\} \middle| \bar{y} = q, k = q \right] = \hat{Y}(T) \approx \frac{T}{\alpha N}.$$

2069 To obtain the expectation of the quadratic term, we similarly denote the following terms with different z_0 :

$$2070$$

$$2071 \quad Z(T) \triangleq \mathbb{E} \left[\left(\sum_{t \leq T} \mathbb{1}\{z_t = k\} \right)^2 \middle| z_0 = q \right],$$

$$2072$$

$$2073 \quad \hat{Z}(T) \triangleq \mathbb{E} \left[\left(\sum_{t \leq T} \mathbb{1}\{z_t = k\} \right)^2 \middle| z_0 \in [N + 1], z_0 \neq q \right].$$

2074 Then the data generation process implies, $\forall T \geq 1$,

$$2075$$

$$2076 \quad Z(T) = p(z_1 = q | z_0 = q) \cdot (1 + 2Y(T - 1) + Z(T - 1)) + p(z_1 = N + 1 | z_0 = q) \cdot Z(T - 1),$$

$$2077$$

$$2078 \quad \hat{Z}(T) = p(z_1 = q | z_0 \neq q) \cdot (1 + 2Y(T - 1) + Z(T - 1)) + p(z_1 \neq q | z_0 \neq q) \cdot \hat{Z}(T - 1),$$

2079 where $2Y(T - 1)$ is due to $\mathbb{E}[(1 + \sum_{2 \leq t \leq T} \cdot)^2] = 1 + 2\mathbb{E}[\sum_{2 \leq t \leq T} \cdot] + \mathbb{E}[(\sum_{2 \leq t \leq T} \cdot)^2]$.

2080 Then the iteration becomes

$$2081$$

$$2082 \quad Z(T) = (1 - \alpha) \cdot (1 + 2Y(T - 1) + Z(T - 1)) + \alpha \cdot \hat{Z}(T - 1)$$

$$2083$$

$$2084 \quad = (1 - \alpha)Z(T - 1) + \alpha\hat{Z}(T - 1) + (1 - \alpha)(1 + 2Y(T - 1)),$$

$$2085$$

$$2086 \quad \hat{Z}(T) = \frac{1}{N} \cdot (1 + 2Y(T - 1) + Z(T - 1)) + \frac{N - 1}{N} \cdot \hat{Z}(T - 1)$$

$$2087$$

$$2088 \quad = \frac{1}{N}Z(T - 1) + \frac{N - 1}{N}\hat{Z}(T - 1) + \frac{1}{N}(1 + 2Y(T - 1)).$$

2089 This gives

$$2090$$

$$2091 \quad Z(T) - \hat{Z}(T) = (1 - \alpha - \frac{1}{N})(Z(T - 1) - \hat{Z}(T - 1)) + (1 - \alpha - \frac{1}{N})(1 + 2Y(T - 1)),$$

$$2092$$

$$2093 \quad \frac{1}{N}Z(T) + \alpha\hat{Z}(T) = \frac{1}{N}Z(T - 1) + \alpha\hat{Z}(T - 1) + \frac{1}{N}(1 + 2Y(T - 1)).$$

2106 Considering the initialization $Z(0) = \hat{Z}(0) = 0$, we have

$$\begin{aligned}
2107 \quad Z(T) - \hat{Z}(T) &= \sum_{t \leq T-1} \left(1 - \alpha - \frac{1}{N}\right)^{T-t} (1 + 2Y(t)) \\
2108 \quad &\approx \sum_{t \leq T-1} \left(1 - \alpha - \frac{1}{N}\right)^{T-t} \left(1 + \frac{2t}{\alpha N} - 2 + \frac{2}{\alpha^2}\right) \\
2109 \quad &\approx \left(-1 + \frac{2}{\alpha^2}\right) \frac{1 - \alpha}{\alpha} + \frac{2(1 - \alpha)}{\alpha^2} \cdot \frac{T}{N}. \\
2110 \quad \frac{1}{N}Z(T) + \alpha\hat{Z}(T) &= \frac{T}{N} + \frac{2}{N} \sum_{1 \leq t \leq T-1} Y(t) \\
2111 \quad &\approx \frac{T}{N} + \frac{2}{N} \sum_{1 \leq t \leq T-1} \left(\frac{t}{\alpha N} - 1 + \frac{1}{\alpha^2}\right) \\
2112 \quad &\approx \frac{T}{N} \left(-1 + \frac{2}{\alpha^2}\right) + \frac{T^2}{\alpha N^2}.
\end{aligned}$$

2123 Then we obtain

$$\begin{aligned}
2124 \quad Z(T) &\approx \frac{T}{N} \left(-\frac{3}{\alpha} + \frac{2}{\alpha^2} + \frac{2}{\alpha^3}\right) + \frac{T^2}{\alpha^2 N^2} + \frac{1 - \alpha}{\alpha} \left(\frac{2}{\alpha^2} - 1\right), \\
2125 \quad \hat{Z}(T) &\approx \frac{T}{\alpha N} \left(-1 + \frac{2}{\alpha^2}\right) + \frac{T^2}{\alpha^2 N^2}.
\end{aligned}$$

2126 Since the data generation process implicitly assumes $z_0 \neq q$, we have the desired expectation as

$$\mathbb{E} \left[\left(\sum_{t \leq T} \mathbb{1}\{z_t = k\} \right)^2 \middle| \bar{y} = q, k = q \right] = \hat{Z}(T) \approx \frac{T}{\alpha N} \left(-1 + \frac{2}{\alpha^2}\right) + \frac{T^2}{\alpha^2 N^2}.$$

2135 \square

2136 **Lemma E.2** ($\bar{y} = q, k = N + 1$). *Following the data generation process, assuming $N, T \gg 1$ and $\alpha = \Theta(1)$, if $\bar{y} = q$ and $k = N + 1$, it holds*

$$\begin{aligned}
2137 \quad &\mathbb{E} \left[\sum_{t \leq T} \mathbb{1}\{z_t = k\} \middle| \bar{y} = q, k = N + 1 \right] \approx \frac{T}{N}, \\
2138 \quad &\mathbb{E} \left[\left(\sum_{t \leq T} \mathbb{1}\{z_t = k\} \right)^2 \middle| \bar{y} = q, k = N + 1 \right] \approx \frac{T}{N} + \frac{T^2}{N^2}.
\end{aligned} \tag{15}$$

2143 *Proof.* For simplicity, we omit the condition of $\bar{y} = q, k = N + 1$ in this proof. Denote

$$\begin{aligned}
2144 \quad Y(T) &\triangleq \mathbb{E} \left[\sum_{t \leq T} \mathbb{1}\{z_t = k\} \middle| z_0 = q \right], \\
2145 \quad \hat{Y}(T) &\triangleq \mathbb{E} \left[\sum_{t \leq T} \mathbb{1}\{z_t = k\} \middle| z_0 \in [N + 1], z_0 \neq q \right].
\end{aligned}$$

2146 Then the data generation process implies, $\forall T \geq 1$,

$$\begin{aligned}
2147 \quad Y(T) &= p(z_1 = q | z_0 = q) \cdot Y(T - 1) + p(z_1 = N + 1 | z_0 = q) \cdot (1 + \hat{Y}(T - 1)), \\
2148 \quad \hat{Y}(T) &= p(z_1 = q | z_0 \neq q) \cdot Y(T - 1) + p(z_1 \in [N] \setminus \{q\} | z_0 \neq q) \cdot \hat{Y}(T - 1).
\end{aligned}$$

2160 The iteration becomes

$$2161 \quad Y(T) = (1 - \alpha) \cdot Y(T - 1) + \alpha \cdot \hat{Y}(T - 1) + \alpha,$$

$$2162 \quad \hat{Y}(T) = \frac{1}{N} \cdot Y(T - 1) + \frac{N - 1}{N} \cdot \hat{Y}(T - 1).$$

2165 This gives

$$2166 \quad Y(T) - \hat{Y}(T) = (1 - \alpha - \frac{1}{N})(Y(T - 1) - \hat{Y}(T - 1)) + \alpha,$$

$$2167 \quad \frac{1}{N}Y(T) + \alpha\hat{Y}(T) = \frac{1}{N}Y(T - 1) + \alpha\hat{Y}(T - 1) + \frac{\alpha}{N}.$$

2170 Consider the initialization $Y(0) = \hat{Y}(0) = 0$. This implies

$$2171 \quad Y(T) - \hat{Y}(T) = \frac{\alpha}{\alpha + \frac{1}{N}} \left(1 - \left(1 - \alpha - \frac{1}{N} \right)^T \right),$$

$$2172 \quad \frac{1}{N}Y(T) + \alpha\hat{Y}(T) = \frac{\alpha}{N}T.$$

2177 Then we obtain

$$2178 \quad Y(T) \approx \frac{T}{N} + 1,$$

$$2179 \quad \hat{Y}(T) \approx \frac{T}{N}.$$

2182 Since the data generation process implicitly assumes $z_0 \neq q$, we have the desired expectation as

$$2183 \quad \mathbb{E} \left[\sum_{t \leq T} \mathbb{1}\{z_t = k\} \middle| \bar{y} = q, k = N + 1 \right] = \hat{Y}(T) \approx \frac{T}{N}.$$

2188 To obtain the expectation of the quadratic term, we similarly denote the following terms with different z_0 :

$$2189 \quad Z(T) \triangleq \mathbb{E} \left[\left(\sum_{t \leq T} \mathbb{1}\{z_t = k\} \right)^2 \middle| z_0 = q \right],$$

$$2190 \quad \hat{Z}(T) \triangleq \mathbb{E} \left[\left(\sum_{t \leq T} \mathbb{1}\{z_t = k\} \right)^2 \middle| z_0 \in [N + 1], z_0 \neq q \right].$$

2197 Then the data generation process implies, $\forall T \geq 1$,

$$2198 \quad Z(T) = p(z_1 = q | z_0 = q) \cdot Z(T - 1) + p(z_1 = N + 1 | z_0 = q) \cdot (1 + 2\hat{Y}(T - 1) + \hat{Z}(T - 1)),$$

$$2199 \quad \hat{Z}(T) = p(z_1 = q | z_0 \neq q) \cdot Z(T - 1) + p(z_1 \neq q | z_0 \neq q) \cdot \hat{Z}(T - 1),$$

2201 where $2\hat{Y}(T - 1)$ is due to $\mathbb{E}[(1 + \sum_{2 \leq t \leq T} \cdot)^2] = 1 + 2\mathbb{E}[\sum_{2 \leq t \leq T} \cdot] + \mathbb{E}[(\sum_{2 \leq t \leq T} \cdot)^2]$.

2203 Then the iteration becomes

$$2204 \quad Z(T) = (1 - \alpha) \cdot Z(T - 1) + \alpha \cdot (1 + 2\hat{Y}(T - 1) + \hat{Z}(T - 1))$$

$$2205 \quad = (1 - \alpha)Z(T - 1) + \alpha\hat{Z}(T - 1) + \alpha(1 + 2\hat{Y}(T - 1)),$$

$$2206 \quad \hat{Z}(T) = \frac{1}{N} \cdot Z(T - 1) + \frac{N - 1}{N} \cdot \hat{Z}(T - 1).$$

2209 This gives

$$2210 \quad Z(T) - \hat{Z}(T) = (1 - \alpha - \frac{1}{N})(Z(T - 1) - \hat{Z}(T - 1)) + \alpha(1 + 2\hat{Y}(T - 1)),$$

$$2211 \quad \frac{1}{N}Z(T) + \alpha\hat{Z}(T) = \frac{1}{N}Z(T - 1) + \alpha\hat{Z}(T - 1) + \frac{\alpha}{N}(1 + 2\hat{Y}(T - 1)).$$

2214 Considering the initialization $Z(0) = \hat{Z}(0) = 0$, we have

$$\begin{aligned}
2215 & \\
2216 & Z(T) - \hat{Z}(T) = \sum_{t \leq T-1} \alpha \left(1 - \alpha - \frac{1}{N}\right)^{T-1-t} (1 + 2\hat{Y}(t)) \\
2217 & \\
2218 & \\
2219 & \approx \sum_{t \leq T-1} \alpha \left(1 - \alpha - \frac{1}{N}\right)^{T-1-t} \left(1 + \frac{2t}{N}\right) \\
2220 & \\
2221 & \approx \frac{2T}{N} + 1, \\
2222 & \\
2223 & \frac{1}{N}Z(T) + \alpha\hat{Z}(T) = \frac{\alpha T}{N} + \frac{2\alpha}{N} \sum_{1 \leq t \leq T-1} \hat{Y}(t) \\
2224 & \\
2225 & \approx \frac{\alpha T}{N} + \frac{2\alpha}{N} \sum_{1 \leq t \leq T-1} \frac{t}{N} \\
2226 & \\
2227 & \approx \frac{\alpha T}{N} + \frac{\alpha T^2}{N^2}. \\
2228 & \\
2229 & \\
2230 & \\
2231 &
\end{aligned}$$

2231 Then we obtain

$$\begin{aligned}
2232 & \\
2233 & Z(T) \approx 3\alpha \frac{T}{N} + \alpha \frac{T^2}{N^2} + \alpha, \\
2234 & \\
2235 & \hat{Z}(T) \approx \frac{T}{N} + \frac{T^2}{N^2}. \\
2236 &
\end{aligned}$$

2237 Since the data generation process implicitly assumes $z_0 \neq q$, we have the desired expectation as

$$\mathbb{E} \left[\left(\sum_{t \leq T} \mathbb{1}\{z_t = k\} \right)^2 \middle| \bar{y} = q, k = N + 1 \right] = \hat{Z}(T) \approx \frac{T}{N} + \frac{T^2}{N^2}.$$

2242 □

2243 **Lemma E.3** ($\bar{y} = q, k \leq N, k \neq q$). *Following the data generation process, assuming $N, T \gg 1$*
2244 *and $\alpha = \Theta(1)$, if $\bar{y} = q$ and $k \in [N] \setminus \{q\}$, it holds*

$$\begin{aligned}
2245 & \\
2246 & \mathbb{E} \left[\sum_{t \leq T} \mathbb{1}\{z_t = k\} \middle| \bar{y} = q, k \in [N] \setminus \{q\} \right] \approx \frac{T}{N}, \\
2247 & \\
2248 & \\
2249 & \mathbb{E} \left[\left(\sum_{t \leq T} \mathbb{1}\{z_t = k\} \right)^2 \middle| \bar{y} = q, k \in [N] \setminus \{q\} \right] \approx \frac{T}{N} + \frac{T^2}{N^2}. \tag{16} \\
2250 & \\
2251 & \\
2252 & \\
2253 &
\end{aligned}$$

2254 *Proof.* For simplicity, we omit the condition of $\bar{y} = q, k \in [N] \setminus \{q\}$ in this proof. Denote

$$\begin{aligned}
2255 & \\
2256 & Y(T) \triangleq \mathbb{E} \left[\sum_{t \leq T} \mathbb{1}\{z_t = k\} \middle| z_0 = q \right], \\
2257 & \\
2258 & \\
2259 & \hat{Y}(T) \triangleq \mathbb{E} \left[\sum_{t \leq T} \mathbb{1}\{z_t = k\} \middle| z_0 \in [N + 1], z_0 \neq q \right]. \\
2260 & \\
2261 & \\
2262 &
\end{aligned}$$

2263 Then the data generation process implies, $\forall T \geq 1$,

$$\begin{aligned}
2264 & Y(T) = p(z_1 = q | z_0 = q) \cdot Y(T - 1) + p(z_1 = N + 1 | z_0 = q) \cdot \hat{Y}(T - 1), \\
2265 & \hat{Y}(T) = p(z_1 = q | z_0 \neq q) \cdot Y(T - 1) \\
2266 & \quad + p(z_1 \in [N] \setminus \{q\} | z_0 \neq q) \cdot (p(z_1 = k | z_1 \sim \text{Uniform}([N] \setminus \{q\})) + \hat{Y}(T - 1)). \\
2267 &
\end{aligned}$$

2268 The iteration becomes

$$2269 \quad Y(T) = (1 - \alpha) \cdot Y(T - 1) + \alpha \cdot \hat{Y}(T - 1),$$

$$2270 \quad \hat{Y}(T) = \frac{1}{N} \cdot Y(T - 1) + \frac{N - 1}{N} \cdot (\hat{Y}(T - 1) + \frac{1}{N - 1}).$$

2273 This gives

$$2274 \quad Y(T) - \hat{Y}(T) = (1 - \alpha - \frac{1}{N})(Y(T - 1) - \hat{Y}(T - 1)) - \frac{1}{N},$$

$$2275 \quad \frac{1}{N}Y(T) + \alpha\hat{Y}(T) = \frac{1}{N}Y(T - 1) + \alpha\hat{Y}(T - 1) + \frac{\alpha}{N}.$$

2278 Consider the initialization $Y(0) = \hat{Y}(0) = 0$. This implies

$$2280 \quad Y(T) - \hat{Y}(T) = \frac{-\frac{1}{N}}{\alpha + \frac{1}{N}} \left(1 - \left(1 - \alpha - \frac{1}{N} \right)^T \right),$$

$$2281 \quad \frac{1}{N}Y(T) + \alpha\hat{Y}(T) = \frac{\alpha}{N}T.$$

2285 Then we obtain

$$2286 \quad Y(T) \approx \frac{T}{N},$$

$$2287 \quad \hat{Y}(T) \approx \frac{T}{N}.$$

2290 Since the data generation process implicitly assumes $z_0 \neq q$, we have the desired expectation as

$$2291 \quad \mathbb{E} \left[\sum_{t \leq T} \mathbb{1}\{z_t = k\} \middle| \bar{y} = q, k = N + 1 \right] = \hat{Y}(T) \approx \frac{T}{N}.$$

2296 To obtain the expectation of the quadratic term, we similarly denote the following terms with different z_0 :

$$2298 \quad Z(T) \triangleq \mathbb{E} \left[\left(\sum_{t \leq T} \mathbb{1}\{z_t = k\} \right)^2 \middle| z_0 = q \right],$$

$$2299 \quad \hat{Z}(T) \triangleq \mathbb{E} \left[\left(\sum_{t \leq T} \mathbb{1}\{z_t = k\} \right)^2 \middle| z_0 \in [N + 1], z_0 \neq q \right].$$

2305 Then the data generation process implies, $\forall T \geq 1$,

$$2306 \quad Z(T) = p(z_1 = q | z_0 = q) \cdot Z(T - 1) + p(z_1 = N + 1 | z_0 = q) \cdot \hat{Z}(T - 1),$$

$$2307 \quad \hat{Z}(T) = p(z_1 = q | z_0 \neq q) \cdot Z(T - 1) + p(z_1 \neq q | z_0 \neq q) \cdot \hat{Z}(T - 1)$$

$$2308 \quad + p(z_1 = k | z_0 \neq q) \cdot (1 + 2\hat{Y}(T - 1)),$$

2311 where $2\hat{Y}(T - 1)$ is due to $\mathbb{E}[(1 + \sum_{2 \leq t \leq T} \cdot)^2] = 1 + 2\mathbb{E}[\sum_{2 \leq t \leq T} \cdot] + \mathbb{E}[(\sum_{2 \leq t \leq T} \cdot)^2]$.

2313 Then the iteration becomes

$$2314 \quad Z(T) = (1 - \alpha) \cdot Z(T - 1) + \alpha \cdot \hat{Z}(T - 1),$$

$$2315 \quad \hat{Z}(T) = \frac{1}{N} \cdot Z(T - 1) + \frac{N - 1}{N} \cdot \hat{Z}(T - 1) + \frac{1}{N}(1 + 2\hat{Y}(T - 1)).$$

2317 This gives

$$2318 \quad Z(T) - \hat{Z}(T) = (1 - \alpha - \frac{1}{N})(Z(T - 1) - \hat{Z}(T - 1)) - \frac{1}{N}(1 + 2\hat{Y}(T - 1)),$$

$$2319 \quad \frac{1}{N}Z(T) + \alpha\hat{Z}(T) = \frac{1}{N}Z(T - 1) + \alpha\hat{Z}(T - 1) + \frac{\alpha}{N}(1 + 2\hat{Y}(T - 1)).$$

2322 Considering the initialization $Z(0) = \hat{Z}(0) = 0$, we have

$$\begin{aligned}
2323 & \\
2324 & Z(T) - \hat{Z}(T) = -\frac{1}{N} \sum_{t \leq T-1} \left(1 - \alpha - \frac{1}{N}\right)^{T-1-t} (1 + 2\hat{Y}(t)) \\
2325 & \\
2326 & \approx -\frac{1}{N} \sum_{t \leq T-1} \left(1 - \alpha - \frac{1}{N}\right)^{T-1-t} \left(1 + \frac{2t}{N}\right) \\
2327 & \\
2328 & \approx -\frac{1}{\alpha N} \left(\frac{2T}{N} + 1\right), \\
2329 & \\
2330 & \frac{1}{N}Z(T) + \alpha\hat{Z}(T) = \frac{\alpha T}{N} + \frac{2\alpha}{N} \sum_{1 \leq t \leq T-1} \hat{Y}(t) \\
2331 & \\
2332 & \approx \frac{\alpha T}{N} + \frac{2\alpha}{N} \sum_{1 \leq t \leq T-1} \frac{t}{N} \\
2333 & \\
2334 & \approx \frac{\alpha T}{N} + \frac{\alpha T^2}{N^2}.
\end{aligned}$$

2339 Then we obtain

$$\begin{aligned}
2340 & \\
2341 & Z(T) \approx \frac{T}{N} + \frac{T^2}{N^2}, \\
2342 & \\
2343 & \hat{Z}(T) \approx \frac{T}{N} + \frac{T^2}{N^2}. \\
2344 &
\end{aligned}$$

2345 Since the data generation process implicitly assumes $z_0 \neq q$, we have the desired expectation as

$$\mathbb{E} \left[\left(\sum_{t \leq T} \mathbb{1}\{z_t = k\} \right)^2 \middle| \bar{y} = q, k \in [N] \setminus \{q\} \right] = \hat{Z}(T) \approx \frac{T}{N} + \frac{T^2}{N^2}.$$

2350 \square

2351 E.2 WHEN $\bar{y} \neq q$

2352 **Lemma E.4** ($\bar{y} \neq q, k = q$). *Following the data generation process, assuming $N, T \gg 1$ and $\alpha = \Theta(1)$, if $\bar{y} \neq q$ and $k = q$, it holds*

$$\begin{aligned}
2353 & \\
2354 & \mathbb{E} \left[\sum_{t \leq T} \mathbb{1}\{z_t = k\} \middle| \bar{y} \neq q, k = q \right] \approx \frac{T}{N}, \\
2355 & \\
2356 & \mathbb{E} \left[\left(\sum_{t \leq T} \mathbb{1}\{z_t = k\} \right)^2 \middle| \bar{y} \neq q, k = q \right] \approx \frac{T}{N} + \frac{T^2}{N^2}. \\
2357 & \\
2358 & \\
2359 & \\
2360 & \\
2361 & \\
2362 & \\
2363 &
\end{aligned} \tag{17}$$

2364 *Proof.* For simplicity, we omit the condition of $\bar{y} \neq q, k = q$ in this proof. Denote

$$\begin{aligned}
2365 & \\
2366 & Y(T) \triangleq \mathbb{E} \left[\sum_{t \leq T} \mathbb{1}\{z_t = k\} \middle| z_0 = q \right], \\
2367 & \\
2368 & \hat{Y}(T) \triangleq \mathbb{E} \left[\sum_{t \leq T} \mathbb{1}\{z_t = k\} \middle| z_0 \in [N+1], z_0 \neq q \right]. \\
2369 & \\
2370 & \\
2371 &
\end{aligned}$$

2372 Then the data generation process implies, $\forall T \geq 1$,

$$\begin{aligned}
2373 & \\
2374 & Y(T) = \hat{Y}(T-1), \\
2375 & \hat{Y}(T) = p(z_1 = q | z_0 \neq q) \cdot (1 + Y(T-1)) + p(z_1 \in [N] \setminus \{q\} | z_0 \neq q) \cdot \hat{Y}(T-1).
\end{aligned}$$

2376 The iteration becomes

$$2377 \quad Y(T) = \hat{Y}(T-1),$$

$$2378 \quad \hat{Y}(T) = \frac{1}{N} \cdot Y(T-1) + \frac{N-1}{N} \cdot \hat{Y}(T-1) + \frac{1}{N}.$$

2381 This gives

$$2382 \quad Y(T) - \hat{Y}(T) = -\frac{1}{N}(Y(T-1) - \hat{Y}(T-1)) - \frac{1}{N},$$

$$2383 \quad \frac{1}{N}Y(T) + \hat{Y}(T) = \frac{1}{N}Y(T-1) + \hat{Y}(T-1) + \frac{1}{N}.$$

2387 Consider the initialization $Y(0) = \hat{Y}(0) = 0$. This implies

$$2388 \quad Y(T) - \hat{Y}(T) = \frac{-\frac{1}{N}}{1 + \frac{1}{N}} \left(1 - \left(-\frac{1}{N} \right)^T \right),$$

$$2389 \quad \frac{1}{N}Y(T) + \hat{Y}(T) = \frac{1}{N}T.$$

2394 Then we obtain

$$2395 \quad Y(T) \approx \frac{T}{N},$$

$$2396 \quad \hat{Y}(T) \approx \frac{T}{N}.$$

2399 Since the data generation process implicitly assumes $z_0 \neq q$, we have the desired expectation as

$$2400 \quad \mathbb{E} \left[\sum_{t \leq T} \mathbb{1}\{z_t = k\} \middle| \bar{y} \neq q, k = q \right] = \hat{Y}(T) \approx \frac{T}{N}.$$

2404 To obtain the expectation of the quadratic term, we similarly denote the following terms with different z_0 :

$$2407 \quad Z(T) \triangleq \mathbb{E} \left[\left(\sum_{t \leq T} \mathbb{1}\{z_t = k\} \right)^2 \middle| z_0 = q \right],$$

$$2408 \quad \hat{Z}(T) \triangleq \mathbb{E} \left[\left(\sum_{t \leq T} \mathbb{1}\{z_t = k\} \right)^2 \middle| z_0 \in [N+1], z_0 \neq q \right].$$

2414 Then the data generation process implies, $\forall T \geq 1$,

$$2415 \quad Z(T) = \hat{Z}(T-1),$$

$$2416 \quad \hat{Z}(T) = p(z_1 = q | z_0 \neq q) \cdot (1 + 2Y(T-1) + Z(T-1)) + p(z_1 \in [N] \setminus \{q\} | z_0 \neq q) \cdot \hat{Z}(T-1),$$

2417 where $2Y(T-1)$ is due to $\mathbb{E}[(1 + \sum_{2 \leq t \leq T} \cdot)^2] = 1 + 2\mathbb{E}[\sum_{2 \leq t \leq T} \cdot] + \mathbb{E}[(\sum_{2 \leq t \leq T} \cdot)^2]$.

2420 Then the iteration becomes

$$2421 \quad Z(T) = \hat{Z}(T-1),$$

$$2422 \quad \hat{Z}(T) = \frac{1}{N}Z(T-1) + \frac{N-1}{N}\hat{Z}(T-1) + \frac{1}{N}(1 + 2Y(T-1)).$$

2425 This gives

$$2426 \quad Z(T) - \hat{Z}(T) = -\frac{1}{N}(Z(T-1) - \hat{Z}(T-1)) - \frac{1}{N}(1 + 2Y(T-1)),$$

$$2427 \quad \frac{1}{N}Z(T) + \hat{Z}(T) = \frac{1}{N}Z(T-1) + \hat{Z}(T-1) + \frac{1}{N}(1 + 2Y(T-1)).$$

2430 Considering the initialization $Z(0) = \hat{Z}(0) = 0$, we have

$$\begin{aligned}
2431 & \\
2432 & Z(T) - \hat{Z}(T) = -\frac{1}{N} \sum_{t \leq T-1} \left(-\frac{1}{N}\right)^{T-1-t} (1 + 2Y(t)) \\
2433 & \\
2434 & \approx -\frac{1}{N} \sum_{t \leq T-1} \left(-\frac{1}{N}\right)^{T-1-t} \left(1 + \frac{2t}{N}\right) \\
2435 & \\
2436 & \approx -\frac{1}{N} - \frac{2T}{N^2}, \\
2437 & \\
2438 & \frac{1}{N}Z(T) + \hat{Z}(T) = \frac{T}{N} + \frac{2}{N} \sum_{1 \leq t \leq T-1} Y(t) \\
2439 & \\
2440 & \approx \frac{T}{N} + \frac{2}{N} \sum_{1 \leq t \leq T-1} \frac{t}{N} \\
2441 & \\
2442 & \approx \frac{T}{N} + \frac{T^2}{N^2}. \\
2443 & \\
2444 & \\
2445 & \\
2446 &
\end{aligned}$$

2447 Then we obtain

$$\begin{aligned}
2448 & Z(T) \approx \frac{T}{N} + \frac{T^2}{N^2}, \\
2449 & \\
2450 & \hat{Z}(T) \approx \frac{T}{N} + \frac{T^2}{N^2}. \\
2451 &
\end{aligned}$$

2452 Since the data generation process implicitly assumes $z_0 \neq q$, we have the desired expectation as

$$\begin{aligned}
2453 & \\
2454 & \mathbb{E} \left[\left(\sum_{t \leq T} \mathbb{1}\{z_t = k\} \right)^2 \middle| \bar{y} = q, k \in [N] \setminus \{q\} \right] = \hat{Z}(T) \approx \frac{T}{N} + \frac{T^2}{N^2}. \\
2455 & \\
2456 &
\end{aligned}$$

□

2457
2458 **Lemma E.5** ($\bar{y} \neq q, k = N + 1$). *Following the data generation process, assuming $N, T \gg 1$ and*
2459 *$\alpha = \Theta(1)$, if $\bar{y} \neq q$ and $k = N + 1$, it holds*

$$\begin{aligned}
2460 & \\
2461 & \mathbb{E} \left[\sum_{t \leq T} \mathbb{1}\{z_t = k\} \middle| \bar{y} \neq q, k = N + 1 \right] \approx \frac{\alpha T}{N}, \\
2462 & \\
2463 & \mathbb{E} \left[\left(\sum_{t \leq T} \mathbb{1}\{z_t = k\} \right)^2 \middle| \bar{y} \neq q, k = N + 1 \right] \approx \frac{\alpha T}{N} + \frac{\alpha^2 T^2}{N^2}. \\
2464 & \\
2465 & \\
2466 & \\
2467 &
\end{aligned} \tag{18}$$

2468 *Proof.* For simplicity, we omit the condition of $\bar{y} \neq q, k = N + 1$ in this proof. Denote

$$\begin{aligned}
2469 & \\
2470 & Y(T) \triangleq \mathbb{E} \left[\sum_{t \leq T} \mathbb{1}\{z_t = k\} \middle| z_0 = q \right], \\
2471 & \\
2472 & \hat{Y}(T) \triangleq \mathbb{E} \left[\sum_{t \leq T} \mathbb{1}\{z_t = k\} \middle| z_0 \in [N + 1], z_0 \neq q \right]. \\
2473 & \\
2474 & \\
2475 &
\end{aligned}$$

2476 Then the data generation process implies, $\forall T \geq 1$,

$$\begin{aligned}
2477 & Y(T) = \hat{Y}(T - 1) + p(z_1 = N + 1 | z_0 = q), \\
2478 & \\
2479 & \hat{Y}(T) = p(z_1 = q | z_0 \neq q) \cdot Y(T - 1) + p(z_1 \in [N] \setminus \{q\} | z_0 \neq q) \cdot \hat{Y}(T - 1). \\
2480 &
\end{aligned}$$

2481 The iteration becomes

$$\begin{aligned}
2482 & Y(T) = \hat{Y}(T - 1) + \alpha, \\
2483 & \hat{Y}(T) = \frac{1}{N} \cdot Y(T - 1) + \frac{N - 1}{N} \cdot \hat{Y}(T - 1).
\end{aligned}$$

2484 This gives
2485

$$2486 \quad Y(T) - \hat{Y}(T) = -\frac{1}{N}(Y(T-1) - \hat{Y}(T-1)) + \alpha,$$

$$2487 \quad \frac{1}{N}Y(T) + \hat{Y}(T) = \frac{1}{N}Y(T-1) + \hat{Y}(T-1) + \frac{\alpha}{N}.$$

2490 Consider the initialization $Y(0) = \hat{Y}(0) = 0$. This implies

$$2492 \quad Y(T) - \hat{Y}(T) = \frac{\alpha}{1 + \frac{1}{N}} \left(1 - \left(-\frac{1}{N} \right)^T \right),$$

$$2493 \quad \frac{1}{N}Y(T) + \hat{Y}(T) = \frac{\alpha}{N}T.$$

2498 Then we obtain

$$2499 \quad Y(T) \approx \frac{\alpha T}{N} + \alpha,$$

$$2500 \quad \hat{Y}(T) \approx \frac{\alpha T}{N}.$$

2504 Since the data generation process implicitly assumes $z_0 \neq q$, we have the desired expectation as

$$2505 \quad \mathbb{E} \left[\sum_{t \leq T} \mathbb{1}\{z_t = k\} \middle| \bar{y} \neq q, k = q \right] = \hat{Y}(T) \approx \frac{\alpha T}{N}.$$

2510 To obtain the expectation of the quadratic term, we similarly denote the following terms with different
2511 z_0 :

$$2512 \quad Z(T) \triangleq \mathbb{E} \left[\left(\sum_{t \leq T} \mathbb{1}\{z_t = k\} \right)^2 \middle| z_0 = q \right],$$

$$2513 \quad \hat{Z}(T) \triangleq \mathbb{E} \left[\left(\sum_{t \leq T} \mathbb{1}\{z_t = k\} \right)^2 \middle| z_0 \in [N+1], z_0 \neq q \right].$$

2520 Then the data generation process implies, $\forall T \geq 1$,

$$2521 \quad Z(T) = \hat{Z}(T-1) + p(z_1 = N+1 | z_0 = q) \cdot (1 + 2\hat{Y}(T-1)),$$

$$2522 \quad \hat{Z}(T) = p(z_1 = q | z_0 \neq q) \cdot Z(T-1) + p(z_1 \in [N] \setminus \{q\} | z_0 \neq q) \cdot \hat{Z}(T-1),$$

2525 where $2\hat{Y}(T-1)$ is due to $\mathbb{E}[(1 + \sum_{2 \leq t \leq T} \cdot)^2] = 1 + 2\mathbb{E}[\sum_{2 \leq t \leq T} \cdot] + \mathbb{E}[(\sum_{2 \leq t \leq T} \cdot)^2]$.

2527 Then the iteration becomes

$$2528 \quad Z(T) = \hat{Z}(T-1) + \alpha(1 + 2\hat{Y}(T-1)),$$

$$2529 \quad \hat{Z}(T) = \frac{1}{N}Z(T-1) + \frac{N-1}{N}\hat{Z}(T-1).$$

2533 This gives

$$2534 \quad Z(T) - \hat{Z}(T) = -\frac{1}{N}(Z(T-1) - \hat{Z}(T-1)) + \alpha(1 + 2\hat{Y}(T-1)),$$

$$2535 \quad \frac{1}{N}Z(T) + \hat{Z}(T) = \frac{1}{N}Z(T-1) + \hat{Z}(T-1) + \frac{\alpha}{N}(1 + 2\hat{Y}(T-1)).$$

2538 Considering the initialization $Z(0) = \hat{Z}(0) = 0$, we have

$$\begin{aligned}
2539 & \\
2540 & Z(T) - \hat{Z}(T) = \alpha \sum_{t \leq T-1} \left(-\frac{1}{N}\right)^{T-1-t} (1 + 2\hat{Y}(t)) \\
2541 & \\
2542 & \approx \alpha \sum_{t \leq T-1} \left(-\frac{1}{N}\right)^{T-1-t} \left(1 + \frac{2\alpha t}{N}\right) \\
2543 & \\
2544 & \approx \frac{2\alpha^2 T}{N} + \alpha, \\
2545 & \\
2546 & \frac{1}{N}Z(T) + \hat{Z}(T) = \frac{\alpha T}{N} + \frac{2\alpha}{N} \sum_{1 \leq t \leq T-1} \hat{Y}(t) \\
2547 & \\
2548 & \approx \frac{\alpha T}{N} + \frac{2\alpha}{N} \sum_{1 \leq t \leq T-1} \frac{\alpha t}{N} \\
2549 & \\
2550 & \approx \frac{\alpha T}{N} + \frac{\alpha^2 T^2}{N^2}.
\end{aligned}$$

2554 Then we obtain

$$\begin{aligned}
2555 & \\
2556 & Z(T) \approx \frac{T}{N}(2\alpha^2 + \alpha) + \frac{\alpha^2 T^2}{N^2} + \alpha, \\
2557 & \\
2558 & \hat{Z}(T) \approx \frac{\alpha T}{N} + \frac{\alpha^2 T^2}{N^2}.
\end{aligned}$$

2560 Since the data generation process implicitly assumes $z_0 \neq q$, we have the desired expectation as

$$\mathbb{E} \left[\left(\sum_{t \leq T} \mathbb{1}\{z_t = k\} \right)^2 \middle| \bar{y} = q, k \in [N] \setminus \{q\} \right] = \hat{Z}(T) \approx \frac{\alpha T}{N} + \frac{\alpha^2 T^2}{N^2}.$$

2565 □

2566 **Lemma E.6** ($\bar{y} \neq q, k = \bar{y}$). *Following the data generation process, assuming $N, T \gg 1$ and*
2567 *$\alpha = \Theta(1)$, if $\bar{y} \neq q$ and $k = \bar{y}$, it holds*

$$\begin{aligned}
2568 & \\
2569 & \mathbb{E} \left[\sum_{t \leq T} \mathbb{1}\{z_t = k\} \middle| \bar{y} \neq q, k = \bar{y} \right] \approx (2 - \alpha) \frac{T}{N}, \\
2570 & \\
2571 & \\
2572 & \mathbb{E} \left[\left(\sum_{t \leq T} \mathbb{1}\{z_t = k\} \right)^2 \middle| \bar{y} \neq q, k = \bar{y} \right] \approx \frac{(2 - \alpha)T}{N} + \frac{(2 - \alpha)^2 T^2}{N^2}.
\end{aligned} \tag{19}$$

2576 *Proof.* For simplicity, we omit the condition of $\bar{y} \neq q, k = \bar{y}$ in this proof. Denote

$$\begin{aligned}
2577 & \\
2578 & Y(T) \triangleq \mathbb{E} \left[\sum_{t \leq T} \mathbb{1}\{z_t = k\} \middle| z_0 = q \right], \\
2579 & \\
2580 & \\
2581 & \hat{Y}(T) \triangleq \mathbb{E} \left[\sum_{t \leq T} \mathbb{1}\{z_t = k\} \middle| z_0 \in [N + 1], z_0 \neq q \right].
\end{aligned}$$

2584 Then the data generation process implies, $\forall T \geq 1$,

$$\begin{aligned}
2585 & Y(T) = \hat{Y}(T - 1) + p(z_1 = \bar{y} | z_0 = q), \\
2586 & \\
2587 & \hat{Y}(T) = p(z_1 = q | z_0 \neq q) \cdot Y(T - 1) + p(z_1 \in [N] \setminus \{q\} | z_0 \neq q) \cdot \hat{Y}(T - 1) + p(z_1 = \bar{y} | z_0 \neq q).
\end{aligned}$$

2588 The iteration becomes

$$\begin{aligned}
2589 & Y(T) = \hat{Y}(T - 1) + (1 - \alpha), \\
2590 & \hat{Y}(T) = \frac{1}{N} \cdot Y(T - 1) + \frac{N - 1}{N} \cdot \hat{Y}(T - 1) + \frac{1}{N}.
\end{aligned}$$

2591

2592 This gives
2593

$$2594 \quad Y(T) - \hat{Y}(T) = -\frac{1}{N}(Y(T-1) - \hat{Y}(T-1)) + (1 - \alpha - \frac{1}{N}),$$

$$2595 \quad \frac{1}{N}Y(T) + \hat{Y}(T) = \frac{1}{N}Y(T-1) + \hat{Y}(T-1) + \frac{2-\alpha}{N}.$$

2598 Consider the initialization $Y(0) = \hat{Y}(0) = 0$. This implies
2599

$$2600 \quad Y(T) - \hat{Y}(T) = \frac{1-\alpha-\frac{1}{N}}{1+\frac{1}{N}} \left(1 - \left(-\frac{1}{N}\right)^T\right),$$

$$2601 \quad \frac{1}{N}Y(T) + \hat{Y}(T) = \frac{2-\alpha}{N}T.$$

2605 Then we obtain
2606

$$2607 \quad Y(T) \approx (1-\alpha) + (2-\alpha)\frac{T}{N},$$

$$2608 \quad \hat{Y}(T) \approx (2-\alpha)\frac{T}{N}.$$

2611 Since the data generation process implicitly assumes $z_0 \neq q$, we have the desired expectation as
2612

$$2613 \quad \mathbb{E} \left[\sum_{t \leq T} \mathbb{1}\{z_t = k\} \middle| \bar{y} \neq q, k = q \right] = \hat{Y}(T) \approx (2-\alpha)\frac{T}{N}.$$

2617 To obtain the expectation of the quadratic term, we similarly denote the following terms with different
2618 z_0 :
2619

$$2620 \quad Z(T) \triangleq \mathbb{E} \left[\left(\sum_{t \leq T} \mathbb{1}\{z_t = k\} \right)^2 \middle| z_0 = q \right],$$

$$2621 \quad \hat{Z}(T) \triangleq \mathbb{E} \left[\left(\sum_{t \leq T} \mathbb{1}\{z_t = k\} \right)^2 \middle| z_0 \in [N+1], z_0 \neq q \right].$$

2627 Then the data generation process implies, $\forall T \geq 1$,
2628

$$2629 \quad Z(T) = \hat{Z}(T-1) + p(z_1 = \bar{y} | z_0 = q) \cdot (1 + 2\hat{Y}(T-1)),$$

$$2630 \quad \hat{Z}(T) = p(z_1 = q | z_0 \neq q) \cdot Z(T-1) + p(z_1 \in [N] \setminus \{q\} | z_0 \neq q) \cdot \hat{Z}(T-1)$$

$$2631 \quad + p(z_1 = \bar{y} | z_0 \neq q) \cdot (1 + 2\hat{Y}(T-1)),$$

2634 where $2\hat{Y}(T-1)$ is due to $\mathbb{E}[(1 + \sum_{2 \leq t \leq T} \cdot)^2] = 1 + 2\mathbb{E}[\sum_{2 \leq t \leq T} \cdot] + \mathbb{E}[(\sum_{2 \leq t \leq T} \cdot)^2]$.
2635

2636 Then the iteration becomes

$$2637 \quad Z(T) = \hat{Z}(T-1) + (1-\alpha)(1 + 2\hat{Y}(T-1)),$$

$$2638 \quad \hat{Z}(T) = \frac{1}{N}Z(T-1) + \frac{N-1}{N}\hat{Z}(T-1) + \frac{1}{N}(1 + 2\hat{Y}(T-1)).$$

2641 This gives
2642

$$2643 \quad Z(T) - \hat{Z}(T) = -\frac{1}{N}(Z(T-1) - \hat{Z}(T-1)) + (1-\alpha-\frac{1}{N})(1 + 2\hat{Y}(T-1)),$$

$$2644 \quad \frac{1}{N}Z(T) + \hat{Z}(T) = \frac{1}{N}Z(T-1) + \hat{Z}(T-1) + \frac{2-\alpha}{N}(1 + 2\hat{Y}(T-1)).$$

2646 Considering the initialization $Z(0) = \hat{Z}(0) = 0$, we have

$$\begin{aligned}
2647 & Z(T) - \hat{Z}(T) = (1 - \alpha - \frac{1}{N}) \sum_{t \leq T-1} (-\frac{1}{N})^{T-1-t} (1 + 2\hat{Y}(t)) \\
2648 & \approx (1 - \alpha - \frac{1}{N}) \sum_{t \leq T-1} (-\frac{1}{N})^{T-1-t} \left(1 + \frac{2(2-\alpha)t}{N}\right) \\
2649 & \approx (1 - \alpha) \left(1 + \frac{2(2-\alpha)T}{N}\right), \\
2650 & \frac{1}{N}Z(T) + \hat{Z}(T) = \frac{(2-\alpha)T}{N} + \frac{2(2-\alpha)}{N} \sum_{1 \leq t \leq T-1} \hat{Y}(t) \\
2651 & \approx \frac{(2-\alpha)T}{N} + \frac{2(2-\alpha)}{N} \sum_{1 \leq t \leq T-1} \frac{(2-\alpha)t}{N} \\
2652 & \approx \frac{(2-\alpha)T}{N} + \frac{(2-\alpha)^2 T^2}{N^2}.
\end{aligned}$$

2653 Then we obtain

$$\begin{aligned}
2654 & Z(T) \approx \frac{T}{N}(2-\alpha)(3-2\alpha) + \frac{(2-\alpha)^2 T^2}{N^2} + (1-\alpha), \\
2655 & \hat{Z}(T) \approx \frac{(2-\alpha)T}{N} + \frac{(2-\alpha)^2 T^2}{N^2}.
\end{aligned}$$

2656 Since the data generation process implicitly assumes $z_0 \neq q$, we have the desired expectation as

$$\mathbb{E} \left[\left(\sum_{t \leq T} \mathbb{1}\{z_t = k\} \right)^2 \middle| \bar{y} = q, k \in [N] \setminus \{q\} \right] = \hat{Z}(T) \approx \frac{(2-\alpha)T}{N} + \frac{(2-\alpha)^2 T^2}{N^2}.$$

2657 \square

2658 **Lemma E.7** ($\bar{y} \neq q, k \leq N, k \neq q, k \neq \bar{y}$). *Following the data generation process, assuming $N, T \gg 1$ and $\alpha = \Theta(1)$, if $\bar{y} \neq q$ and $k \in [N] \setminus \{\bar{y}, q\}$, it holds*

$$\begin{aligned}
2659 & \mathbb{E} \left[\sum_{t \leq T} \mathbb{1}\{z_t = k\} \middle| \bar{y} \neq q, k \in [N] \setminus \{\bar{y}, q\} \right] \approx \frac{T}{N}, \\
2660 & \mathbb{E} \left[\left(\sum_{t \leq T} \mathbb{1}\{z_t = k\} \right)^2 \middle| \bar{y} \neq q, k \in [N] \setminus \{\bar{y}, q\} \right] \approx \frac{T}{N} + \frac{T^2}{N^2}.
\end{aligned} \tag{20}$$

2661 *Proof.* For simplicity, we omit the condition of $\bar{y} \neq q, k \in [N] \setminus \{\bar{y}, q\}$ in this proof. Denote

$$\begin{aligned}
2662 & Y(T) \triangleq \mathbb{E} \left[\sum_{t \leq T} \mathbb{1}\{z_t = k\} \middle| z_0 = q \right], \\
2663 & \hat{Y}(T) \triangleq \mathbb{E} \left[\sum_{t \leq T} \mathbb{1}\{z_t = k\} \middle| z_0 \in [N+1], z_0 \neq q \right].
\end{aligned}$$

2664 Then the data generation process implies, $\forall T \geq 1$,

$$\begin{aligned}
2665 & Y(T) = \hat{Y}(T-1), \\
2666 & \hat{Y}(T) = p(z_1 = q | z_0 \neq q) \cdot Y(T-1) + p(z_1 \in [N] \setminus \{q\} | z_0 \neq q) \cdot \hat{Y}(T-1) + p(z_1 = k | z_0 \neq q).
\end{aligned}$$

2700 The iteration becomes

$$2701 \quad Y(T) = \hat{Y}(T-1) + (1-\alpha),$$

$$2702 \quad \hat{Y}(T) = \frac{1}{N} \cdot Y(T-1) + \frac{N-1}{N} \cdot \hat{Y}(T-1) + \frac{1}{N}.$$

2703 Note that these two equations are exactly the same as those in Lemma E.4 with same initialization as
2704 $Y(0) = \hat{Y}(0) = 0$. Therefore, we have

$$2705 \quad Y(T) \approx \frac{T}{N},$$

$$2706 \quad \hat{Y}(T) \approx \frac{T}{N}.$$

2707 Since the data generation process implicitly assumes $z_0 \neq q$, we have the desired expectation as

$$2708 \quad \mathbb{E} \left[\sum_{t \leq T} \mathbb{1}\{z_t = k\} \middle| \bar{y} \neq q, k = q \right] = \hat{Y}(T) \approx \frac{T}{N}.$$

2709 To obtain the expectation of the quadratic term, we similarly denote the following terms with different
2710 z_0 :

$$2711 \quad Z(T) \triangleq \mathbb{E} \left[\left(\sum_{t \leq T} \mathbb{1}\{z_t = k\} \right)^2 \middle| z_0 = q \right],$$

$$2712 \quad \hat{Z}(T) \triangleq \mathbb{E} \left[\left(\sum_{t \leq T} \mathbb{1}\{z_t = k\} \right)^2 \middle| z_0 \in [N+1], z_0 \neq q \right].$$

2713 Then the data generation process implies, $\forall T \geq 1$,

$$2714 \quad Z(T) = \hat{Z}(T-1),$$

$$2715 \quad \hat{Z}(T) = p(z_1 = q | z_0 \neq q) \cdot Z(T-1) + p(z_1 \in [N] \setminus \{q\} | z_0 \neq q) \cdot \hat{Z}(T-1)$$

$$2716 \quad + p(z_1 = \bar{k} | z_0 \neq q) \cdot (1 + 2\hat{Y}(T-1)),$$

2717 where $2\hat{Y}(T-1)$ is due to $\mathbb{E}[(1 + \sum_{2 \leq t \leq T} \cdot)^2] = 1 + 2\mathbb{E}[\sum_{2 \leq t \leq T} \cdot] + \mathbb{E}[(\sum_{2 \leq t \leq T} \cdot)^2]$.

2718 Then the iteration becomes

$$2719 \quad Z(T) = \hat{Z}(T-1),$$

$$2720 \quad \hat{Z}(T) = \frac{1}{N} Z(T-1) + \frac{N-1}{N} \hat{Z}(T-1) + \frac{1}{N} (1 + 2\hat{Y}(T-1)).$$

2721 Again note that, since $Y(T) \approx \hat{Y}(T)$, these two equations are the same as those in Lemma E.4.
2722 Therefore, we have

$$2723 \quad Z(T) \approx \frac{T}{N} + \frac{T^2}{N^2},$$

$$2724 \quad \hat{Z}(T) \approx \frac{T}{N} + \frac{T^2}{N^2}.$$

2725 Since the data generation process implicitly assumes $z_0 \neq q$, we have the desired expectation as

$$2726 \quad \mathbb{E} \left[\left(\sum_{t \leq T} \mathbb{1}\{z_t = k\} \right)^2 \middle| \bar{y} = q, k \in [N] \setminus \{q\} \right] = \hat{Z}(T) \approx \frac{T}{N} + \frac{T^2}{N^2}.$$

2727

□

2754 **F PROOF OF THEOREM 2: TRAINING DYNAMICS OF THE ATTENTION LAYER**

2755 We consider the following simplified 1-layer model for the noisy in-context recall task.

$$\begin{aligned}
2756 \quad x_t &\triangleq \mathbf{W}_E(z_t) + \widetilde{\mathbf{W}}_E(z_{t-1}) \in \mathbb{R}^d, \\
2757 \quad \phi(x_T, x_{1:T}) &\triangleq \sum_{t \leq T} [\sigma(x_T^\top \mathbf{W}_{QK} x_{1:T})]_t \cdot \mathbf{W}_V x_t \in \mathbb{R}^d, \\
2758 \quad \xi_{\text{attn}}(x_{1:T}) &\triangleq \mathbf{W}_U \phi(x_T, x_{1:T}) \in \mathbb{R}^{N+1}, \\
2759 \quad \xi_{\text{ff}}(x_{1:T}) &\triangleq \mathbf{W}_U F(x_T) = \mathbf{W}_U \mathbf{W}_F x_T \in \mathbb{R}^{N+1},
\end{aligned} \tag{21}$$

2760 With zero initialization of \mathbf{W}_{QK} , \mathbf{W}_V , \mathbf{W}_F , we analyze the training dynamics of these three matrices in three phases:

- 2761 1. \mathbf{W}_F learns the noise association in $O(\frac{1}{\eta})$ time,
- 2762 2. \mathbf{W}_V learns to be identity for all tokens $k \in [N + 1]$,
- 2763 3. \mathbf{W}_{QK} attends to any position t such that $z_{t-1} = q$ and $z_t = \bar{y}$.

2764 **Assumption F.1.** *In this section, we make the following assumptions*

- 2765 1. (orthonormal embedding) $\mathbf{W}_E(i)^\top \mathbf{W}_E(j) = \widetilde{\mathbf{W}}_E(i)^\top \widetilde{\mathbf{W}}_E(j) = \mathbb{1}\{i = j\}$ and $\mathbf{W}_E(i)^\top \widetilde{\mathbf{W}}_E(j) = 0$ for any $i, j \in [N + 1]$.
- 2766 2. (Feed-forward learns noise association) After phase 1, the prediction for noise always satisfies $\hat{p}(N + 1|z_{1:T}) = \alpha$ for any $z_{1:T} \in [N + 1]^{\otimes T}$. If \hat{p} deviates from α , \mathbf{W}_F will learn the noise association in a more quick speed than the other weights, so that it is fair to assume $\hat{p} = \alpha$ for computing gradients of these weights.
- 2767 3. (Infinite samples) $m \rightarrow \infty$ so the training loss L is population loss.
- 2768 4. $\alpha \leq 1.5 - \sqrt{5}/2 \approx 0.38$. This is to ensure the sign $\mathbf{W}_U(j)^\top (-\nabla_{\mathbf{w}_V} L) \mathbf{W}_E(k) > 0$ for any $j = k \leq N$ in (23).

2769 **Phase 1:** In this phase, the impact of $\widetilde{\mathbf{W}}_E(z_{T-1})$ on \mathbf{W}_F and \mathbf{W}_V is negligible compared with that of $\mathbf{W}_E(z_T)$ because Z_{T-1} is close to uniform in $[N + 1]$ while $z_T = q$ is fixed.

2770 Lemma D.1 gives

$$\mathbf{W}_U(k)^\top (-\nabla_{\mathbf{w}_F} L) \mathbf{W}_E(q) = \begin{cases} \Theta(1), & \text{if } k = N + 1, \\ \Theta(\frac{1}{N}), & \text{if } k \leq N. \end{cases}$$

2771 Lemma D.2 gives

$$\mathbf{W}_U(j)^\top (-\nabla_{\mathbf{w}_V} L) \mathbf{W}_E(k) = \begin{cases} \Theta(\frac{1}{N}), & \text{if } j = N + 1, \forall k, \\ \Theta(\frac{1}{N^2}), & \text{if } j \leq N, \forall k. \end{cases} \tag{22}$$

2772 Note that the entries of the above projection have the following signs, with details as $-\mu$ in Table 3,

$$\mathbf{W}_U(j)^\top (-\nabla_{\mathbf{w}_V} L) \mathbf{W}_E(k) \begin{cases} > 0, & \text{if } (j = N + 1) \text{ or } (j = k) \text{ or } (j = q, k = N + 1), \\ < 0, & \text{otherwise.} \end{cases} \tag{23}$$

2773 The arguments in Appendix B.3 show

$$\mathbf{W}_E(j)^\top (-\nabla_{\mathbf{w}_{QK}} L) \mathbf{W}_E(q) = \begin{cases} -\Theta(\frac{1}{N^2}), & \text{if } j = N + 1, \\ \Theta(\frac{1}{N^3}), & \text{if } j \leq N. \end{cases} \tag{24}$$

2774 Therefore, during this phase, \mathbf{W}_F learns the noise association with effective graident norm of $\Theta(1)$ as $\mathbf{W}_U(N + 1)^\top (-\nabla_{\mathbf{w}_F} L) \mathbf{W}_E(q) = \Theta(1)$. Meanwhile, \mathbf{W}_F moves in the other directions

2808 uniformly in $\Theta(\frac{1}{N})$ as $\mathbf{W}_U(k)^\top (-\nabla_{\mathbf{W}_F} L) \mathbf{W}_E(q) = \Theta(\frac{1}{N})$ for any $k \leq N$, which in fact ensures
 2809 $\hat{p}(k|z_{1:T}) = \frac{1-\hat{p}(N+1|z_{1:T})}{N}$ for any $k \leq N$ and $z_{1:T} \in [N+1]^{\otimes T}$.
 2810

2811 After $O(\eta^{-1})$ steps in this phase, we have $\hat{p}(N+1|z_{1:T}) = \alpha$ and $\hat{p}(k|z_{1:T}) = \frac{1-\alpha}{N}$ for any $k \leq N$
 2812 and $z_{1:T}$.

2813 **Phase 2:** Assume $\hat{p}(N+1|\cdot) = \alpha$ starting from the beginning of this phase as discussed above. Due
 2814 to symmetry for the rest k channels, we have $\hat{p}(k|\cdot) = \frac{1-\alpha}{N}$. Note that the attention scores in $\phi(\cdot, \cdot)$
 2815 are still close to uniform, *i.e.*, $[\sigma(x_T^\top \mathbf{W}_{QK} x_{1:T})]_t \approx \frac{1}{T}$, since the update of \mathbf{W}_{QK} is in $O(N^{-2})$
 2816 whose impact on attention scores is also in $O(N^{-2})$ through $\exp(x) \approx 1+x$ for $x \approx 0$. Then we
 2817 track the movement of \mathbf{W}_V under these conditions.
 2818

2819 Since $m \rightarrow \infty$, taking $\bar{x} \triangleq \frac{1}{T} \sum_{i=1}^T x_i$, $\mu_k \triangleq \mathbb{E}[\bar{x}|y=k]$ and $\hat{\mu}_k \triangleq \mathbb{E}[\frac{\hat{p}(k|\bar{x})}{p(y=k)} \bar{x}] = \mathbb{E}[\bar{x}]$ since
 2820 $\hat{p}(k|\bar{x}) = \alpha \mathbb{1}\{k=N+1\} + \frac{1-\alpha}{N} \mathbb{1}\{k \leq N\} = p(y|k)$, Lemma H.1 gives
 2821

$$\begin{aligned} 2822 \nabla_{\mathbf{W}_V} L &= \sum_{k=1}^{N+1} p(y=k) \mathbf{W}_U(k) (\mathbb{E}[\bar{x}] - \mathbb{E}[\bar{x}|y=k])^\top \\ 2823 &= \sum_{k=1}^N p(y=k) \mathbf{W}_U(k) (\mathbb{E}[\bar{x}] - \mathbb{E}[\bar{x}|y=k])^\top \\ 2824 &= \sum_{k=1}^N \frac{1-\alpha}{N} \mathbf{W}_U(k) (\mathbb{E}[\bar{x}] - \mathbb{E}[\bar{x}|y=k])^\top \\ 2825 &= -\frac{1-\alpha}{N^2} \sum_{k=1}^N \mathbf{W}_U(k) (\mathbf{W}_E(k) - \overline{\mathbf{W}}_E + \widetilde{\mathbf{W}}_E(k) - \widetilde{\overline{\mathbf{W}}}_E)^\top, \end{aligned}$$

2834 where the second equality is due to $\mathbb{E}[\bar{x}] = \mathbb{E}[\bar{x}|y=N+1]$ due to $y=N+1$ is uniform for any
 2835 correct token $\bar{y} \leq N$, and the last equality is from
 2836

$$2837 \mathbb{E}[\bar{x}] - \mathbb{E}[\bar{x}|y=k] \approx -\frac{1}{N} (\mathbf{W}_E(k) - \overline{\mathbf{W}}_E) - \frac{1}{N} (\widetilde{\mathbf{W}}_E(k) - \widetilde{\overline{\mathbf{W}}}_E)$$

2840 with $\overline{\mathbf{W}}_E = N^{-1} \sum_{i=1}^N \mathbf{W}_E(i)$, $\widetilde{\overline{\mathbf{W}}}_E = N^{-1} \sum_{i=1}^N \widetilde{\mathbf{W}}_E(i)$ because $\mathbb{E}[\bar{x}] = \mathbb{E}_y[\mathbb{E}_x[\bar{x}|y]]$, and the
 2841 expected number of the tuple (q, \hat{y}) in a context length T is $\Theta(\frac{T}{N})$ by comparing Lemma E.6 and E.7.
 2842

2843 Therefore, the gradient for \mathbf{W}_V has the following structure
 2844

$$\begin{aligned} 2845 \mathbf{W}_U(j)^\top (-\nabla_{\mathbf{W}_V} L) \mathbf{W}_E(k) &\approx \frac{1}{N^2} \mathbb{1}\{j=k\} + O\left(\frac{1}{N^3}\right), \forall j, k \leq N, \\ 2846 & \\ 2847 \mathbf{W}_U(j)^\top (-\nabla_{\mathbf{W}_V} L) \widetilde{\mathbf{W}}_E(k) &\approx \frac{1}{N^2} \mathbb{1}\{j=k\} + O\left(\frac{1}{N^3}\right), \forall j, k \leq N. \end{aligned} \quad (25)$$

2850 Denote steps of phase 1 and phase 2 as t_1 and t_2 . Combined with the structure of \mathbf{W}_V in phase 1 as
 2851 in Eq.(22,23), ignoring projections that are $O(N^{-3})$ or negative, \mathbf{W}_V has the following structure
 2852 after phase 2
 2853

$$\begin{aligned} 2854 \mathbf{W}_U(j)^\top \mathbf{W}_V \mathbf{W}_E(k) &= \begin{cases} \Theta(\eta t_1 N^{-1}), & \text{if } j=N+1, \forall k, \\ \Theta(\eta t_1 N^{-2} + \eta t_2 N^{-2}), & \text{if } j=k \leq N, \\ \Theta(\eta t_1 N^{-2}), & \text{if } j=q, k=N+1, \end{cases} \\ 2855 & \\ 2856 \mathbf{W}_U(j)^\top \mathbf{W}_V \widetilde{\mathbf{W}}_E(k) &= \Theta(\eta t_2 N^{-2}), \text{ if } j=k \leq N. \end{aligned} \quad (26)$$

2858 **Phase 3:** now assume \mathbf{W}_V has the structure in Eq(26). The model still predicts $\hat{p}_{\mathbf{W}}(k|z) = \alpha \mathbb{1}\{k =$
 2859 $N+1\} + \frac{1-\alpha}{N} \mathbb{1}\{k \leq N\}$ because the above projections of \mathbf{W}_V onto $\mathbf{W}_U(j : j \leq N)$ is $o(\frac{1}{N})$.
 2860
 2861

Meanwhile, the attention scores are uniform as $\frac{1}{T}$ as $\mathbf{W}_{QK} \approx 0$. Therefore, the gradient of \mathbf{W}_{QK} is

$$\begin{aligned} \nabla \mathbf{W}_{QK} L &= \frac{1}{T} \sum_{k=1}^{N+1} \sum_{t \leq T} p(y=k) (\mathbb{E}[(\mathbf{W}_U(k)^\top \mathbf{W}_V x_t) \cdot x_T(x_t - \bar{x})^\top] \\ &\quad - \mathbb{E}[(\mathbf{W}_U(k)^\top \mathbf{W}_V x_t) \cdot x_T(x_t - \bar{x})^\top | y=k]) \\ &= \frac{1-\alpha}{TN} \sum_{k=1}^N \sum_{t \leq T} (\mathbb{E}[(\mathbf{W}_U(k)^\top \mathbf{W}_V x_t) \cdot x_T(x_t - \bar{x})^\top] \\ &\quad - \mathbb{E}[(\mathbf{W}_U(k)^\top \mathbf{W}_V x_t) \cdot x_T(x_t - \bar{x})^\top | y=k]), \end{aligned}$$

where $\bar{x} = T^{-1} \sum_{t \leq T} x_t$ and the last equality holds due to the condition of $y = N+1$ uniform for any correct token $\hat{y} \leq N$. Then, considering the above structure of \mathbf{W}_V , we notice that $\mathbf{W}_U(j)^\top \mathbf{W}_V x_t \approx \beta_1 \mathbb{1}\{z_t = j\} + \beta_2 \mathbb{1}\{z_{t-1} = j\}$ with $\beta_1 = \eta t_1 N^{-2} + \eta t_2 N^{-2}$ and $\beta_2 = \eta t_2 N^{-2}$ for any $j, k \leq N$. Here note that we ignore the projection of $j = q, k = N+1$ in Eq(26) because $\hat{y} = q$ is with probability $1/N = o(1)$ so that it will not influence much the following derivation.

Plug-in $\mathbf{W}_U(j)^\top \mathbf{W}_V x_t$ and we get

$$\mathbf{W}_E(q)^\top (-\nabla \mathbf{W}_{QK} L) (\mathbf{W}_E(b_1) + \widetilde{\mathbf{W}}_E(b_2)) = \frac{1-\alpha}{TN} \sum_{k \leq N} \sum_{t \leq T} \mathbb{E}[A_{k,b_1,b_2}^{(t)} | y=k] - \mathbb{E}[A_{k,b_1,b_2}^{(t)}] \quad (27)$$

where

$$\begin{aligned} A_{k,b_1,b_2}^{(t)} &= (\beta_1 \mathbb{1}\{z_t = k\} + \beta_2 \mathbb{1}\{z_{t-1} = k\}) \\ &\quad \cdot \left(\mathbb{1}\{z_t = b_1\} - \frac{\sum_{s \leq T} \mathbb{1}\{z_s = b_1\}}{T} + \mathbb{1}\{z_{t-1} = b_2\} - \frac{\sum_{s \leq T} \mathbb{1}\{z_{s-1} = b_2\}}{T} \right). \end{aligned}$$

Now we are to control $\Delta_{k,b_1,b_2} \triangleq \sum_{t \leq T} \mathbb{E}[A_{k,b_1,b_2}^{(t)} | y=k] - \mathbb{E}[A_{k,b_1,b_2}^{(t)}]$ for different choices of b_1, b_2 . Note that b_1 and b_2 co-exist by sum in $A_{k,b_1,b_2}^{(t)}$, so the additivity of expectation allows us to discuss choices of b_1, b_2 separately and then combine the results. Denote

$$\begin{aligned} B_{k,b_1}^{(t)} &= (\beta_1 \mathbb{1}\{z_t = k\} + \beta_2 \mathbb{1}\{z_{t-1} = k\}) \left(\mathbb{1}\{z_t = b_1\} - \frac{\sum_{s \leq T} \mathbb{1}\{z_s = b_1\}}{T} \right), \\ C_{k,b_2}^{(t)} &= (\beta_1 \mathbb{1}\{z_t = k\} + \beta_2 \mathbb{1}\{z_{t-1} = k\}) \left(\mathbb{1}\{z_{t-1} = b_2\} - \frac{\sum_{s \leq T} \mathbb{1}\{z_{s-1} = b_2\}}{T} \right). \end{aligned} \quad (28)$$

Controlling $\sum_{t \leq T} \mathbb{E}[B_{k,b_1}^{(t)} | y=k] - \mathbb{E}[B_{k,b_1}^{(t)}]$:

- If $b_1 = k$, from Lemma E.6 and E.7, we have

$$\begin{aligned} &\mathbb{E} \left[\sum_{t \leq T} \beta_1 \mathbb{1}\{z_t = k\} \mathbb{1}\{z_t = k\} \middle| y=k \right] - \mathbb{E} \left[\sum_{t \leq T} \beta_1 \mathbb{1}\{z_t = k\} \mathbb{1}\{z_t = k\} \right] = \beta_1 (1-\alpha) \frac{T}{N}. \\ &\mathbb{E} \left[- \sum_{t \leq T} \beta_1 \mathbb{1}\{z_t = k\} \frac{\sum_{s \leq T} \mathbb{1}\{z_s = k\}}{T} \middle| y=k \right] - \mathbb{E} \left[- \sum_{t \leq T} \beta_1 \mathbb{1}\{z_t = k\} \frac{\sum_{s \leq T} \mathbb{1}\{z_s = k\}}{T} \right] \\ &= -\mathbb{E} \left[\beta_1 T^{-1} (\sum_{s \leq T} \mathbb{1}\{z_s = k\})^2 \middle| y=k \right] + \mathbb{E} \left[\beta_1 T^{-1} (\sum_{s \leq T} \mathbb{1}\{z_s = k\})^2 \right] \\ &= \beta_1 T^{-1} \left(\frac{T}{N} + \frac{T^2}{N^2} - \frac{(2-\alpha)T}{N} - \frac{(2-\alpha)^2 T^2}{N^2} \right) = o \left(\beta_1 \frac{T}{N} \right). \end{aligned}$$

The terms involving $\mathbb{1}\{z_{t-1} = k\}$ are negligible as $O(T/N^2)$. Therefore, we have

$$\sum_{t \leq T} \mathbb{E}[B_{k,k}^{(t)} | y=k] - \mathbb{E}[B_{k,k}^{(t)}] = \beta_1 (1-\alpha) \frac{T}{N}. \quad (29)$$

2916
2917
2918
2919
2920
2921
2922
2923
2924
2925
2926
2927
2928
2929
2930
2931
2932
2933
2934
2935
2936
2937
2938
2939
2940
2941
2942
2943
2944
2945
2946
2947
2948
2949
2950
2951
2952
2953
2954
2955
2956
2957
2958
2959
2960
2961
2962
2963
2964
2965
2966
2967
2968
2969

- If $b_1 \neq k$, all terms are $O(T/N^2)$ because
 - If $b_1 \leq N$, it holds $p(z_t = b_1 | z_{t-1} = k) = 1/N$ with the expected number of k in context of length L being $\Theta(T/N)$ from lemmas in Appendix E.
 - If $b_1 = N + 1$, it holds $p(z_t = N + 1 | z_{t-1} = k) = O(1/N) \cdot \mathbb{1}\{k = q\}$ and the expected number of q in context of length T is $\Theta(T/N)$ from Lemma E.1 and E.4.
 - $\mathbb{E}[\sum_t \mathbb{1}\{z_{t-1} = k\} \#b_1/T] = \mathbb{E}[\#k \cdot \#b_1/T] = O(T/N^2)$ no matter it is with condition $y = k$ or not.

Therefore, for any $b_1 \neq k$, we have

$$\sum_{t \leq T} \mathbb{E}[B_{k,b_1}^{(t)} | y = k] - \mathbb{E}[B_{k,b_1}^{(t)}] = o(T/N). \quad (30)$$

Controlling $\sum_{t \leq T} \mathbb{E}[C_{k,b_2}^{(t)} | y = k] - \mathbb{E}[C_{k,b_2}^{(t)}]$:

- If $b_2 = q$, Lemma E.4 gives

$$\begin{aligned} & \mathbb{E} \left[\sum_{t \leq T} \beta_1 \mathbb{1}\{z_t = k\} \left(\mathbb{1}\{z_{t-1} = q\} - \frac{\#q}{T} \right) \middle| y = k \right] \\ & - \mathbb{E} \left[\sum_{t \leq T} \beta_1 \mathbb{1}\{z_t = k\} \left(\mathbb{1}\{z_{t-1} = q\} - \frac{\#q}{T} \right) \right] \\ & = (1 - p(\hat{y} = k)) \cdot \mathbb{E} \left[\sum_{t \leq T} \beta_1 \mathbb{1}\{z_t = k\} \left(\mathbb{1}\{z_{t-1} = q\} - \frac{\#q}{T} \right) \middle| y = k \right] + o\left(\beta_1 \frac{T}{N}\right) \\ & \approx \beta_1 (1 - \alpha) \frac{T}{N}, \end{aligned}$$

where the last equality is from $p(z_t = k | \bar{y} = k, z_{t-1} = q) = 1 - \alpha$.

All the other terms are negligible with the same reason as above.

Therefore, we have

$$\sum_{t \leq T} \mathbb{E}[C_{k,q}^{(t)} | y = k] - \mathbb{E}[C_{k,q}^{(t)}] = \beta_1 (1 - \alpha) \frac{T}{N}. \quad (31)$$

- If $b_2 = k$, similar to the above discussion about $B_{k,k}$, we have

$$\sum_{t \leq T} \mathbb{E}[C_{k,k}^{(t)} | y = k] - \mathbb{E}[C_{k,k}^{(t)}] = \beta_2 (1 - \alpha) \frac{T}{N}. \quad (32)$$

Note that the key difference is that here we use β_2 instead of β_1 , and $\beta_2 < \beta_1$.

- If $b_2 \neq q$ and $b_2 \neq k$, similar to the discussion for Eq(30), we have

$$\sum_{t \leq T} \mathbb{E}[C_{k,b_2}^{(t)} | y = k] - \mathbb{E}[C_{k,b_2}^{(t)}] = o(T/N). \quad (33)$$

Therefore, combining the above results in Eq(29, 30, 31, 32, 33), taking sums of the corresponding B and C from Eq(28) gives

$$\Delta_{k,b_1,b_2} = \begin{cases} \beta_1 (1 - \alpha) TN^{-1} + \beta_1 (1 - \alpha) TN^{-1}, & \text{if } b_1 = k, b_2 = q, \\ \beta_1 (1 - \alpha) TN^{-1} + \beta_2 (1 - \alpha) TN^{-1}, & \text{if } b_1 = k, b_2 = k, \\ \beta_1 (1 - \alpha) TN^{-1}, & \text{if } b_1 = k, \text{ other } b_2, \\ \beta_1 (1 - \alpha) TN^{-1}, & \text{if } b_1 \neq k, b_2 = q, \\ \beta_2 (1 - \alpha) TN^{-1}, & \text{if } b_1 \neq k, b_2 = k, \\ O(TN^{-1}), & \text{otherwise.} \end{cases}$$

To take the summation over all $k \leq N$ in Eq(27), we discuss the following cases of b_1 and b_2 for $\mathbf{W}_E(q)^\top (-\nabla_{\mathbf{W}_{QK}} L)(\mathbf{W}_E(b_1) + \widehat{\mathbf{W}}_E(b_2))$.

2970
2971
2972
2973
2974
2975
2976
2977
2978
2979
2980
2981
2982
2983
2984
2985
2986
2987
2988
2989
2990
2991
2992
2993
2994
2995
2996
2997
2998
2999
3000
3001
3002
3003
3004
3005
3006
3007
3008
3009
3010
3011
3012
3013
3014
3015
3016
3017
3018
3019
3020
3021
3022
3023

- If $b_1 \leq N, b_1 \neq b_2, b_2 = q$:
 - when $k = b_1$, we take Δ_{k,b_1,b_2} under the condition of $b_1 = k, b_2 = q$.
 - when $k \neq b_1$, we take Δ_{k,b_1,b_2} under the condition of $b_1 \neq k, b_2 = q$. Note that there are $(N - 1)$ such k .

Therefore, it holds

$$\mathbf{W}_E(q)^\top (-\nabla_{\mathbf{W}_{QK}} L)(\mathbf{W}_E(b_1) + \widetilde{\mathbf{W}}_E(q)) = \frac{1 - \alpha}{TN} \beta_1 (1 - \alpha) T (1 + N^{-1}). \quad (34)$$

- If $b_1 = b_2 = q$:
 - when $k = b_1$, we take Δ_{k,b_1,b_2} under the condition of $b_1 = k, b_2 = k$ to achieve a lower bound of the gap later.
 - when $k \neq b_1$, we take Δ_{k,b_1,b_2} under the condition of $b_1 \neq k, b_2 = q$. Note that there are $(N - 1)$ such k .

Therefore, it holds

$$\mathbf{W}_E(q)^\top (-\nabla_{\mathbf{W}_{QK}} L)(\mathbf{W}_E(b_1) + \widetilde{\mathbf{W}}_E(q)) \geq \frac{1 - \alpha}{TN} (\beta_1 (1 - \alpha) T + \beta_2 (1 - \alpha) TN^{-1}). \quad (35)$$

- If $b_1 = N + 1, b_2 = q$: for any $k \leq N$, it holds $k \neq b_1$, so we take Δ_{k,b_1,b_2} under the condition of $b_1 \neq k, b_2 = q$. Therefore, it holds

$$\mathbf{W}_E(q)^\top (-\nabla_{\mathbf{W}_{QK}} L)(\mathbf{W}_E(N + 1) + \widetilde{\mathbf{W}}_E(q)) = \frac{1 - \alpha}{TN} \beta_1 (1 - \alpha) T. \quad (36)$$

- If $b_2 \neq q, \forall b_1$: To get an upper bound of the projection length, we take Δ_{k,b_1,b_2} under the condition of $b_1 = k, b_2 = k$ or $b_1 \neq k, b_2 = k$. Therefore, it holds

$$\mathbf{W}_E(q)^\top (-\nabla_{\mathbf{W}_{QK}} L)(\mathbf{W}_E(b_1) + \widetilde{\mathbf{W}}_E(b_2)) \leq \frac{1 - \alpha}{TN} (\beta_1 + 2\beta_2) (1 - \alpha) TN^{-1}. \quad (37)$$

Comparing the above four cases, for any $\bar{y} \leq N$, the attention weight \mathbf{W}_{QK} to attend more to $x_t = \mathbf{W}_E(\bar{y}) + \widetilde{\mathbf{W}}_E(q)$ than to $x_t = \mathbf{W}_E(N + 1) + \widetilde{\mathbf{W}}_E(q)$, with

$$\begin{aligned} \mathbf{W}_E(q)^\top (-\nabla_{\mathbf{W}_{QK}} L)(\mathbf{W}_E(\bar{y}) + \widetilde{\mathbf{W}}_E(q)) - \mathbf{W}_E(q)^\top (-\nabla_{\mathbf{W}_{QK}} L)(\mathbf{W}_E(N + 1) + \widetilde{\mathbf{W}}_E(q)) \\ \geq \frac{(1 - \alpha)^2}{N^2} \beta_2. \end{aligned}$$

Meanwhile, any other setting of b_1, b_2 has smaller projection in $(-\nabla_{\mathbf{W}_{QK}} L)$.

In summary, \mathbf{W}_{QK} has the following patterns

1. it learns to attend to indices t such that $z_{t-1} = q$ is the trigger word,
2. when there are multiple t_i 's such that $z_{t_i-1}=q$, it learns to attend to those with $z_t = \bar{y}$ more than $z_t = N + 1$.

G LINEAR ASSOCIATIVE MEMORY

G.1 EXPERIMENTS AND DISCUSSIONS

In Section 3, we showed that *fully* truncating a feed-forward layer can be helpful for reasoning. We now present a setting where noisy associations are stored in a rank-one subspace of a layer, so that *intermediate* levels of truncation are more useful to remove noise.

Model and data. We consider a simple associative memory setting where the goal is learn a fixed permutation from input tokens to output tokens (w.l.o.g. taken to be the identity), with a linear model similar to Cabannes et al. (2024). Consider a learnable weight matrix $\mathbf{W} \in \mathbb{R}^{d \times d}$. Consider embeddings for n input tokens as $\{e_i\}_{i=1}^n \subset \mathbb{R}^d$ and embeddings for c output tokens as $\{u_i\}_{i=1}^c \subset \mathbb{R}^d$. In contrast to Cabannes et al. (2024), we consider an additional ‘‘common noise’’

output token $c = n + 1$, which is chosen for any input with probability $\alpha \in (0, 1)$. For any input $x \in [n]$, the target distribution $p_\alpha(\cdot|x)$ is defined by

$$p_\alpha(y|x) = (1 - \alpha) \cdot \mathbb{1}\{y = x\} + \alpha \cdot \mathbb{1}\{y = c\}. \tag{38}$$

In other words, the last channel (c) for output is the **common noise** with probability α for any input. The training dataset \mathcal{D}_α consists of uniformly distributed inputs $x \in [n]$, and outputs conditionally sampled as $y|x \sim p_\alpha(\cdot|x)$.

Given any pair of input and output tokens, the associative memory model takes the form

$$f(i, j; \mathbf{W}) \triangleq \langle u_j, \mathbf{W}e_i \rangle, \quad \forall i, j \in [n] \times [c], \tag{39}$$

When $k \leq d$, we denote the rank- k approximation of f as $f^{(k)}$ by replacing \mathbf{W} with $\mathbf{W}^{(k)}$, where $\mathbf{W}^{(k)}$ is the rank- k approximation of \mathbf{W} .

Training. During training, the dataset \mathcal{D}_α is generated with non-zero noise probability $\alpha > 0$. At test time, the dataset \mathcal{D}_0 is without noise as $\alpha = 0$, so the computed loss is called **pure-label loss**. The model is trained with Gradient Descent (GD) subjected to cross-entropy loss.

Experiments with randomness. Assume both $\{e_i\}_{i=1}^n$ and $\{u_i\}_{i=1}^c$ are i.i.d. uniformly drawn from sphere \mathbb{S}^{d-1} . Also assume the model is initialized as $\mathbf{W}_{i,j} \sim \mathcal{N}(0, \frac{1}{d})$. Due to randomness from embeddings and model initialization, let's first conduct 20 runs of experiments to obtain significant factors before moving the theoretical argument.

Note that *only full models are trained*, and we track loss for low-rank models by conducting SVD in each step without manipulating training. In Figure 5, we illustrate the pure-label loss *v.s.* training steps for models of different ranks, where $n = 3$, $\alpha = 0.03$ and $d = 8$ or 12 . It turns out, while the full model (rank ≥ 3) has a constant pure-label loss (~ 0.03 , dependent on α), the rank-2 model is very likely to have a significant loss than the full model. Meanwhile, the larger d has more stable results than small d .

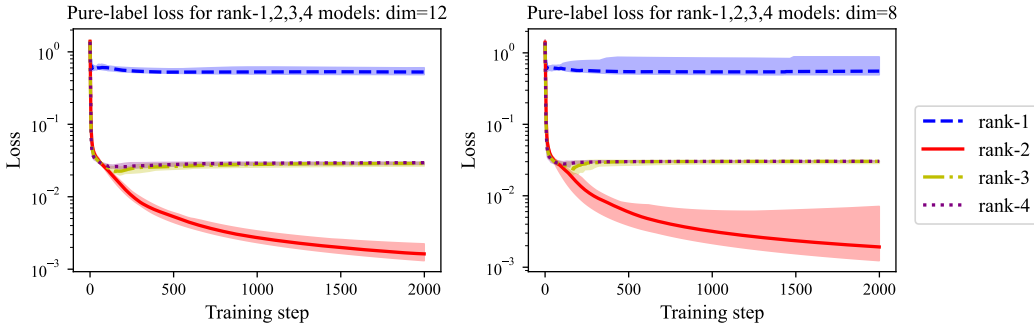


Figure 18: Pure-label loss for rank-1,2,3,4 models with $n = 3$, $\alpha = 0.03$ and $d = 12$ (left) or 8 (right). *Only full models are trained*, and we report low-rank results by conducting SVD in each step without manipulating the training. In both figures, the experiments are run for 20 times to examine the randomness. For each rank, we plot curves of the median, 25% and 75% out of 20 runs. It turns out: i) rank-2 models are very likely to have significantly lower pure-label loss than full models (rank ≥ 3), and ii) the larger dimension d has more stable results.

Therefore, we can qualify the following important factors for this model:

- i. d *v.s.* n, c : when $d \gg n, c$, random drawn embeddings tend to be orthogonal to each other, with inner product in $O(1/\sqrt{d})$. If $n, c = \Omega(d)$, embeddings will be in strong correlations, making the problem extremely difficult to understand. Cabannes et al. (2024) also discussed about such particle interaction in associative memory.
- ii. Low-rank subspace storing the noise. In Figure 18, the rank-1 subspace between the full and rank-2 models is responsible to store the noise, removing which will induce a model ideally predicting the ground-truth without noise. This is understandable if the embeddings are orthogonal, as shown in Theorem 3.

- iii. α v.s. n . When n is large, orthogonal embeddings still induces a low-rank subspace storing the noise, but α decides whether the low-rank subspace corresponds to the smallest singular values of \mathbf{W} . If not, it requires more careful manipulation of the spectrum instead of low-rank approximation of \mathbf{W} .

G.2 PROOF OF THEOREM 3

Now we present a theoretical analysis of this problem with some assumptions.

Assumption G.1 (Orthonormality). *Embeddings of input and output tokens are orthonormal, i.e., $e_i^\top e_j = \mathbb{1}\{i = j\}, \forall i, j$ and $u_i^\top u_j = \mathbb{1}\{i = j\}, \forall i, j$.*

Assumption G.2 (Initialization). *The learnable matrix \mathbf{W} is initialized from $\mathbf{0}$ when $t = 0$.*

Theorem 5 (Restatement of Theorem 3). *Assume Assumptions G.1 and G.2 hold, considering $n = 2, c = 3$ and $\alpha \in (0.2, 0.4)$, we train the full model $f(\cdot, \cdot; \mathbf{W})$ with gradient flow. Denote $P(i, j; \mathbf{W})$ as the model's predicted probability for output j conditioned on input i . Then, for $t \rightarrow \infty$ and $i \in \{1, 2\}$, we have*

$$\begin{aligned} P(i, j; \mathbf{W}) &= (1 - \alpha) \cdot \mathbb{1}\{j = i\} + \alpha \cdot \mathbb{1}\{j = c\}, \\ P(i, j; \mathbf{W}^{(1)}) &= (1 - \Theta(t^{-1/2})) \cdot \mathbb{1}\{j = i\} + \Theta(t^{-1/2}) \cdot \mathbb{1}\{j = c\}. \end{aligned}$$

Remark 1. Note that here the assumption $\alpha \in (0.2, 0.4)$ is a technical choice. In experiments, any value $\alpha \in (0, 0.4)$ still has the same result.

Proof. W.l.o.g., we assume the embeddings are standard basis in \mathbb{R}^d . For any \mathbf{W} , the gradient $\nabla_{\mathbf{W}} L$ can be decomposed as

$$\nabla_{\mathbf{W}} L = \gamma_1 \begin{bmatrix} 1 \\ -1 \\ 0 \end{bmatrix} [1 \quad -1 \quad 0] + \gamma_2 \begin{bmatrix} 1 \\ 1 \\ -2 \end{bmatrix} [1 \quad 1 \quad 0]. \quad (40)$$

Since \mathbf{W} initializes from zero, this implies \mathbf{W} can always be decomposed with the same basis

$$\mathbf{W} = \beta_1 \begin{bmatrix} 1 \\ -1 \\ 0 \end{bmatrix} [1 \quad -1 \quad 0] + \beta_2 \begin{bmatrix} 1 \\ 1 \\ -2 \end{bmatrix} [1 \quad 1 \quad 0]. \quad (41)$$

Then gradient flow gives the following ODE

$$\begin{aligned} \dot{\beta}_1 &= -\gamma_1 = \frac{\exp(-\beta_1 + \beta_2) - \exp(\beta_1 + \beta_2)}{\exp(-\beta_1 + \beta_2) + \exp(\beta_1 + \beta_2) + \exp(-2\beta_2)} + 1 - \alpha \\ &= \frac{\exp(-2\beta_1) - 1}{\exp(-2\beta_1) + \exp(-\beta_1 - 3\beta_2) + 1} + 1 - \alpha, \\ \dot{\beta}_2 &= -\gamma_2 = \frac{3 \exp(-2\beta_2)}{\exp(-\beta_1 + \beta_2) + \exp(\beta_1 + \beta_2) + \exp(-2\beta_2)} - 3\alpha \\ &= \frac{3 \exp(-\beta_1 - 3\beta_2)}{\exp(-2\beta_1) + \exp(-\beta_1 - 3\beta_2) + 1} - 3\alpha. \end{aligned} \quad (42)$$

Denoting $a = -2\beta_1, b = -\beta_1 - 3\beta_2$, the ODE becomes

$$\begin{aligned} \dot{a} &= \frac{2 - 2 \exp(a)}{\exp(a) + \exp(b) + 1} - 2 + 2\alpha, \\ \dot{b} &= \frac{2 - 8 \exp(b)}{\exp(a) + \exp(b) + 1} - 2 + 10\alpha. \end{aligned} \quad (43)$$

Lemma H.3 gives the solution as, when $t \rightarrow \infty$,

$$a \rightarrow -\log(t) - \log(1 - \alpha)(4 - 2\alpha), \quad b \rightarrow \log \frac{\alpha}{1 - \alpha}.$$

For the full model, taking the scores $\mathbf{W}_{1,:}$ of the first input token as an example, we have $\mathbf{W}_{11} = \beta_1 + \beta_2$, $\mathbf{W}_{12} = -\beta_1 + \beta_2$, $\mathbf{W}_{13} = -2\beta_2$, so the margins are

$$\mathbf{W}_{11} - \mathbf{W}_{12} = 2\beta_1 = -a, \mathbf{W}_{11} - \mathbf{W}_{13} = \beta_1 + 3\beta_2 = -b.$$

For the rank-1 model (assuming $\beta_1 > \beta_2$), the margins are

$$\mathbf{W}_{11}^{(1)} - \mathbf{W}_{12}^{(1)} = 2\beta_1, \mathbf{W}_{11}^{(1)} - \mathbf{W}_{13}^{(1)} = \beta_1.$$

The proof finishes by computing softmax on the margins. \square

H USEFUL LEMMAS

Lemma H.1. *Let p be a data distribution on $(x, y) \in \mathbb{R}^d \times [N]$. Consider training data as m i.i.d. samples $\mathcal{D} \triangleq \{(x_i, y_i)\}_{i=1}^m \subset \mathbb{R}^d \times [N+1]$ from p . Consider the following classification problem, with fixed output embeddings \mathbf{W}_U :*

$$\hat{L}(\mathbf{W}) = \frac{1}{m} \sum_{i=1}^m [l(y_i, \mathbf{W}_U \mathbf{W} x_i)].$$

The gradients take the following form: denoting $\hat{p}_{\mathbf{W}}(k|x_i)$ as the current predicted probability of class k in $[N+1]$ classes for input x_i ,

$$\nabla_{\mathbf{W}} \hat{L}(\mathbf{W}) = \frac{1}{m} \sum_{i=1}^m \left[\sum_{k=1}^{N+1} (\hat{p}_{\mathbf{W}}(k|x_i) - \mathbb{1}\{y_i = k\}) \mathbf{W}_U(k) x_i^\top \right].$$

When $m \rightarrow \infty$, the above equation becomes

$$\nabla_{\mathbf{W}} L(\mathbf{W}) = \sum_{k=1}^{N+1} p(y = k) \mathbf{W}_U(k) (\hat{\mu}_k - \mu_k)^\top,$$

where $\mu_k \triangleq \mathbb{E}[x|y = k]$ and $\hat{\mu}_k \triangleq \mathbb{E}_x[\frac{\hat{p}_{\mathbf{W}}(k|x)}{p(y=k)} x]$.

Remark 2. This lemma is from Lemma 2 in Bietti et al. (2023).

Proof. Recall the form of the cross-entropy loss for classification with K classes:

$$l(y, \epsilon) = - \sum_{k=1}^K \mathbb{1}\{y = k\} \log \frac{e^{\xi_k}}{\sum_j e^{\xi_j}}.$$

Its derivatives take the form

$$\frac{\partial l}{\partial \xi_k}(y, \xi) = s(\xi)_k - \mathbb{1}\{y = k\},$$

where $s(\xi)_k = \frac{e^{\xi_k}}{\sum_j e^{\xi_j}}$.

The gradient of L is then given by

$$\begin{aligned} \nabla_{\mathbf{W}} \hat{L}(\mathbf{W}) &= \frac{1}{m} \sum_{i=1}^m \left[\sum_{k=1}^{N+1} \frac{\partial l}{\partial \xi_k}(y_i, \mathbf{W}_U \mathbf{W} x_i) \nabla_{\mathbf{W}} (\mathbf{W}_U(k)^\top \mathbf{W} x_i) \right] \\ &= \frac{1}{m} \sum_{i=1}^m \left[\sum_{k=1}^{N+1} (\hat{p}_{\mathbf{W}}(k|x_i) - \mathbb{1}\{y_i = k\}) \mathbf{W}_U(k) x_i^\top \right]. \end{aligned}$$

When $m \rightarrow \infty$, the above equation becomes

$$\begin{aligned} \nabla_{\mathbf{W}} L(\mathbf{W}) &= \sum_{k=1}^{N+1} \mathbf{W}_U(k) \mathbb{E}[\hat{p}_{\mathbf{W}}(k|x) x^\top] - \sum_{k=1}^{N+1} \mathbb{E}[\mathbb{1}\{y = k\} \mathbf{W}_U(k) \mathbb{E}[x|y]^\top] \\ &= \sum_{k=1}^{N+1} \mathbf{W}_U(k) \mathbb{E}[\hat{p}_{\mathbf{W}}(k|x) x^\top] - \sum_{j,k} p(y = k) \mathbb{1}\{j = k\} \mathbf{W}_U(k) \mathbb{E}[x|y = j]^\top \\ &= \sum_{k=1}^{N+1} p(y = k) \mathbf{W}_U(k) (\hat{\mu}_k - \mu_k)^\top. \end{aligned}$$

3186

□

3187

3188 **Lemma H.2.** Consider a sequence $\{S_t\}_{t \geq 1}$ with $S_t = a^t \cdot t$ where $a \neq 1$. Then $\sum_{1 \leq t \leq T} S_t =$
 3189 $\frac{a(1-a^T)}{(a-1)^2} + \frac{a^{T+1} \cdot T}{a-1}$.

3190

3191

3192 *Proof.* Denote $X_t \triangleq \sum_{1 \leq t \leq T} S_t$. Then we have $a \cdot X_t = \sum_{2 \leq t \leq T+1} a^t \cdot (t-1)$. Hence, it holds
 3193 $(a-1)X_t = -\sum_{2 \leq t \leq T} a^t - a + a^{T+1} \cdot T = -\frac{a(1-a^T)}{1-a} + a^{T+1} \cdot T$. Therefore, we have

3194

3195

3196

$$X_t = \frac{a(1-a^T)}{(a-1)^2} + \frac{a^{T+1} \cdot T}{a-1}.$$

3197

□

3198

3199 **Lemma H.3.** Consider the following ODE with $a(0) = b(0) = 0$ and $\alpha \in (0.2, 0.4)$,

3200

3201

3202

3203

3204

3205

3206

3207

3208

3209

3210

3211

3212

3213

3214

3215

3216

3217

3218

3219

3220

3221

3222

3223

3224

3225

3226

3227

3228

3229

3230

3231

3232

3233

3234

3235

3236

3237

3238

3239

Proof. The ODE can be re-written as

$$\begin{aligned} \dot{a} &= 2 \cdot \frac{(\alpha - 2) \exp(a) + (\alpha - 1) \exp(b) + \alpha}{\exp(a) + \exp(b) + 1} \triangleq \frac{2D}{\exp(a) + \exp(b) + 1}, \\ \dot{b} &= 10 \cdot \frac{(\alpha - \frac{1}{5}) \exp(a) + (\alpha - 1) \exp(b) + \alpha}{\exp(a) + \exp(b) + 1} \triangleq \frac{10E}{\exp(a) + \exp(b) + 1}. \end{aligned}$$

At $t = 0$, it holds $\dot{a}(0) < 0$, $\dot{b}(0) < 0$ since $D = 3\alpha - 3 < 0$, $E = 3\alpha - \frac{6}{5} < 0$. Hence, a and b start to decrease from $t = 0$. The ending of the decreasing happens when one of D and E gets positive. Let's show D and E will never be positive when $\alpha \in (0.2, 0.4)$ by contradiction.

Assume time T_1 is when one of D and E equals to 0 for the first time. This means $E = 0$, because, for any time t , it always holds $D < E$ since $\exp(a) > 0$ for any $a \in \mathbb{R}$. Then at T_1 , we have $\dot{a} < 0$, $\dot{b} = 0$, which means $\exp(a)$ will decrease for any small time window $\Delta t > 0$ and $\exp(b)$ stays unchanged. Together with $\alpha > 0.2$, this means it has $E < 0$ again at time $T_1 + \Delta t$. Therefore, it is possible for E to be 0, but E will never be positive. Meanwhile, this also guarantees D will always be negative because $D < E$.

Then, we make an observation that when D is always negative and E is always non-positive, the decreasing nature of a will have $D \approx E$ when $t \rightarrow \infty$ by $\exp(a) \approx 0$. This implies $b = \log \frac{\alpha}{1-\alpha}$. Then, by taking $\exp(a) = \beta \cdot t^{-\gamma}$, the ODE gives

3230

3231

3232

3233

3234

3235

3236

3237

3238

3239

$$-\gamma \frac{1}{t} = \frac{(2\alpha - 4)\beta \cdot t^{-\gamma}}{\beta \cdot t^{-\gamma} + \frac{1}{1-\alpha}},$$

which gives $\gamma = 1$, $\beta = \frac{1}{(1-\alpha)(4-2\alpha)}$.

Therefore, when $t \rightarrow \infty$, we have

$$a \rightarrow \log \left(\frac{1}{(1-\alpha)(4-2\alpha)} t^{-1} \right), \quad b \rightarrow \log \frac{\alpha}{1-\alpha}.$$

□

3240 I INPUT EXAMPLES FOR LLMs

3241

3242 I.1 EXAMPLES FOR PREPOSITIONS

3243

3244 For experiments in Appendix C.1, we use two synthetic datasets: inputs are 30 prepositions, and
3245 inputs are 40 incomplete sentences ending with a preposition.

3246 The 30 prepositions are:

3247

3248 "about", "above", "across", "after", "against", "along", "around", "at", "before", "behind", "below",
3249 "beneath", "beside", "between", "by", "during", "for", "from", "in", "inside", "into", "near", "of",
3250 "on", "over", "through", "to", "under", "with", "without".

3251 Generated by Claude 3 (Anthropic, 2024), the 40 incomplete sentences are:

3252

3253 ["Inspired painter gazed at pristine canvas, envisioning next creation about", "Children's delighted
3254 squeals filled yard as they frolicked, stumbling across", "Singer inhaled deeply, calming nerves before
3255 gracing stage before", "Ominous storm clouds amassed, promising downpour that would soon roll
3256 in", "Awestruck trekker admired breathtaking summit vista, looking over", "Rich aroma of freshly
3257 roasted beans permeated cozy cafe, enticing during", "With deft sleight of hand, illusionist made
3258 coin vanish, leaving spectators in awe without", "Majestic oak stood tall, branches reaching skyward
3259 above", "Gentle waves caressed shoreline, soothing rhythm lulling along", "Meticulous investigator
3260 scoured crime scene, searching for any evidence left behind", "Radiant sunbeams filtered through
3261 sheer curtains, warming hardwood floor beneath", "Concert pianist's nimble fingers glided across
3262 ivory keys, room resonating with melody around", "Crickets' evening chorus filled silent field from
3263 nearby meadow during", "Jubilant laughter resounded down corridor as jovial group headed towards
3264 celebration without", "Struggling poet tapped pen restlessly, seeking words to capture elusive emotion
3265 beneath", "Soothing patter of raindrops danced on windowpane, inviting serene relaxation with",
3266 "Mouthwatering scent of fresh bread beckoned passersby into cozy bakery without", "Mighty waves
3267 thundered against jagged cliffs, echoing roar along rugged shoreline around", "Seasoned trekker
3268 carefully navigated winding trail, cautiously avoiding exposed roots and rocks beneath", "Graceful
3269 ballerina flowed across stage, movements blending seamlessly with melody during", "Crackling
3270 campfire cast dancing shadows across gathered faces around", "Vibrant brush strokes danced across
3271 canvas, bold hues bursting into life before", "Photographer framed breathtaking sunset, capturing
3272 fleeting beauty over glistening ocean without", "Stern librarian hushed raucous group, reminding
3273 them to stay quiet inside", "Ink flowed from author's pen, words brimming with raw passion as page
3274 filled during", "Earthy aroma of freshly steeped tea perfumed air, inviting moment of serenity along",
3275 "Masterful guitarist's fingers danced nimbly across strings, room alive with haunting melody around",
3276 "Meticulous chef artfully garnished plate, adding delicate finishing touches over", "Indomitable
3277 marathoner pushed through punishing final stretch, fortitude driving every stride before", "Engrossed
3278 scientist examined specimen's intricate structures through microscope beneath", "Nervous thespian
3279 steadied breathing, striding into dazzling spotlight, delivering flawless performance with", "Skilled
3280 artist's pencil glided gracefully, deftly capturing subject's essence without", "Weary hiker paused
3281 to catch breath, marveling at sweeping panorama from lofty peak above", "Deep in thought, writer
3282 drummed fingers, seeking perfect phrasing to convey profound emotion without", "Lost in reverie,
3283 violinist swayed gently, fingers dancing across delicate strings during", "Painter's brushstrokes burst
3284 into radiant life, canvas ablaze with vivid sunset hues over", "Adept photographer framed picturesque
3285 scene, preserving landscape's beauty without", "World-renowned chef meticulously garnished plate,
3286 each component strategically placed around", "Dedicated researcher scrutinized specimen under
3287 microscope, documenting minute details beneath", "Seasoned actor inhaled deeply, embodying
3288 character as bright lights engulfed stage with",].

3286

3287 I.2 MORE EXAMPLES OF FACTUAL RECALL

3288 We consider more examples of factual recall with pairs of input and output shown in Table 5.

3289

3290

3291

3292

3293

3294
3295
3296
3297
3298
3299
3300
3301
3302
3303
3304
3305
3306
3307
3308
3309
3310
3311
3312
3313
3314
3315
3316
3317
3318
3319
3320
3321
3322
3323
3324
3325
3326
3327
3328
3329
3330
3331
3332
3333
3334
3335
3336
3337
3338
3339
3340
3341
3342
3343
3344
3345
3346
3347

Table 5: Inputs and Outputs of Factual Knowledge

Input	Target output
The Great Wall is located in	China
Mount Kilimanjaro is located in	Tanzania
The Nobel Prize is awarded in	Sweden
The Statue of Liberty stands in	New York Harbor
Vatican City is enclosed within	Rome
The Acropolis is situated in	Athens
The Sydney Opera House is located on	Bennelong Point
The Galápagos Islands belong to	Ecuador
The Aurora Borealis can be seen in	Norway
The Amazon River flows through	Brazil
The Andes Mountains extend through	Chile
Machu Picchu is found in	Peru
The Kremlin is located in	Moscow
Uluru is a landmark found in	Australia
Petra is an archaeological city in	Jordan
Angkor Wat is located in	Cambodia
The city of Toronto is in	Canada
The city of Barcelona is in	Spain
The city of Mumbai is in	India
The Eiffel Tower is located in	Paris

J SYNTHETIC IOI TASK

Data and task. Here we consider a synthetic data model similar to the IOI task Wang et al. (2022), with additional noise. Consider a vocabulary $\mathcal{V} = \{1, 2, \dots, N, N + 1\}$. The token $\tau \triangleq N + 1$ is the generic noise token. We fix a *trigger* token $q \in [N]$, which governs in-context recall, and a context length T . Each sequence of tokens $z_{1:T} = [z_1, z_2, \dots, z_T]$ is generated as follows:

- i. Sample a correct *output* token \bar{y} and a different *distractor* token y^D uniformly in $[N]$.
- ii. Sample three indices $i_1, i_2, i_3 \in [T - 2]$ such that their distances are no smaller than 2. (This is for non-overlapping.)
- iii. Set $z_{i_1} = z_{i_2} = z_{i_3} = q$. Among the three indices $i_1 + 1, i_2 + 1, i_3 + 1$, random select one of them with $z_{i_k+1} = \bar{y}$ with the other two as $z_{i_k+1} = y^D$.
- iv. Set $z_T = q$ and sample $z_{T+1} \sim p_{\alpha, \bar{y}}(\cdot)$ with

$$p_{\alpha, \bar{y}}(x) = \begin{cases} 1 - \alpha, & \text{if } x = \bar{y}, \\ \alpha, & \text{if } x = \tau, \\ 0, & \text{otherwise.} \end{cases}$$

- v. Random fill with tokens from $\mathcal{V} \setminus \{q\}$ into the remaining positions in $[T + 1] \setminus \{i_1, i_1 + 1, i_2, i_2 + 1, i_3, i_3 + 1, T, T + 1\}$.

The key difference between the above data and noisy in-context recall in Section 3 is that, in addition to detecting the tokens \bar{y} and y^D after the trigger q , this task also requires counting to decide which of \bar{y} and y^D appear more. This mechanism is exactly the definition of the correct IO token in Wang et al. (2022).

Most of the other settings are the same as that in Section 3, including the training procedure, the architecture of a transformer layer, dimensionality and the vocabulary size.

Results. Figure 19 shows the test performance for models with layers $L = 3, 4, 5, 6, 7$, where the models are trained with SGD. **Dropping the last-layer MLP** consistently improves the test performance across all models. Figure 20 shows the test performance for $L = 3, 4, 5$ trained with Adam (Kingma, 2014). **Truncating the last MLP’s input weights** with $\rho = 0.01$ significantly

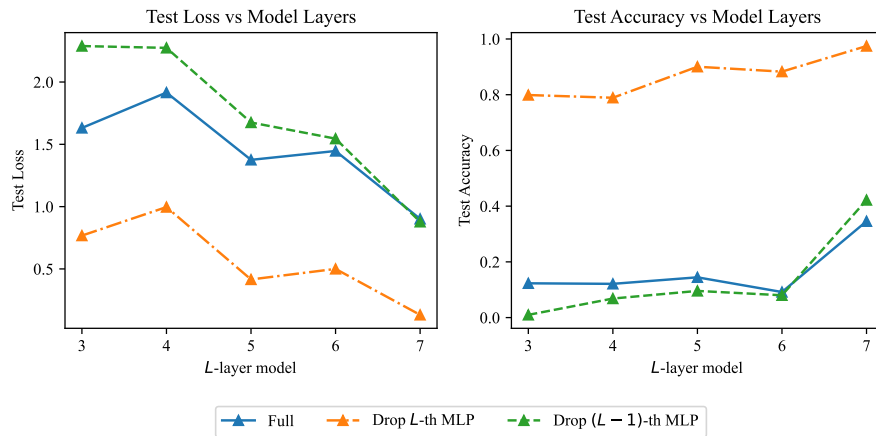


Figure 19: **Synthetic IOI trained with SGD**: test loss and accuracy for transformers with different layers. Dropping the last-layer MLP consistently improves the test accuracies across all models.

improves the performance for $L = 3, 4$. We also note that the model fails to converge for $L = 5$, possibly because we do not use any normalization technique in the architecture, so the Adam training is less stable for deep transformers.

3402
 3403
 3404
 3405
 3406
 3407
 3408
 3409
 3410
 3411
 3412
 3413
 3414
 3415
 3416
 3417
 3418
 3419
 3420
 3421
 3422
 3423
 3424
 3425
 3426
 3427
 3428
 3429
 3430
 3431
 3432
 3433
 3434
 3435
 3436
 3437
 3438
 3439
 3440
 3441
 3442
 3443
 3444
 3445
 3446
 3447
 3448
 3449
 3450
 3451
 3452
 3453
 3454
 3455



Figure 20: **Synthetic IOI trained with Adam**: test loss and accuracy for transformers with layers $L = 3, 4, 5$. Truncating the last-layer MLP’s input weights with $\rho = 0.01$ improves the test performances for $L = 3, 4$, while the model fails to converge for $L = 5$.